

**Phenylpropanoids and long chain fatty acid  
derivatives in the interaction of  
*Arabidopsis thaliana* and *Verticillium longisporum***

Dissertation  
zur Erlangung des  
mathematisch-naturwissenschaftlichen Doktorgrades  
"Doctor rerum naturalium"  
der Georg-August-Universität Göttingen

vorgelegt von  
Stefanie König (geb. Götze)  
aus Hannover

Göttingen 2011

Referent:

Prof. Dr. Ivo Feußner

Korreferent:

Prof. Dr. Wolfgang Dröge-Laser

Tag der mündlichen Prüfung:

14. Oktober 2011

# INDEX

<b>1</b>	<b>INTRODUCTION .....</b>	<b>1</b>
1.1	Plant defense responses .....	1
1.2	Verticillium species .....	3
1.2.1	<i>Verticillium longisporum</i> .....	3
1.2.2	Infection cycle .....	4
1.2.3	Plant defense in response to <i>Verticillium</i> infection .....	5
1.3	Preliminary data generated by metabolite fingerprinting .....	6
1.4	Phenylpropanoids .....	7
1.4.1	General biosynthesis of phenylpropanoids .....	7
1.4.2	Flavonoids .....	9
1.4.3	Lignin and lignans .....	9
1.4.4	Sinapate esters .....	11
1.5	Suberin and cutin .....	11
1.5.1	Structure of cutin and suberin .....	11
1.5.2	Enzymes involved in cutin and suberin monomer biosynthesis .....	13
1.5.3	Involvement in plant-pathogen interactions .....	13
1.6	Sphingolipids .....	14
1.6.1	Biosynthesis of sphingolipids .....	15
1.6.2	$\alpha$ -Hydroxylated fatty acids .....	16
1.6.3	Involvement in abiotic and biotic stress .....	17
1.7	Goals of the thesis .....	18
<b>2</b>	<b>MATERIALS AND METHODS .....</b>	<b>19</b>
2.1	Materials .....	19
2.1.1	Chemicals .....	19
2.1.2	Enzymes and size markers .....	19
2.1.3	Kits .....	20
2.1.4	Equipment .....	20
2.1.5	Consumables .....	20
2.1.6	Software .....	21
2.1.7	Plant lines .....	21
2.1.8	Microorganisms .....	22
2.1.9	Plasmids .....	22
2.1.10	Oligonucleotides .....	22
2.1.11	Media .....	24
2.2	Methods .....	25
2.2.1	Fungal growth and cultivation .....	25
2.2.2	Fungal toxicity tests .....	25
2.2.3	Plant growth and cultivation .....	25
2.2.4	Plant treatments .....	26

2.2.4.1	Infection with <i>V. longisporum</i> .....	26
2.2.4.2	Infection with <i>Golovinomyces cichoracearum</i> .....	26
2.2.4.3	Hygromycin selection .....	26
2.2.4.4	BASTA selection .....	27
2.2.5	Leaf area measurements .....	27
2.2.6	Crossing of Arabidopsis plants .....	27
2.2.7	Analytical methods .....	27
2.2.7.1	Undirected metabolite fingerprinting by UPLC-MS measurements .....	27
2.2.7.2	Determination of sinapate esters, flavonoids and indoles .....	29
2.2.7.3	Determination of lignan glucosides and monolignol glucosides .....	29
2.2.7.4	Determination of residual bound lipids (suberin and cutin monomers) .....	30
2.2.7.5	Determination of ceramides and glucosylceramides .....	31
2.2.7.6	Determination of multiple phytohormones by HPLC-MS/MS .....	32
2.2.7.7	Synthesis of 4-methoxy-indol-3-ylmethyl-glucosinolate .....	34
2.2.8	Molecular biological methods .....	34
2.2.8.1	DNA isolation from bacterial cultures, solutions and gel pieces .....	34
2.2.8.2	Extraction of genomic DNA of Arabidopsis leaves .....	34
2.2.8.3	Amplification of DNA fragments by polymerase chain reaction .....	35
2.2.8.4	PCR based genotyping of SALK-lines .....	35
2.2.8.5	Quantification of <i>V. longisporum</i> -DNA in inoculated plants .....	36
2.2.8.6	Separation of DNA by electrophoresis .....	36
2.2.8.7	Restriction and ligation of DNA .....	36
2.2.8.8	LR-Clonase reaction .....	36
2.2.8.9	Sequencing reaction .....	37
2.2.8.10	Transformation of competent <i>E. coli</i> cells .....	37
2.2.8.11	Preparation of competent <i>A. tumefaciens</i> cells .....	37
2.2.8.12	Transformation of <i>A. tumefaciens</i> .....	38
2.2.8.13	Transformation of Arabidopsis .....	38
2.2.8.14	Cloning strategy for the complementation of <i>fah1xfah2</i> .....	38
2.2.8.15	Cloning strategy for the promotor GUS fusions .....	38
2.2.8.16	Determination of transcript levels .....	39
2.2.8.16.1	RNA extraction .....	39
2.2.8.16.2	cDNA synthesis .....	39
2.2.9	Microscopy of <i>V. longisporum</i> infected plant material .....	40
2.2.9.1	Paraffin embedding .....	40
2.2.9.2	Lignin staining of embedded plant material .....	40
2.2.10	GUS staining .....	40
2.2.11	Statistics .....	41
<b>3</b>	<b>RESULTS .....</b>	<b>42</b>
<b>3.1</b>	<b>Infection of Arabidopsis plants with <i>V. longisporum</i> .....</b>	<b>42</b>
<b>3.2</b>	<b>Undirected metabolite fingerprinting in <i>V. longisporum</i> infected tissue using UPLC-MS(TOF) .....</b>	<b>44</b>
3.2.1	Leaf material .....	44
3.2.2	Root material .....	48
<b>3.3</b>	<b>Phenylpropanoids and indoles in the interaction of Arabidopsis and <i>V. longisporum</i> .</b>	<b>49</b>
3.3.1	Quantification of selected markers .....	49
3.3.2	Microscopic analysis of lignin accumulation in hypocotyls and petioles .....	52
3.3.3	Expression analysis of genes of the phenylpropanoid pathway .....	53

3.3.4	Infection of mutant plants of the detected metabolic pathways.....	54
3.3.4.1	Infection of the indole mutant <i>cyp79b2/b3</i> .....	55
3.3.4.2	Infection of sinapate ester mutants .....	55
3.3.4.3	Coniferin and infection.....	57
3.3.4.4	Lignans and infection .....	60
3.3.5	Relevance of the phenylpropanoid and indole markers for the development of infection symptoms.....	61
3.3.6	Undirected metabolite fingerprinting to find markers involved in symptom development of Arabidopsis challenged with <i>V. longisporum</i> .....	64
<b>3.4</b>	<b>Analysis of hydroxy and dicarboxy fatty acids in the interaction of Arabidopsis and <i>V. longisporum</i> .....</b>	<b>66</b>
3.4.1	Suberin and cutin .....	66
3.4.1.1	Composition of cutin and suberin monomers in infected plants.....	66
3.4.1.2	Infection of suberin mutants with different infection methods .....	67
3.4.2	$\alpha$ -Hydroxy fatty acids .....	69
3.4.2.1	Characterization of T-DNA insertion lines of <i>AtFAH1</i> and <i>AtFAH2</i> .....	69
3.4.2.2	Expression analysis of <i>AtFAH1</i> and <i>AtFAH2</i> by GUS staining .....	71
3.4.2.3	Ceramide and glucosylceramide analysis.....	72
3.4.2.4	Metabolite fingerprinting of the <i>fah1xfah2</i> mutant.....	74
3.4.2.5	Phytohormone analysis in the <i>fah1xfah2</i> mutant .....	76
3.4.2.6	Biotic stress response .....	78
3.4.2.6.1	Infection of <i>fah</i> mutants with powdery mildew ( <i>G. cichoracearum</i> ).....	78
3.4.2.6.2	Infection of the <i>fah1xfah2</i> mutant with <i>V. longisporum</i> .....	79
<b>4</b>	<b>DISCUSSION .....</b>	<b>80</b>
<b>4.1</b>	<b>Undirected metabolite fingerprinting .....</b>	<b>80</b>
4.1.1	Root metabolites .....	81
<b>4.2</b>	<b>Phenylpropanoids .....</b>	<b>82</b>
4.2.1	Sinapate esters in the defense response of Arabidopsis .....	83
4.2.2	Lignin and lignans in the defense response of Arabidopsis .....	84
4.2.3	Monolignols and its glucosides in the defense response of Arabidopsis .....	87
<b>4.3</b>	<b>Indole glucosinolates in the defense response of Arabidopsis.....</b>	<b>89</b>
<b>4.4</b>	<b>Polar metabolites involved in symptom development .....</b>	<b>89</b>
<b>4.5</b>	<b>Cutin and suberin.....</b>	<b>91</b>
<b>4.6</b>	<b>Sphingolipids.....</b>	<b>92</b>
4.6.1	Changes in sphingolipid metabolism of the <i>fah1xfah2</i> mutant.....	92
4.6.2	Growth phenotype of <i>fah1xfah2</i> plants.....	93
4.6.3	Response of the <i>fah1xfah2</i> mutant to infection with different fungi.....	95
<b>5</b>	<b>SUMMARY .....</b>	<b>97</b>
<b>6</b>	<b>REFERENCES .....</b>	<b>99</b>
<b>7</b>	<b>ABBREVIATIONS .....</b>	<b>113</b>

---

<b>8</b>	<b>APPENDIX .....</b>	<b>116</b>
8.1	Infection markers detected by metabolite fingerprinting analyses .....	116
8.2	Quantification of infection markers of root dip infected plants .....	118
8.3	Mutants examined in infections with <i>V. longisporum</i> .....	119
8.4	Infection of the <i>cyp79b2/b3</i> mutant with <i>V. longisporum</i> .....	120
8.5	Infection and metabolite analysis of sinapate ester mutants.....	121
8.6	Infection of C4H:F5H plants with <i>V. longisporum</i> .....	123
8.7	Lignans in the infection with <i>V. longisporum</i> .....	124
8.8	Infection of JA mutants with <i>V. longisporum</i> .....	125
8.9	Determination of ceramides and glucosylceramides in the <i>fah</i> mutants.....	127

# 1 Introduction

As sessile organisms, plants have to cope with different biotic and abiotic stress situations. To defend themselves against pathogens, they developed different strategies which reach from preformed barriers to systemic resistance. In the field, productivity as well as quality is often affected by these interactions. Therefore knowledge about mechanisms that confer to resistance in plants is important for breeding and establishment of resistant genetically modified plants. The following work focuses on metabolites involved in plant pathogen interactions. The model plant *Arabidopsis thaliana* is used to determine metabolic reactions in response to the root pathogen *Verticillium longisporum*.

## 1.1 Plant defense responses

Plant pathogens can be divided into different categories based on their infection behavior. Biotrophic pathogens like *Golovinomyces cichoracearum* need the living cell to feed and grow (Vogel & Somerville, 2000). In contrast to this, necrotrophic pathogens like for example *Botrytis cinerea* kill their host cells and feed from the remaining dead tissue. To induce cell death they excrete phytotoxic metabolites and induce oxidative burst (van Kan, 2006). Some pathogens cannot be grouped into one of these categories because they act as both: biotrophs and necrotrophs. The behavior of these so called hemibiotrophs is dependent on their life cycle or the outer conditions (Glazebrook, 2005). One example for hemibiotrophic pathogens are the *Verticillium* species on which this work is focused (Fradin & Thomma, 2006).

Plants evolved various defense strategies to cope with invading pathogens. Some of them are constitutively activated and some of them are induced upon infection. The first barrier against invading pathogens is the cuticle of the leaf and fruit epidermis, or the suberin layer of the exo- and endodermis of the roots (Kolattukudy, 2001). Both are structural related polymers which consist of unpolar fatty acid derivatives (reviewed in Pollard et al, 2008). Their synthesis and function will be further described in section 1.5. One strategy of pathogens to overcome this barrier is the excretion of degrading enzymes, which hydrolyze the polymer, for example cutinases excreted by *Fusarium* species (Kolattukudy, 2001). Other strategies to overcome the barrier are the penetration through wounds or stomata or the formation of appressoria (Howard et al, 1991; Melotto et al, 2008).

Next to this barrier, plants deposit different antimicrobial metabolites during normal growth. These preformed defense metabolites are called phytoanticipins (VanEtten et al,

1994). They are usually stored in specialized cells and tissues or lay in vacuoles and organelles (Bednarek & Osbourn, 2009; Morrissey & Osbourn, 1999). One prominent example are the glucosinolates ( $\beta$ -thioglucoside-N-hydroxysulfates) of the *Brassicaceae* including *Arabidopsis*. Upon tissue damage, the glucosinolates get in contact with myrosinases ( $\beta$ -thioglucosidases), which hydrolyze them to different toxic products like isothiocyanates, nitriles and thiocyanates (Fahey et al, 2001). Three major groups of glucosinolates based on the origin of the side chain are known in *Arabidopsis*: indole glucosinolates (tryptophan derived side chain), aliphatic glucosinolates (methionine derived side chain) and aromatic glucosinolates (phenylalanine derived side chain). They are involved in defense against feeding insects, but also antimicrobial activity is described (Bednarek et al, 2009; Clay et al, 2009).

Antimicrobial secondary metabolites can also be synthesized *de novo* in response to infection. These metabolites are called phytoalexins and are part of the induced defense response of the plant (Hammerschmidt, 1999; VanEtten et al, 1994). In *Arabidopsis* camalexin, which derives from the indole pathway, is known as the characteristic phytoalexin. Its synthesis is induced by a variety of pathogens but it does not lead to resistance against all of them (Glawischnig, 2007).

For the induction of a defense response, plants are able to detect pathogen associated molecular patterns (PAMPs) or pathogen delivered effectors with special receptors and proteins (reviewed in Jones & Dangl, 2006). Whereas PAMPs elicit a rather unspecific answer, the response to effectors is more specific, faster and stronger. First a local response, which is restricted to the infected and surrounding cells, is activated. It is accompanied by oxidative burst, hypersensitive reaction (HR) and the synthesis of phytoalexins. Additionally, the cell wall in the surrounding tissue is reinforced by callose deposition, stronger lignification and embedding of phenylpropanoids in the cell wall (Dixon et al, 1994; Lamb & Dixon, 1997; Nürnberger & Lipka, 2005). Biosynthesis and function of phenylpropanoids and lignin involved in defense are further described in section 1.4. All these reactions are important to capture and kill the pathogens in the infected cells and to hinder the outspread into the neighboring cells by strengthening the cell wall. Next to the local resistance plants can evolve a systemic resistance which is based on a signal that is transferred through the plant. It confers long lasting resistance to a wide range of microorganisms. The inducer of this so-called systemic acquired resistance (SAR) is the phytohormone salicylic acid (SA), which is activated by HR or by the infection itself (Durrant & Dong, 2004). SAR is based on changes in gene expression and leads to further synthesis of phytoalexins and pathogenesis related proteins (PR proteins), which are described to have antimicrobial activity (van Loon et al, 2006).

SAR is defined to be the form of resistance especially against biotrophic microorganisms because cell death is induced (reviewed in Glazebrook, 2005). Responses to necrotrophic fungi especially involve jasmonic acid (JA) and ethylene as plant hormones which induce defense related gene expression.

## 1.2 *Verticillium* species

*Verticillium* species are soil borne fungi which cause vascular diseases in various plant species in the moderate and subtropic climate (Pegg & Brady, 2002). They belong to the phylum of the Ascomycota. In the genus *Verticillium* six plant pathogenic species are included (Barbara & Clewes, 2003) of which *V. dahliae* and *V. albo-atrum* are the most wide spread and best studied species. The host range of especially *V. dahliae* is rather broad and includes many important crop plants like sunflower, cotton, potato and tomato but also trees and woody plants are infected by the fungus. Infection symptoms in these plants are quite variable and include growth depression, wilt, chlorosis and necrosis as well as brown coloration of the vascular tissue (Beckman, 1987).

### 1.2.1 *Verticillium longisporum*

The introduction of *V. longisporum* as new species in the phylum *Verticillium* was controversially discussed in the beginning. Karapapa et al (1997) proposed it as a new species based on molecular and morphological differences and suggested it to be a hybrid of *V. dahliae* and *V. albo-atrum*. Later it was shown that indeed the spores are nearly twice as long as in *V. dahliae* species and that the morphology of the microsclerotia differs (Zeise & von Tiedemann, 2001). Additionally, the DNA content was estimated to be 1.75 times the one of *V. dahliae*, suggesting *V. longisporum* to be a parasexual hybrid. Phylogenetic studies based on seven nuclear loci recently showed that *V. longisporum* may have evolved in different ways (Inderbitzin et al, 2011). Here the authors discuss that it originated three times in independent hybridization events. All hybrids share one common parent of a so far unknown taxon that hybridized with *V. dahliae* lineage D2 and D3 as well as with an additional species of unknown taxon.

*V. longisporum* not only differs in its morphology and molecular pattern but also in its host range from *V. dahliae*. The main hosts of this species are cruciferous plants which are not infected by *V. dahliae* (Zeise & von Tiedemann, 2002; Zhou et al, 2006). *V. longisporum* is an important pathogen in oilseed rape cultivation in Northern Europe (Dunker et al, 2008; Johansson et al, 2006a). The yield depression can be expected between 10 - 50 % based on soil and climatic conditions (Dunker et al, 2008). Symptoms caused in the field are chlorosis and necrosis of lateral branches and leaves, brown coloration of the stems and

premature ripening, but no wilting. The symptoms of infection are lately visible and can be easily mixed up with symptoms of senescence or of infection by other fungi (Dunker et al, 2008). One problem of this disease are the long lasting microsclerotia in the soil which cannot be diminished. Different strategies to reduce the fungal inoculums like chemical fumigation, solarisation or crop rotation are all rather ineffective (Fradin & Thomma, 2006). Another problem is that there are no fungicides available once the plants are infected as well as yet no resistant cultivars are on the market (Rygulla et al, 2007). There are different efforts in the resynthesis of resistant plants by interspecific hybridization of *Brassica rapa* and *Brassica oleracea*. In *B. oleracea* different lines are known to be resistant against *V. longisporum*, which are therefore promising candidates for hybridization (Rygulla et al, 2007).

### **1.2.2 Infection cycle**

The infection cycle of *V. dahliae* and *V. longisporum* is quite comparable (Johansson et al, 2006a). As already described, these pathogens possess a hemibiotrophic life cycle (Fig. 1). It starts with microsclerotia which are abundant in contaminated soils and can rest there for many years (Wilhelm, 1955). The microsclerotia are dark melanized thick-walled hyphae which are stimulated to germinate by root exudates (Mol et al, 1995). After germination *V. longisporum* hyphae get in contact with the root hairs and generate a hyphal network (Eynck et al, 2007). The hyphae enter the roots through the junction of epidermal cells or directly grow into the cells. Afterwards they grow inter- and intracellular to the central cylinder where they have to pass the endodermis (Eynck et al, 2007). It is proposed that the infection takes place in young parts of the roots where no endodermis is developed yet or at sides of damage of this barrier (Bishop & Cooper, 1983; Pegg & Brady, 2002). After entering the xylem, the fungus stays most of its life cycle in this nutrient poor environment. It spreads through the plant by generating conidia which are transported upwards with the xylem stream in the plant. These spores can be trapped at the end of vessel cells where they germinate and invade the neighboring vessels (Bishop & Cooper, 1983). In contrast to *V. dahliae*, *V. longisporum* is restricted to individual vessels, which may be the cause of the absence of wilting symptoms in these infections (Eynck et al, 2007). After the plant becomes senescent, the fungus spreads from the xylem into the whole tissue. At this point the necrotrophic or saprophytic phase starts. In the dead plant tissue the fungus forms new microsclerotia which find their way back into the soil with the plant debris.

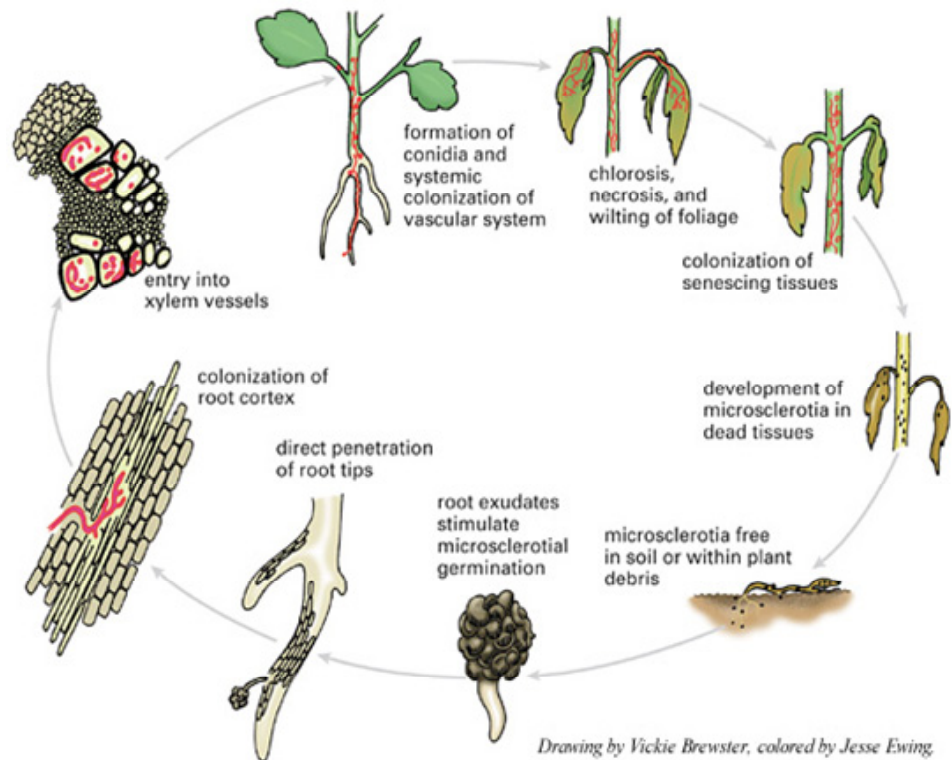


**Fig. 1: Infection cycle of *Verticillium* species** (from Berlinger & Powelson, 2000)

### 1.2.3 Plant defense in response to *Verticillium* infection

The knowledge about resistance mechanisms in plants in answer to *V. longisporum* infection is scarce. More is known in relation to *V. dahliae* infections. Two different levels of resistance are described here: One in the prevascular phase where the fungus grows in the root cortex but is not able to grow further into the vascular system (Eynck et al, 2007; Talboys, 1972). Here the endodermis as well as quick deposition of lignin in the surrounding tissue might act as barriers against further outspread of the fungus (Griffiths, 1971; Talboys, 1972).

Resistance in the vascular phase is described by rapid deposition of suberin and other xylem coating material (Lee et al, 1992; Lulai, 2005; Robb et al, 1991). Additionally the vessels may be occluded by gels, gums or other deposits (Pegg & Brady, 2002). Both mechanisms lead to lowering the outspread of the fungus to the neighboring vessels. Also induction of PR proteins and phytoalexins like elemental sulfur and phenolic compounds are described to diminish fungal growth (Benhamou, 1995; Gayoso et al, 2010; Talboys, 1972; Tjamos et al, 2005; Williams et al, 2002).

In the *V. longisporum* - *Brassica napus* interaction some responses, similar to the ones described for *V. dahliae* in different plants, were described. Deposition of phenolic compounds and generation of vessel occlusions were shown in *B. napus* response to

*V. longisporum* infection (Eynck et al, 2009). A resistant and a non-resistant cultivar were analyzed showing that the induction of phenolic compounds is correlated with disease severity and with less amounts of *V. longisporum*-DNA (VL-DNA) in the plants. Another study concerning the plants answer to *V. longisporum* infection showed that SA and its glucoside are enriched in infected xylem sap of root and hypocotyls of *B. napus* plants (Ratzinger et al, 2009). Floerl et al (2008) could show that different proteins are induced in the apoplast of infected *B. napus* plants. Some of those proteins were identified: an endochitinase, a peroxidase, a PR-4 protein, and a  $\alpha$ -1,3-glucanase. Additionally it could be shown that xylem sap from infected plants lead to reduction in fungal growth.

Because the work with the model plant *Arabidopsis* provides many advantages, *V. longisporum* infection was also studied in this species. Different publications showed that it is a suitable host to study the *V. longisporum* pathosystem (Floerl et al, 2010; Häffner et al, 2010; Johansson et al, 2006b). In *Arabidopsis* infection leads to stunting of the leaves, comparable to the stunting of the stem of *B. napus* plants in the greenhouse. At later stages chlorosis and necrosis of the leaves occur. It was already investigated that these symptoms are not related to water or nutrient depletion (Floerl et al, 2010). In this thesis *Arabidopsis* was used as host to study the interaction on the metabolic level.

### 1.3 Preliminary data generated by metabolite fingerprinting

This thesis is based on unpublished preliminary data generated by Dr. Kirstin Feussner (Göttingen). Undirected metabolite fingerprinting using UPLC-MS(TOF) was performed to analyze the differences in the metabolites of control and *V. longisporum* infected *Arabidopsis* leaves. Two major classes of metabolites that were affected in response to the infection could be identified in this analysis (Tab. 1). In the polar phase of extraction phenylpropanoids especially sinapate esters were detected to accumulate at early time points of infection (10 days post infection (dpi)). In the non-polar phase different long chain and very long chain fatty acid derivatives (dicarboxy fatty acids and hydroxy fatty acids) were found to be affected in response to the infection. Based on their structure it was deduced that these fatty acid derivatives may derive from cutin or suberin because all of them could be part of these polymers. In addition the detected  $\alpha$ -hydroxy fatty acids could also be part of sphingolipids.

All three different metabolite classes will be further analyzed in this thesis. Their biosynthesis and their putative function in plant pathogen interactions will be described in the following parts of the introduction.

**Tab. 1: Markers identified by undirected metabolite fingerprinting of control and infected *Arabidopsis* leaves.**

Leaves of 10 dpi and 35 dpi control and *V. longisporum* infected plants were extracted by two phase partitioning. Samples were measured by UPLC-MS(TOF) and metabolites that differ in their amounts between those samples were identified. In the polar phase of infection phenylpropanoids were detected and in the non-polar phase fatty acid derivatives were found to be affected. ↑: higher intensity in infected plants, ↓: lower intensity in infected plants.

compound	10 dpi	35 dpi
1-O-sinapoyl-β-D-glucose	↑	↑
1,2-bis-O-sinapoyl-β-D-glucose	↑	↑
sinapic acid		↑

compound	10 dpi	35 dpi
<b>α,ω-dicarboxylic acids</b>		
docosanedioic acid	↓	↑
tetracosanedioic acid	↓	↑
<b>hydroxy fatty acids</b>		
hydroxy tricosanoic acid		↑
hydroxy tetracosanoic acid	↓	↑
hydroxy tetracosenoic acid		↑
hydroxy pentacosanoic acid		↑
hydroxy pentacosenoic acid		↑
hydroxy hexacosanoic acid		↑
hydroxy hexacosenoic acid		↑
hydroxy dotriacontanoic acid		↑
<b>α-hydroxy fatty acids</b>		
α-hydroxy palmitic acid		↑
α-hydroxy docosanoic acid		↑

## 1.4 Phenylpropanoids

### 1.4.1 General biosynthesis of phenylpropanoids

The biosynthetic group of phenylpropanoids contains lignin, flavonoids and cinnamic acid conjugates which are all ubiquitously found in higher plants. Also in the synthesis of mixed polymers like suberin and cutin this pathway is involved.

Fig. 2 shows the core phenylpropanoid pathway in *Arabidopsis* from which all specific metabolic groups are synthesized (reviewed in Boerjan et al, 2003; Davin et al, 2008; Vanholme et al, 2010; Vogt, 2010). The pathway starts with phenylalanine that derives from the shikimate pathway. Phenylalanine is converted to cinnamic acid by the phenylalanine ammonia lyase (PAL) which catalyses the deamination of this amino acid. The reaction is one branch point between secondary and primary metabolism. Cinnamic acid may be further hydroxylated and methylated on the aromatic ring. The traditional view of this pathway describes these reactions on the level of free hydroxy cinnamic acid (Fig. 2, horizontal upper pathway in grey). But recent studies verified that 3-hydroxylation

and -methylation is preferentially catalyzed on the level of the shikimate and coenzyme A (CoA) conjugates and the 5-hydroxylation and -methylation on the level of hydroxycinnamoyl aldehydes and alcohols (Fig.2) (reviewed in Humphreys & Chapple, 2002). Furthermore it was shown that the synthesis of ferulic acid and sinapic acid derives from the activity of a hydroxycinnamaldehyde dehydrogenase (HCALDH) which converts coniferyl aldehyde and sinapyl aldehyde back to ferulic and sinapic acid (Nair et al, 2004). The rate limiting step for this pathway is the reaction of the cinnamate-4-hydroxylase (C4H), which provides carbon sources for all end products of the pathway. For the entry to guaiacyl and syringyl lignin the cinnamate-3-hydroxylase (C3'H) catalyses the rate limiting step (Davin et al, 2008). The final products deriving from this pathway (Fig. 2, in blue) and their functions in the plant are addressed in the following part.

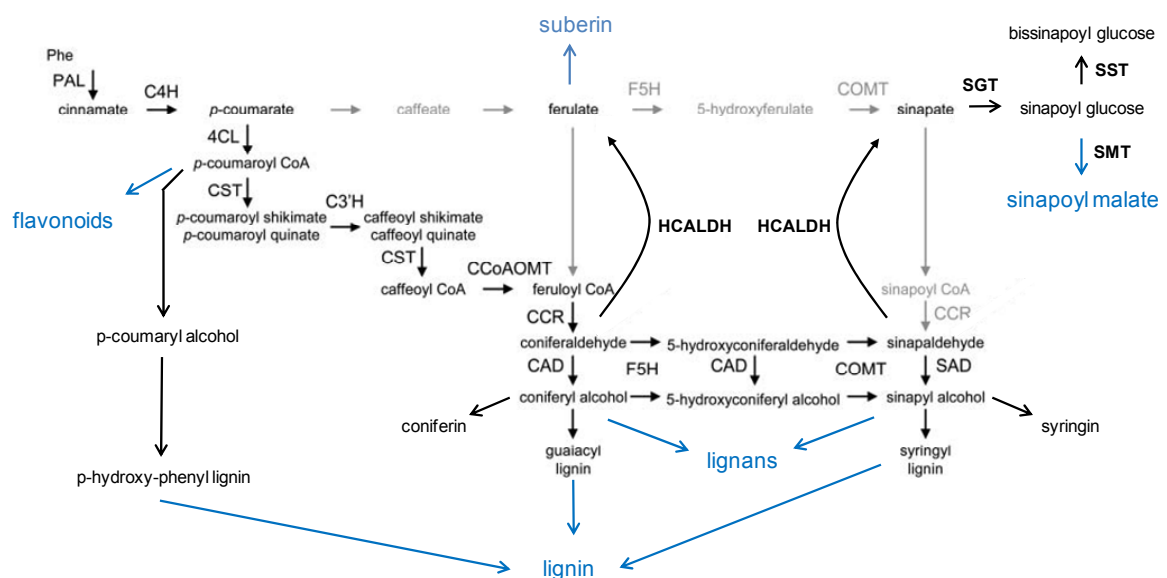


**Fig. 2: Phenylpropanoid pathway in Arabidopsis (modified from Nair et al, 2004).**

The upper horizontal pathway shows the previous view of the biosynthesis of monolignols and sinapate esters (in grey) and the revised version is shown below in black. Terminal metabolites deriving from this pathway are marked in blue. Involved enzymes with abbreviations: caffeoyl CoA O-methyltransferase (CCoAOMT), cinnamate-4-hydroxylase (C4H), (hydroxy)cinnamyl alcohol dehydrogenase (CAD), (hydroxy)cinnamoyl CoA reductase (CCR), p-coumaroyl shikimate/quinic acid 3'-hydroxylase (C3'H), 4-coumarate CoA ligase (4CL), ferulate-5-hydroxylase (F5H), hydroxycinnamoyl CoA:shikimate/quinic acid hydroxycinnamoyltransferase (CST), phenylalanine ammonia-lyase (PAL), caffeic acid/5-hydroxyferulic acid O-methyltransferase (COMT), sinapyl alcohol dehydrogenase (SAD), UDP glucose:sinapic acid glucosyltransferase (SGT), sinapoyl glucose:malate sinapoyltransferase (SMT), sinapoyl glucose:sinapoyl glucose sinapoyltransferase (SST), hydroxycinnamaldehyde dehydrogenase (HCALDH).

### 1.4.2 Flavonoids

Flavonoids derive from *p*-coumarate and are synthesized by the chalcone synthase (CHS), the initial enzyme of the flavonoid biosynthesis. It catalyses the condensation of malonyl-CoA with *p*-coumaryl-CoA in a series of decarboxylation, condensation and cyclization reactions (Jez et al, 2002). The further conversion of the CHS product in the flavonoid pathway yields flavones, isoflavones, flavanones and anthocyanins. Due to different modifications of the core structure a large variety of these metabolites exist in several plant species.

One function of flavonoids is the protection of the plant against UV light. Their synthesis is induced upon UV-B light exposure and mutants with reduced amounts of flavonoids are more susceptible against this treatment (Landry, 1995). But this function seems not only be due to the strong absorption in the UV-B wavelength of these metabolites but also to their antioxidative capacity (Dixon & Paiva, 1995).

Flavonoids also have an important function in plant defense against pathogens. They can be found in different plant species and have a widespread ability to inhibit spore germination of various plant pathogens (reviewed in Harborne & Williams, 2000). One example are the antifungal isoflavonoids from legumes like kievitone, pisatin and maackiain (Morrissey & Osbourn, 1999). In addition antifungal activity of different flavonoids like hesperitin, flavones, kaempferol and genistein against *V. albo-atrum* was shown in *in vitro* tests (Picman et al, 1995). In *Arabidopsis* the response of flavonoid genes to infection is comparably weak which might be due to the development of indole phytoalexins in this species (Naoumkina et al, 2010)

### 1.4.3 Lignin and lignans

Lignin derives from the monolignols coniferyl alcohol, sinapyl alcohol and *p*-coumaryl alcohol (Fig. 3). They are transported to the cell wall where they undergo oxidative polymerization. The dehydrogenation of the monolignols to phenolic radicals is catalyzed by peroxidases or laccases. The resulting radicals are coupled to form a dimer which is further connected to the next monomer. The mechanism of this coupling is still controversially discussed. Davin & Lewis (2005) predicted the guidance of this reaction by proteins harboring dirigent sides for controlled coupling. Boerjan et al (2003) and Vanholme et al (2010) preferred on the other hand the theory of non-enzymatic random coupling which might be dependent on the chemical nature of the monolignols and the conditions of the cell walls (Vanholme et al, 2010). The lignin monomer composition is not equally in all tissues. Xylem vessel lignin consists primarily of coniferyl alcohol derived guaiacyl lignin units whereas the secondary cell wall of fibers predominantly harbors lignin

with syringyl lignin units which derive from sinapyl alcohol (Boerjan et al, 2003; Davin & Lewis, 2005).

Lignin is an important polymer not only for normal development but also in plant defense reactions. It makes the cell wall more resistant against mechanical pressure applied during fungal penetration and also less accessible against cell wall degrading enzymes (Bechinger et al, 1999). Specific lignin accumulation upon infection is described in different plant-pathogen interactions (de Ascensao & Dubery, 2003; Hano et al, 2006; Menden et al, 2007; Wuyts et al, 2006). But not only as mechanical barrier, also a possible role of lignin and the precursors in chemical defense is proposed (Naoumkina et al, 2010).

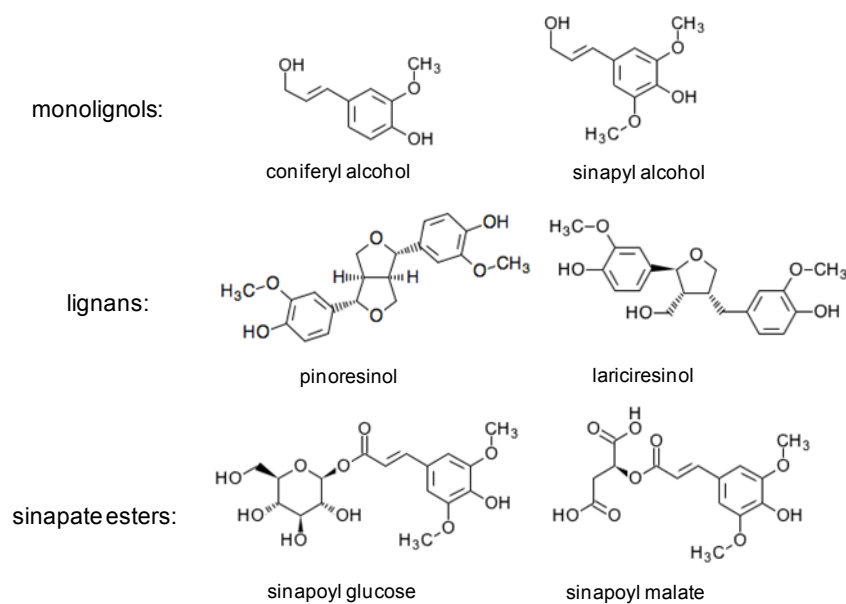


**Fig. 3: Structures of selected phenylpropanoid metabolites.**

The biosynthesis of lignans is closely related to the one of lignin. Lignans are dimers of monolignols and can be found in a large variety in different plant species (Fig. 3). One common pathway for the initial synthesis exists (reviewed in Davin et al, 2008): Two coniferyl alcohol molecules are connected with the help of peroxidases and laccases in a similar manner like in lignin synthesis. But in this case dirigent proteins (DIR) responsible for stereospecific coupling are involved which have been first described in *Forsythia* cell culture (Umezawa et al, 1990). Recently, also in *Arabidopsis* the activity of one of its 25 putative DIR genes was described (Pickel et al, 2010). The resulting product of this coupling is pinoresinol. It is further reduced by pinoresinol reductases (PR) to lariciresinol and further to secoisolariciresinol and mateiresinol. Lignans received much attention because of their health promoting effects in humans, like reduction of the risk of certain

cancers and cardiovascular diseases (reviewed in Adlercreutz, 2007). The primary role of lignans in plants is described mainly in defense against pathogens. Several known lignans are tested *in vitro* to have antibacterial and antifungal activity (Akiyama et al, 2007; Carpinella et al, 2003; Carpinella et al, 2005). Lignan depositions in heartwood of western red cedar not only serve to shut off non-productive water and nutrient transport but also to reinforce the resistance to wood rotting fungi. Also *de novo* formation upon fungal attack is described (Gang et al, 1999).

#### **1.4.4 Sinapate esters**

Sinapate esters are a unique metabolic group of the *Brassicaceae* (reviewed in Milkowski & Strack, 2010). They are synthesized from sinapic acid which is glucosylated by UDP-glucose glucosyltransferases. The resulting sinapoyl glucose serves as energy rich substrate for the synthesis of sinapoyl malate and of minor amounts of bis-sinapoyl glucose in the leaves and sinapoyl choline in the seeds. Involved enzymes in the leaves are the sinapoyl glucose:malate sinapoyltransferase (SMT) and the sinapoyl glucose:sinapoyl glucose sinapoyltransferase (SST) (Fraser et al, 2007; Lehfeldt et al, 2000; Lorenzen et al, 1996). Sinapoyl malate is highly concentrated in leaves of *Arabidopsis* and serves as UV-B light protective substance in the leaves (Landry, 1995). A distinct role in plant defense has not been described so far.

### **1.5 Suberin and cutin**

#### **1.5.1 Structure of cutin and suberin**

Suberin and cutin are biopolymers which both form a barrier from the plant to the environment. Cutin can be found in the cuticle, which consists of epicuticular waxes that are encrusted in the polymer matrix of cutin (Kunst & Samuels, 2003). This layer is deposited at the outer part of the epidermal cell wall and protects leaves and fruits from uncontrolled water loss, UV radiation and mechanical damage by phytopathogens and herbivory insects (Nawrath, 2006). Cutin is composed mainly of C16 and C18  $\omega$ -hydroxy fatty acids which can harbor additional mid chain hydroxy and epoxy groups. Also glycerol and small amounts of phenolics can be found. The cutin composition in *Arabidopsis* differs from this general description in some respect. It more resembles the composition of suberin. The predominant monomers in this species are  $\alpha,\omega$ -dicarboxylic fatty acids of C16 and C18 length (Franke et al, 2005, Bonaventure et al, 2004) and additionally  $\alpha$ -hydroxy fatty acids and fatty acids can be found (Franke et al, 2005).

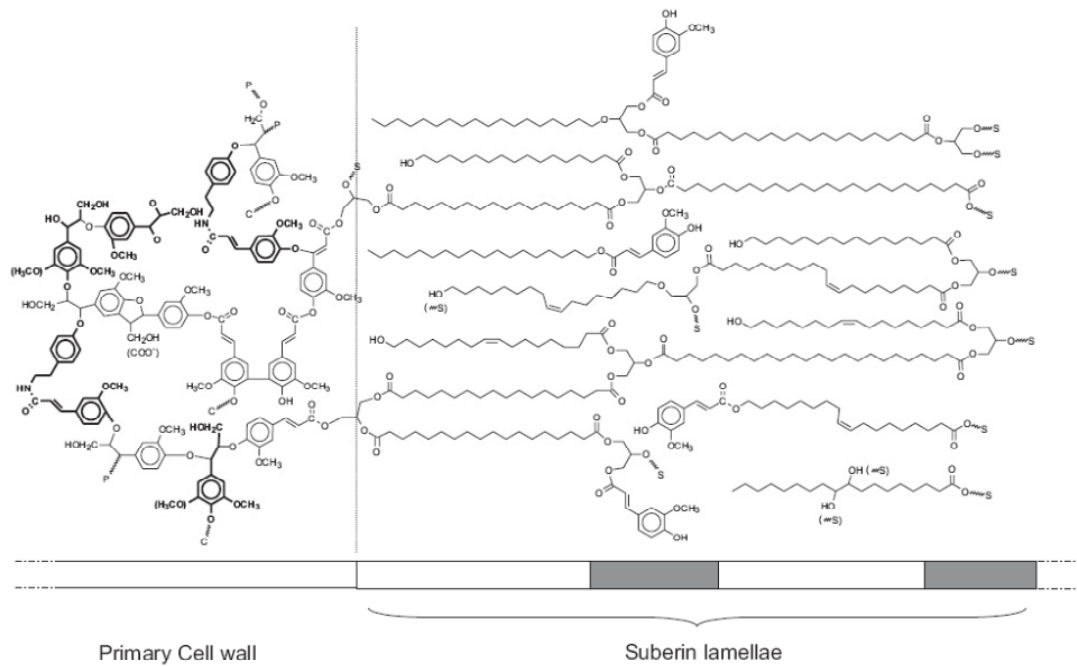


**Fig. 4: Hypothetical structure of suberin** (from Bernards et al 2002).

Suberin can be found in the roots of the plants. It is deposited in the peridermis, hypodermis and exodermis as well as in the casparian strips of the endodermis (Kolattukudy, 2001). Suberin is a barrier against uncontrolled water, solute and mineral transport as well as protection against opportunistic pathogen invasion. It is also formed in response to wounding and pathogen attack (Baxter et al, 2009; Nawrath, 2002). Being a more complex polymer than cutin, suberin consists of a polyaromatic domain build by phenylpropanoids (especially ferulic acid) and a polyaliphatic domain build by fatty acids and derivatives (Fig. 4) (Bernards, 2002). The main monomers in aliphatic suberin are  $\omega$ -hydroxy fatty acids and  $\alpha,\omega$ -dicarboxylic fatty acids in chain length of C16-C26 as well as glycerol. In addition fatty alcohols, unsubstituted fatty acids and  $\alpha$ -hydroxy fatty acids can be found (Franke et al, 2005).

The linkage of the monomers is not fully elucidated yet in both polymers. It is known that they are mainly connected by primary alcohol ester linkages and that ester linkages to mid chain hydroxyl groups form branches or cross links in the polymer (Li-Beisson, 2011). In suberin the aliphatic polymer is attached by an polyaromatic domain which forms the link to the primary cell wall (Fig. 4) (Bernards, 2002; Graça & Santos, 2007).

### 1.5.2 Enzymes involved in cutin and suberin monomer biosynthesis

Enzymes involved in cutin and suberin monomer formation derive from the same families for both polymers (reviewed in Li-Beisson, 2011). Much research has been done on this topic throughout the last years.

The long chain acyl CoA synthases (LACS) LACS 1 and 2 activate fatty acids to acyl-CoA esters in the cutin monomer synthesis (Schnurr et al, 2004). For very long chain fatty acid monomers (C20-C24) additional elongation steps by 3-ketoacyl-CoA synthase genes occurs (Franke et al, 2009; Lee et al, 2009). The CYP86 family is involved in the  $\omega$ -hydroxylation of the fatty acids (Compagnon et al, 2009; Höfer et al, 2008; Xiao et al, 2004) and for the following dehydrogenation step to the dicarboxy fatty acids one putative candidate was described by Kurdyukov et al (2006b). This so-called *hothead* mutant is deficient in its ability to oxidize long chain  $\omega$ -hydroxy fatty acids leading to a decrease in  $\alpha,\omega$ -dicarboxy fatty acids. Finally also glycerol phosphate acyltransferases (GPAT) were shown to be involved in the synthesis of cutin (GPAT4, 6 and 8, Li et al, 2007) and of suberin (GPAT5, Beisson et al, 2007). Most of the involved enzymes were identified by the analysis of mutants which showed a reduced amount of cutin or suberin monomers or a change in the composition of these monomers. In which order the enzymes act to generate  $\omega$ -oxidized acylglycerols is not known so far (Pollard et al, 2008).

For the transport of the monomers across the plasma membrane and the cell wall and the following polymerization not much is known up to now. One ABC transporter involved in this process has been identified (Bird et al, 2007) and some candidate proteins are assumed to play a role in polymerization, like GDSL-motif carboxylesterases and lipase-like proteins of the family of BODYGUARD (BDG) (Kurdyukov et al, 2006a; Suh et al, 2005).

### 1.5.3 Involvement in plant-pathogen interactions

As described above suberin and the cuticle act as passive defense and first barrier against pathogens. But different studies showed that they also have additional functions. Cuticle components for example serve as signals for pathogens to recognize their host. In *Fusarium solani*  $\omega$ -hydroxy fatty acids from cutin trigger the expression of the cutinase gene in the germinating fungus, which leads to the liberation of more cutin monomers (Woloshuk & Kolattukudy, 1986). The importance of this induction of cutinase expression by cutin monomers and the induction of appressoria formation by these monomers was also described for *Magnaporthe griseae* and *Erysiphe graminis* (Francis et al, 1996; Gilbert et al, 1996).

Changes in susceptibility to various pathogens were shown in different cutin mutants. Mutants with perturbed cuticle (*lasc2*, *bdg* or CUTE (cutinase expressing plants)) were shown to be more resistant against *B. cinerea* (Bessire et al, 2007). This resistance is probably due to the release of fungitoxic compounds through the damaged cuticle in these mutants. Also faster elicitor diffusion through the cuticle leading to stronger defense gene expression was discussed (Bessire et al, 2007; Chassot et al, 2007; Tang et al, 2007). In contrast to this, the double mutant *gpat4/gpat8* with also a strong reduction in cutin monomers shows enhanced susceptibility towards the necrotrophic fungi *Alternaria brassicola* (Li et al, 2007). Also in infections with *Pseudomonas syringae* a higher susceptibility of cutin mutants was found. *Lacs2* and *cyp86a2* plants, which have both less than 30% residual cutin, show enhanced susceptibility to this pathogen (Tang et al, 2007; Xiao et al, 2004). It was discussed that the cuticle of this mutant is probably more permeable for the host factor leading to stronger elicitation of *P. syringae* genes (Tang et al, 2007), or that the increased water flow in the stomatal chamber where the pathogen invades, increases the growth of the pathogen.

Further support exists that also cutin monomers itself act as signal substances which can be perceived by the plant cell to induce defense responses (Park et al, 2008; Schweizer et al, 1996). Park et al (2008) could show that the cutin monomer 16-hydroxy palmitic acid induces synthesis of glycine rich proteins, the expression of PR-genes and of accumulation of H<sub>2</sub>O<sub>2</sub> in Arabidopsis leaves. All these examples show that the interaction of pathogens with the cuticle is rather complex and could be an important process during infection.

For suberin such detailed infection studies with mutants are not available. But different examples show the implication of suberin in plant pathogens interaction. Lee et al (1992) could show that tomato plants resistant to infection with *V. albo-atrum* show more and rapid suberin coating in the xylem than the susceptible line. This situation was also shown in *Phytophthora sojae* infected soybean lines (Ranathunge et al, 2008).

## 1.6 Sphingolipids

Sphingolipids are a ubiquitous class of lipids and membrane components of eukaryotic and some prokaryotic cells. Plant sphingolipids can be divided into four different classes: ceramides, glucosylceramides, inositolphosphoryl ceramides (IPC) and free long chain bases (LCB) (Fig. 5) (Pata et al, 2010). LCBs are the basic building block of the more complex ceramides. They have predominantly a chain length of 18 C atoms, are hydroxylated at C-1 and C-3 and have an amino group at C-2. An additional hydroxy group can be introduced at C-4. Also desaturation in position  $\Delta 4$  and  $\Delta 8$  is possible. A

ceramide is formed by N-acylation of the LCB. The fatty acid can have various chain lengths from C16 to C26 and can be  $\alpha$ -hydroxylated. The ceramide can be further attached to a polar head group at the hydroxyl group of the LCB in C-1 position to form complex sphingolipids. Depending of the head group, glucosylceramides and inositolphosphoryl ceramides are the products. The different modifications in the molecules like chain length modification, hydroxylation and desaturation yield to at least 168 species in Arabidopsis (Markham & Jaworski, 2007). Also phosphorylated LCB can be found in plants.

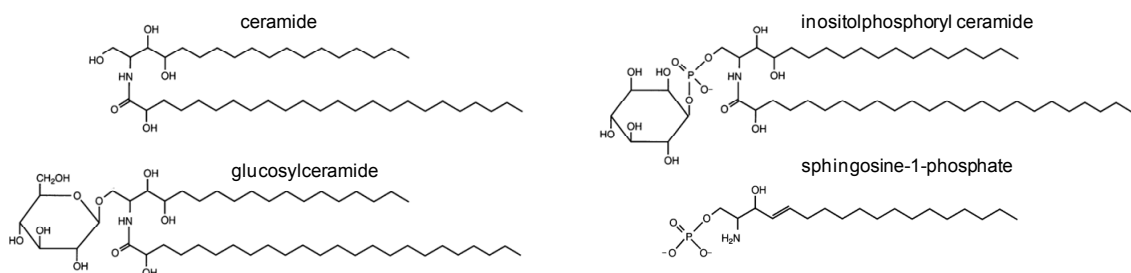


**Fig. 5: Structure of sphingolipids in plants** (modified from Lynch & Dunn, 2004).

Ceramides can be converted to glucosylceramides and inositolphosphoryl ceramides by the attachment of a polar head group to the LCB. Additionally, free LCBs occur in plant cells. They can be also phosphorylated, as it is shown in this example.

### 1.6.1 Biosynthesis of sphingolipids

The biosynthesis (reviewed in Lynch & Dunn, 2004; Sperling & Heinz, 2003) of sphingolipids starts with the synthesis of LCBs by condensation of acyl-CoA with L-serine yielding 3-ketosphinganine (Fig. 6). This first reaction step is catalyzed by the serine palmitoyltransferase and is regarded as the key regulatory step in sphingolipid biosynthesis. The resulting 3-ketosphinganine is further reduced in a NADPH dependent reaction to sphinganine by the 3-ketosphinganine reductase. The sphinganine can be acylated to form ceramides on a CoA dependent (by ceramides synthases) or independent pathway (by ceramidases). The following attachment of a polar head group is accomplished by the glucosylceramide synthase and the IPC synthase. Modifications either at the LCBs or at the fatty acids like hydroxylations or desaturations can occur at different levels of this biosynthesis. Whereas hydroxylation occurs also on free sphinganine, hydroxylation of the fatty acid might occur primary following ceramide synthesis (Lynch & Dunn, 2004). IPC synthase seems to prefer ceramides with  $\alpha$ -hydroxy fatty acid moieties (Bromley et al, 2003).

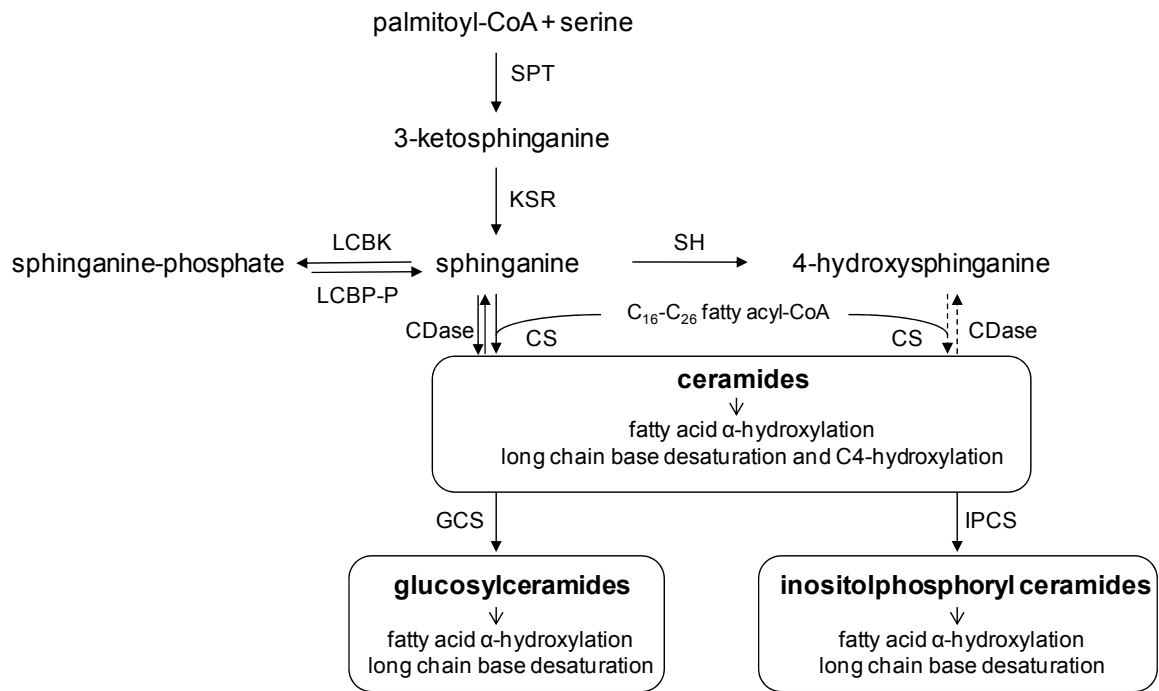


**Fig. 6: Spingolipid biosynthesis in plants** (modified from Pata et al, 2010 and Dunn et al, 2004).

All reactions in plain lines have been demonstrated *in vitro*. The CDase can have also a reverse ceramide synthase activity utilizing free fatty acids as substrate, in contrast to the CS which utilizes fatty acids CoA esters. The substrates for fatty acid  $\alpha$ -hydroxylation and long chain base desaturation still need to be determined. Involved enzymes and abbreviations: serine palmitoyl transferase (SPT), 3-ketosphinganine reductase (KSR), sphinganine-4-hydroxylase (SH), long chain base kinase (LCBK), long chain base phosphate phosphate (LCBP-P), ceramide synthase (CS), ceramidase (CDase), glucosylceramide synthase (GCS), inositolphosphoryl ceramide synthase (IPCS).

### 1.6.2 $\alpha$ -Hydroxylated fatty acids

The role of the  $\alpha$ -hydroxylated fatty acid moiety in *Arabidopsis* is of special interest in this thesis. In *Arabidopsis* two *Fatty Acid Hydroxylase* (*AtFAH1* and 2) genes are known which were detected by database searches. It was shown that both can restore  $\alpha$ -hydroxylase activity in yeast mutants lacking this enzyme activity (Mitchell & Martin, 1997; Nagano et al, 2009). Preferred substrates of the hydroxylase are presumably ceramides and not free fatty acids, although direct data for this assumption are missing (Sperling & Heinz, 2003; Warnecke & Heinz, 2003). For the  $\alpha$ -hydroxylase in *Tetrahymena pyriformis* it was shown that it has indeed a preference for complex sphingolipids and ceramides (Kaya et al, 1984). Additional information about the *Arabidopsis* genes was provided by Nagano et al (2009). They showed that *AtFAH1* and *AtFAH2* interact in plant cells with cytochrome *b5* (*Cytb5*) and this complex further interacts with the cell death suppressor *AtBI-1*. The authors showed that in overexpressor mutants of *AtBI-1* higher amounts of esterified

$\alpha$ -hydroxy fatty acids can be detected in the plants. They assumed that AtBI-1 regulates cell death by interaction with AtFAH resulting in changes in the amount of  $\alpha$ -hydroxylated ceramides. Additionally these authors could show that AtFAH2 is restricted to the ER when expressed in onion cells. The link of the involvement of  $\alpha$ -hydroxylated ceramides in suppression of cell death was also shown by Townley et al (2005). They showed that non-hydroxylated ceramides induce programmed cell death (PCD) in Arabidopsis cells while  $\alpha$ -hydroxylated ceramides do not.

### 1.6.3 Involvement in abiotic and biotic stress

Known functions of sphingolipids are described in the review of Pata et al (2010). Apart from other functions sphingolipids are implicated in abiotic and biotic stress situations. Glucosylceramides are important structural membrane components that increase the stability of the membrane. It was observed that the proportion of glucosylceramides in plasma membranes of freezing-tolerant plants is lower than in freezing-sensitive plants and that the glucosylceramide content is reduced following cold acclimation (Imai et al, 1995; Lynch & Steponkus, 1987). In chilling resistant plants  $\alpha$ -hydroxy monounsaturated very long chain fatty acids in glucosylceramides seems to accumulate (Cahoon et al, 1991; Uemura & Yoshida, 1984) whereas in chilling sensitive plants more saturated  $\alpha$ -hydroxylated fatty acids were found (Imai et al, 1995). Also in drought stress a change in glucosylceramides was reported as well as in aluminum stress. Sensitive cultivars of *Triticum aestivum* showed a decrease of glucosylceramides in response to aluminum exposure whereas the resistant cultivar showed a slight increase (Zhang et al, 1997).

Next to these abiotic stress also implication in pathogen interactions are described in different publications. Two different fungal toxins are known that interfere with sphingolipid metabolism: the AAL-toxin derived from *Alternaria alternata f. sp. lycopersici* and fumonisin B1 (FB1) from *Fusarium verticillioides*. Both are inhibitors of the ceramide synthase leading to increased levels of free LCBs, which further leads to induction of reactive oxygen intermediates (ROI) and to PCD (Shi et al, 2007; Wang et al, 1996). Feeding experiments showed that free LCBs induce ROI production whereas phosphorylated sphinganine blocks ROI production and PCD (Shi et al, 2007). Implication of free LCBs in PCD was also found in the *accelerated cell death 11* mutant (*acd11*) (Brodersen et al, 2002). The mutant is defective in a sphingosine transporter, which leads to PCD and induction of PR genes. Next to the LCBs also ceramides were shown to be involved in PCD. The *acd5* mutant is defective in a ceramide kinase and accumulates its substrates leading to PCD and to increased resistance to the biotrophic powdery mildew infection (Liang et al, 2003; Greenberg et al, 2000; Wang et al, 2008). The same was shown for a mutant defective in an IPC synthase leading to ceramide accumulation, PCD

and resistance to powdery mildew (Wang et al, 2008). A specific glucosylceramide of *Magnaporthe grisea* also promotes hypersensitive reaction in rice (Koga et al, 1998). It was shown to be a general elicitor that protects the plant from a variety of diseases (Umemura et al, 2000). All these examples show that sphingolipids can have an important role in plant pathogen interactions especially in the induction of PCD.

## 1.7 Goals of the thesis

Previous data showed that sinapate esters as well as long chain fatty acid derivatives are affected in their amounts in *Arabidopsis* upon *V. longisporum* infection. The aim of this thesis was to identify the roles of these metabolites during the infection.

The first goal was to repeat the undirected approach to verify the obtained data and to find further infection related markers especially in the described pathways. To quantify these metabolites, directed analysis of phenylpropanoids and suberin/cutin monomers were to be established based on methods described in the literature. For functional analysis of the phenylpropanoid pathway mutants, like the *fah1-2* mutant, were to be tested. This mutant is not able to synthesize sinapate and its esters and was to be used to test the importance of these compounds for the outspread of the fungus in the plant. Additionally, identified phenylpropanoids were to be examined *in vitro* for their toxicity on fungal growth to get further information about the function of identified metabolites.

Suberin mutants were to be analyzed in infections, to examine the function of an intact suberin layer in the early infection situation and to test a possible signaling role of those monomers. For the synthesis of  $\alpha$ -hydroxy fatty acids in sphingolipids, no mutants have been described until the beginning of the thesis. Therefore the goal was to analyze T-DNA insertion lines of both genes and to generate double mutant plants. These mutants were also to be further characterized in their sphingolipid profile as well as their behavior in the infection with *V. longisporum*.

## 2 Materials and methods

### 2.1 Materials

#### 2.1.1 Chemicals

<i>chemicals</i>	<i>supplier</i>
Acetonitrile	Fisher Scientific, Schwerte, Germany
Agar	Duchefa Biochemie, Haarlem, The Netherlands
Agarose	Invitrogen, Karlsruhe, Germany
Carbenicillin	Duchefa Biochemie, Haarlem, The Netherlands
Ceramide standards	Avanti Polar Lipids, Inc., Alabaster, USA
Hexane (HPLC grade)	Acros, Geel, Belgium
Hydroxy fatty acid standards	Matreya, Pleasant Gap, USA
Hygromycin	Invitrogen, Karlsruhe, Germany
Kanamycin	Duchefa Biochemie, Haarlem, The Netherlands
Lignan standards	Phytolab, Vestenbergsgreuth, Germany
Methanol (HPLC grade)	Acros, Geel, Belgium
Murashige & Skoog medium	Duchefa Biochemie, Haarlem, The Netherlands
BASTA	Bayer Cropscience, Monheim, Germany
Wuxal	Aglucon, Düsseldorf, Germany

All other chemicals were obtained from Roth (Karlsruhe, Germany), Merck (Darmstadt, Germany), Fluka (Steinheim, Germany) or Sigma (Deisenhofen, Germany).

#### 2.1.2 Enzymes and size markers

<i>enzymes</i>	<i>supplier</i>
DNase I	MBI Fermentas, St. Leon Rot, Germany
GeneRuler 1kb DNA-Ladder	MBI Fermentas, St. Leon Rot, Germany
LR clonase-Mix	Invitrogen, Karlsruhe, Germany
MasterAmp <i>Tfl</i> -DNA-Polymerase	EPICENTRE Biotechnologies, Madison, USA
<i>Phusion</i> High Fidelity DNA-Polymerase	Finnzymes, Espoo, Finland
Restriction endonucleases	MBI Fermentas, St. Leon Rot, Germany
RevertAid H Minus M-MuLV reverse Transcriptase	MBI Fermentas, St. Leon Rot, Germany
$\beta$ -Glucosidase from almonds	Sigma-Aldrich, Steinheim, Germany
T4-DNA-Ligase	MBI Fermentas, St. Leon Rot, Germany
Takara <i>Ex Taq</i> DNA Polymerase	Takara Bio Inc, Madison, USA

### 2.1.3 Kits

<i>kit</i>	<i>supplier</i>
NucleoSpin Extract II Kit	Machery & Nagel, Düren, Germany
NucleoSpin Plasmid Kit	Machery & Nagel, Düren, Germany
ABI Prism BigDye Terminator Cycle Sequencing Ready Reaction Kit	Applied Biosystems, Darmstadt, Germany

### 2.1.4 Equipment

<i>equipment</i>	<i>supplier</i>
Agilent 1100 HPLC system	Agilent, Waldbronn, Germany
Applied Biosystems 3200 hybrid triple quadrupole/linear ion trap mass spectrometer	MDS Sciex, Ontario, Canada
Aquity UPLC BEH SHIELD RP 18 column (1x100 mm, 1.7 µm particle size)	Waters Corporation, Milford, USA
Aquity UPLC system	Waters Corporation, Milford, USA
C18 column (EC 250/2 Nucleosil 120-5)	Macherey & Nagel, Düren, Germany
Capillary HP-5 column (30 m x 0.25 mm, 0.25 µm coating thickness; J & W Scientific).	Agilent, Waldbronn, Germany
Chip ion source TriVersa NanoMate	Advion Biosciences, Ithaca, USA
Climate chambers	YORK Refrigeration, YORK Industriekälte GmbH & Co. KG, Mannheim, Germany
EC 50/2 Nucleodure C18 gravity column	Macherey & Nagel, Düren, Germany
Fluorescence Stereo Microscope BX51	Olympus, Hamburg, Germany
GC6890 Gas chromatograph with flame ionization detection	Agilent, Waldbronn, Germany
Lyophilisator	Leybold Heraeus GmbH, Köln, Germany
Mastercycler personal	Eppendorf AG, Hamburg, Germany
Percival CU-36L/D	Percival Scientific Inc, Perry, USA
Stereo microscope SZX12	Olympus, Hamburg, Germany
TOF-MS LCT Premier	Waters Corporation, Milford, USA
UPLC eLambda 800 nm PDA detector	Waters Corporation, Milford, USA
UV imager raytest IDA	Raytest, Straubenhardt, Germany

### 2.1.5 Consumables

<i>material</i>	<i>supplier</i>
Polysine slides	Thermo Scientific, Braunschweig, Germany
Sand Nr. 12262	Vitakraft, Bremen, Germany
Seramis substrate	Mars GmbH, Mogendorf, Germany
Soil: Frühstorfer Erde, Str. 1 fein	Industrie Erdwerk Archut, Lauterbach-Wallenrod, Germany
Strata SI-1 silica cartridges	Phenomenex, Torrance, USA

### 2.1.6 Software

<i>software</i>	<i>supplier</i>
Analyst software	Applied Biosystems, Darmstadt, Germany
Bildanalyseprogramm 1.0.4.6	DatInf GmbH, Tübingen, Germany
GC ChemStation software	Agilent, Waldbronn, Germany
HPLC ChemStation software	Agilent, Waldbronn, Germany
ImageJ 1.44p	Wayne Rasband, National Institute of Health, USA
MarVis	Georg August University, Göttingen, Germany
MassLynxTM software	Waters Corporation, Milford, USA

### 2.1.7 Plant lines

<i>name</i>	<i>Atg</i>	<i>plant line</i>	<i>obtained from</i>
Col 0			Nottingham Arabidopsis Stock Centre
<i>fah1-2</i>	At4g36220	CS6172	Nottingham Arabidopsis Stock Centre
<i>ref1-s</i>	At3g24503	SALK_027911	Nottingham Arabidopsis Stock Centre
<i>sng1-1</i>	At3g24503	N3737	Nottingham Arabidopsis Stock Centre
UGT72E1-OE	At3g50740		D. Bowles, University of York
UGT72E2-OE	At5g66690		D. Bowles, University of York
UGT72E3-OE	At5g26310		D. Bowles, University of York
C4H:F5H	At4g36220		C. Chapple, Purdue University
<i>atpr1-1xatpr2</i>	At1g32100 At4g13660	SALK_058467 SALK_123621	T. Umezawa, Kyoto University
<i>nac42</i>	At2g43000	N536474	W. Dröge-Laser, University Würzburg
NAC42_6	At2g43000		W. Dröge-Laser, University Würzburg
NAC42_20	At2g43000		W. Dröge-Laser, University Würzburg
<i>cyp79b2/b3</i>	At4g39950 At2g22330		W. Dröge-Laser, University Würzburg
<i>cad4</i>	At4g39330	SAIL_1265_A06	Nottingham Arabidopsis Stock Centre
<i>cad5</i>	At4g34230	SALK_040062	Nottingham Arabidopsis Stock Centre
<i>cyp86a1-2</i>	At5g58860	SALK_104083	M. Pollard, Michigan State University
<i>cyp86b1-2</i>	At5g23190	SALK_130265	M. Pollard, Michigan State University
<i>gpat5-1</i>	At3g11430	SALK_018117	M. Pollard, Michigan State University
<i>fah1</i>	At2g34770	SALK_140660	M. Pollard, Michigan State University
<i>fah2</i>	At4g20870	SAIL_862_H01	Nottingham Arabidopsis Stock Centre
<i>coi1-t</i>	At2g39940	SALK_035548	A. Mosblech, University Göttingen
<i>dde2-2</i>	At5g42650	N65993	

All plant lines in this table are *Arabidopsis thaliana* lines of the ecotype Columbia 0.

### 2.1.8 Microorganisms

<i>organism</i>	<i>strain</i>	<i>obtained from</i>
<i>E. coli</i>	XL1-blue	Stragene, Heidelberg, Germany
<i>E. coli</i>	DH5 $\alpha$	Invitrogen, Karlsruhe, Germany
<i>Agrobacterium tumefaciens</i>	EHA 105	
<i>Verticillium longisporum</i>	VL43	A. von Tiedemann, University Göttingen

### 2.1.9 Plasmids

<i>vector</i>	<i>selection marker</i>	<i>resistance gene</i>	<i>obtained from</i>
pJet2.1/blunt	carbenicillin		MBI Fermentas, St. Leon Rot, Germany
pUC18entry	carbenicillin		E. Hornung, Göttingen
pCambia3300.GC	kanamycin	BASTA	E. Hornung, Göttingen
pCambia1300.GS	kanamycin	hygromycin	E. Hornung, Göttingen

### 2.1.10 Oligonucleotides

Oligonucleotides for RT-PCR:

<i>Atg</i>	<i>primer name</i>	<i>primer sequence (5' – 3')</i>
At4g34230	CAD5_rev	ATGGCTCAAGTGCATGATGA
	CAD5_for	AGTGGAGGTGGGATCAGATG
At4g37990	CAD8_for	AAGTCGGAGTTGGGTGTTTG
	CAD8_rev	CAGGTAGCTCGAGTGGCTTC
At4g15490	UGT84A3_rev	CCTCCATTGTCGAGTTCCAT
	UGT84A3_for	CAAGCTTTCTTCACCCTTCG
At4g36220	F5H_rev	ACTCCGTTAAGGCCCACTCT
	F5H_for	TCCGGTCGGTCTCTTGTAAC
At3g50740	UGT72E1_rev	TGAGTCCGGCTAACAAAACC
	UGT72E1_for	TGGTTATGCCTGGATGTGAA
At2g30490	C4H_rev	TTCCCCACTCGATAGACCAC
	C4H_for	GACGGTTCCTTTCTTCACCA
At4g23690	DIR6_rev	CGGAAATACTTAGCCCCTTG
	DIR6_for	CTCTTCAAAGCCCTCTTCTCA
At2g37040/At3g53260	PAL1/2_rev	ATTCTCCTCAAATGTCTCAAATC
	PAL1/2_for	GCGATTCACGGTGGTAACTT
At1g49240	AtActin_rev	AGGTCTCCATCTCTTGCTCG
	AtActin_for	GCTGGATTCGCTGGAGATGA
At4g37970	CAD6_rev	ATCAAATGGCTTCTCCGTTG
	CAD6_for	TTGGAGACAAAGTCGGTGTG

At4g37980	CAD7_rev CAD7_for	CCTTCATTTGTTTCGGGTCA AAGTCTTGTTCTGTGGAATTTGC
At4g39330	CAD1_rev CAD1_for	CGTCACTTCCTCCAACCATT CTTGCGAATCTTGTGACCAA
At3g21560	UGT84A2_rev UGT84A2_for	GCTGCGAGTCTAACCCTCC ATCTAGAGCTGGTCGGCAA
At4g34050	CCoAOMT1_rev CCoAOMT1_for	CGACGGCAGATAGTGATTCC AAGCTCGTTAACGCCAAGAA
At3g19450	CAD4neu_rev CAD4neu_for	AAGCCTCTCAAACGCAATGT CTGATCCAGCAGAGATGCAA
At4g20870	LP_FAH4.1neu RP_FAH4.1	CTTCGCAGCGGCTTTAATAC ACTTGTGTTTCAGGTTGGTCATC
At2g34770	LP_FAH1 RP_FAH1	CCTTGATTTTCAGGTTGGTCATC GAGCATGCCTCCACCAAAC

Oligonucleotides for genotyping of SALK/SAIL lines:

<i>line</i>	<i>primer name</i>	<i>primer sequence (5' – 3')</i>
primer for insertion in SALK lines	LBb1	GCGTGGACCGCTTGCTGCAACT
primer for insertion in SAIL lines	LB_SAIL	GCCTTTTCAGAAATGGATAAATAGCCT TGCTTCC
<i>ref1-s</i>	LP_027911 RP_027911	TTGTCAATATCAGCGTCGTTG TGTGGTTTGTATGCTACTTTCATG
<i>fah1</i>	RP_828 (=LP) LP_828 (=RP)	TGGCAGAAGACCAATAATTCTG TGTTTGGCAAGATAACCAACC
<i>fah2</i>	LP_863 RP_863	TTTGAGCAGTTTTTACTCGC AATTCAAAGACCAAATTCTGAAT
<i>cad4</i>	LP_1265 RP_1265	LTAGGTGAGGTGTTGGAAGTGG ACATTCGTTGGACAAACAAGC
<i>cad5</i>	LP_040062 RP_040062	GGAATAATGGAGGCAGAGAGG CCTCTTAGGCCTGGTTGTTTC

Oligonucleotides for complementation of *fah1xfah2* and promoter-GUS fusions:

<i>primer name</i>	<i>primer sequence (5' – 3')</i>
FAH2_Sall_for	ACGGTTCGACATGGTTGCAGAACGATACACAGTC
FAH2_EcoRI_rev	ACGGAATTCTTAGCTCTTCTTCGCAGCGGC
GUS_NotIa	ACGGCGGCCGCATGGTAGATCTGAGGGTAAATTTTC
GUS_Sallb	ACGGTTCGACTCACACGTGATGGTGTGATGGTGTATG
FAH1_prom_Salla	ACGGTTCGACTATTTACTCAAGAAGAGACCGAC
FAH1_NotIb	ACGGCGGCCGCCTTCCTCATAATCTTCTCCAAGATG
FAH2_prom_XhoIa	ACGCTCGAGGCGGATCTGTGTCTGTGATTTATG
FAH1_NotIb	ACGGCGGCCGCCTTCCTGATATTCTTCGCCAAGATG

**2.1.11 Media**

<u>Czapek Dox (CD):</u>	sucrose	30 g l <sup>-1</sup>
	NaNO <sub>3</sub>	3.0 g l <sup>-1</sup>
	KCl	0.5 g l <sup>-1</sup>
	MgSO <sub>4</sub> x 7H <sub>2</sub> O	0.5 g l <sup>-1</sup>
	Fe(III) SO <sub>4</sub> x 7H <sub>2</sub> O	0.01 g l <sup>-1</sup>
	K <sub>2</sub> HPO <sub>4</sub>	1.0 g l <sup>-1</sup>

PDB medium (Sigma-Aldrich): 24 g l<sup>-1</sup>

PDA medium (Roth): 39 g l<sup>-1</sup>

LB medium:

peptone	10 g l <sup>-1</sup>
yeast extract	5 g l <sup>-1</sup>
NaCl	10 g l <sup>-1</sup>

for solid media addition of 1.5 % (w/v) agar

YEB medium:

beef extract	5 g l <sup>-1</sup>
yeast extract	1 g l <sup>-1</sup>
peptone	5 g l <sup>-1</sup>
saccharose	5 g l <sup>-1</sup>
MgSO <sub>4</sub>	2 mM

for solid media addition of 1.5 % (w/v) agar

½ Murashige & Skoog (MS): MS salt 2.2 g l<sup>-1</sup>  
saccharose 10 g l<sup>-1</sup> (20 g l<sup>-1</sup> for infections)  
pH to 5.8 with KOH  
for solid media addition of 1 % (w/v) agar or 0.4 % (w/v) gelrite

Antibiotics:

Antibiotics were added to the media according to the resistance of the bacteria/plants. In case of *V. longisporum* streptomycin was added.

carbenicillin: 100 µg ml<sup>-1</sup>

kanamycin: 25 µg ml<sup>-1</sup>

hygromycin: 20 µg ml<sup>-1</sup>

rifampicin: 50 µg ml<sup>-1</sup>

streptomycin: 10 µg ml<sup>-1</sup>

## 2.2 Methods

### 2.2.1 Fungal growth and cultivation

*V. longisporum* was grown in PDB medium. For inoculation of 200 ml PDB medium 1 ml spore glycerol stock was used ( $1 \times 10^6$  spores  $\text{ml}^{-1}$ ). The fungal culture was grown under permanent shaking for 2 weeks at 20 °C in the dark. To induce sporulation the mycelium was transferred to CD medium for 2-4 days. The spores were harvested by draining the culture through miracloth and collecting of the spores by centrifugation (4000 x g, 10 min). Spores were washed four times with tap water. For the infection experiments they were diluted to the desired concentration with tap water.

### 2.2.2 Fungal toxicity tests

To test the influence of different plant metabolites on *V. longisporum* growth, the fungus was grown on PDA supplemented with these substances solved in methanol (1-100  $\mu\text{M}$ ). As control, plates containing an equal amount of methanol (0.05-0.3 %) were prepared. The plates were inoculated with 2.5  $\mu\text{l}$  spore stock solution (2500 spores) and stored in the dark at 20 °C. Photos of the colonies were taken under the binocular and the corresponding colony area was measured by the Bildanalyseprogramm 1.0.4.6 from DatInf.

### 2.2.3 Plant growth and cultivation

Arabidopsis plants were grown either on soil or under sterile conditions on MS medium. For soil grown plants, seeds were sown on steamed (8 h, 80 °C) soil and stratified for 2 days in the dark at 4 °C. The plants were grown either under long day (16 h light/8 h dark) or under short day conditions (8 h light/16 h dark) in climate chambers at 22 °C, 60 % humidity and light intensity of 120-150  $\mu\text{mol m}^{-2} \text{s}^{-1}$ .

For sterile growth on  $\frac{1}{2}$  MS medium, seeds were first sterilized. This was performed by incubation of the seeds in 6 % (v/v) Na-hypochloride solution with 0.1 % Tween20 for 15 min. Seeds were washed four times with sterile water and plated onto petridishes with solid  $\frac{1}{2}$  MS medium. After stratification for 2 days at 4 °C in the dark plants were grown in growth chambers either under long day or under short day conditions.

## 2.2.4 Plant treatments

### 2.2.4.1 Infection with *V. longisporum*

Infections of Arabidopsis plants with *V. longisporum* were performed with two different methods:

For root cut infections, Arabidopsis plants were grown for 3.5 weeks on ½ MS plates under short day conditions (or 2.5 weeks for long day conditions). For infections, the plants were carefully pulled out of the medium, roots were cut 1 cm above the tip and flooded into the soil with 10 ml *V. longisporum* spore solution ( $1.5 \times 10^{-6} \text{ ml}^{-1}$ ) or with tap water (control plants). Plants were grown in climate chambers under conditions mentioned above (2.2.3).

For root dip infections, seeds were sown on a sand:soil mixture (1:1) with a layer of seramis at the bottom. The sand:soil mixture was well watered with 0.1 % Wuxal before seeds were added. The plates were covered with plastic foil to maintain high humidity. After stratification at 4 °C for 2 days, plants were grown for 20 days under short day conditions in climate chambers. After 7 days the foil was removed and the plates were covered with a plastic hood. For the infection, plants were uprooted and the roots were carefully washed with tap water. After incubation in spore solution ( $3-4 \times 10^5 \text{ spores ml}^{-1}$ ) for 35 min or in tap water (controls), plants were transferred into the soil. Plants were then grown under high humidity conditions covered with a plastic hood for 2 days and afterwards under normal short day conditions.

### 2.2.4.2 Infection with *Golovinomyces cichoracearum*

The infection was performed in the group of Prof. Lipka (Göttingen) by Marnie Schwarz. Arabidopsis plants were grown under short day conditions for 4 weeks. For inoculation they were placed into an inoculation tower and dusted from above with fungal spores. For this, pumpkin plants infected with *G. cichoracearum* were shaken above the plants.

### 2.2.4.3 Hygromycin selection

Hygromycin selection was performed as described in Harrison et al (2006). The complemented *fah1xfah2* seeds were grown on ½ MS growth medium supplemented with 20 mg l<sup>-1</sup> hygromycin. After 2 days of stratification at 4 °C in the dark, plates were incubated for 6 h in the light. To induce hypocotyl growth, plants were transferred in the dark for 3 days at room temperature before they were grown in growth chambers at long day conditions. Resistant seedlings had long hypocotyls after this procedure whereas the

ones of non-resistant plants stayed short. After 3 days in the light, resistant seedlings were transferred to soil.

#### **2.2.4.4 BASTA selection**

Seeds were sown on soil and one week after germination plants were sprayed with 1 mM BASTA. This treatment was repeated one week later. Non-resistant plants get yellow and die. Resistant plants were replanted in new pots approximately 3 weeks after the first treatment.

#### **2.2.5 Leaf area measurements**

Pictures of each plant were taken from the top and the projected leaf area was determined by a special software program called Bildanalyseprogramm 1.0.4.6.

#### **2.2.6 Crossing of Arabidopsis plants**

For crossing of Arabidopsis plants petals, sepals and the anthers of a young flower of the receptor plants were removed. From the donor plant pollen carrying anthers were taken and dipped onto the uncovered stigma of the mother plant. Afterwards the stigma was wrapped into plastic foil for 3-4 days. All flowers, buds and siliques near the treated stigma were removed.

#### **2.2.7 Analytical methods**

##### **2.2.7.1 Undirected metabolite fingerprinting by UPLC-MS measurements**

*Extraction with MTBE:* For metabolic fingerprinting of *fah1xfah2* plants leaf material was extracted using a two-phase extraction with methyl-*tert*-butylether according to (Matyash et al, 2008) also described in 2.2.7.6.

*Extraction with chloroform/methanol:* For metabolic fingerprinting of *V. longisporum* infected plants the material was extracted using a two-phase extraction with chloroform and methanol. 80 mg homogenized plant material was mixed with 1 ml methanol and shaken for 10 min at 70 °C. After centrifugation for 10 min at 13500 x g, 1 ml of the supernatant was transferred into a glass vial, 1 ml ddH<sub>2</sub>O was added and the samples were stored at 4 °C. The pellet was extracted with 500 µl chloroform at 10 min at 37 °C. The mixture was filtered with a glass syringe through a filter (2 µm PTFE, Whatman 4 mm) and combined with the methanol/H<sub>2</sub>O extract. The mixed extracts were stored over night at 4 °C to separate the different phases. Samples were centrifuged at 450 x g for 20 min.

1.8 ml of the upper phase (methanol/H<sub>2</sub>O) was transferred into a new tube, dried under a stream of N<sub>2</sub> and solved in 200 µl methanol. The samples were shaken for 5 min and again dried. The residue was solved in 10 µl methanol by 10 min shaking, 10 µl acetonitrile was added and after additional 10 min shaking 180 µl ddH<sub>2</sub>O was added. After centrifugation at 13500 x g for 10 min the supernatant was used for the measurement.

The lower phase (chloroform) of the two-phase solvent system was transferred into a reaction tube and dried under a stream of N<sub>2</sub>. 30 µl methanol was added and the tubes were shaken for 10 min, 10 µl acetonitrile was added and after 10 min shaking 75 µl ddH<sub>2</sub>O was added. After centrifugation at 13500 x g for 10 min the supernatant was used for the measurement.

*Measurement:* The metabolic fingerprinting was performed with modifications as described in Nahlik et al (2010).

The analysis was performed twice for each sample by Ultra Performance Liquid Chromatography (UPLC) coupled with a photo diode array detector (PDA) and an orthogonal time-of-flight mass spectrometer (TOF-MS). For LC an ACQUITY UPLC BEH SHIELD RP18 column was used at a temperature of 40 °C, a flow rate of 0.2 ml min<sup>-1</sup> and with a binary gradient of solvent A (water/formic acid (100:0.1 (v/v))) and solvent B (acetonitrile/formic acid (100:0.1 (v/v))). The following gradient was applied for the analysis of the samples of the polar extraction phase: 0-0.5 min 10 % solvent B, 0.5-3 min from 10 % to 28 % solvent B, 3-8 min from 28 % up to 95 % solvent B, 8-10 min 95 % solvent B and 10-14 min 10 % solvent B and for the analysis of the samples of the unpolar extraction phase: 0-0.5 min 46 % solvent B, 0.5-5.5 min 46 to 99 % solvent B, 5.5-10 min 100 % solvent B and 10-13 min 46 % solvent B.

The TOF-MS was operated in W optics to ensure a mass resolution larger than 10,000 in negative as well as positive electrospray ionization (ESI) mode. Data were acquired by MassLynx 4.1 software in centroided format over a mass range of m/z 50 - 1200 (negative ionization mode) and m/z 85 -1200 (positive ionization mode) with a scan duration of 0.5 s and an interscan delay of 0.1 s. The capillary and the cone voltage were maintained at 2,700 V and 30 V and the desolvation and source temperature at 350 °C and 80 °C, respectively. Nitrogen was used as cone (30 l h<sup>-1</sup>) and desolvation gas (800 l h<sup>-1</sup>). The Dynamic Range Enhancement (DRE) mode was used for data recording. All analyses were monitored by using Leucine-enkephaline ([M-H]<sup>-</sup> 554.2615 or [M+H]<sup>+</sup> 556.2771 as well as its <sup>13</sup>C isotopomer [M-H]<sup>-</sup> 555.2615 or its double <sup>13</sup>C isotopomer [M+H]<sup>+</sup> 558.2836 as lock spray reference compound at a concentration of 0.5 µg ml<sup>-1</sup> in acetonitrile/water (50:50 (v/v)) and a flow rate of 30 µl min<sup>-1</sup>.

*Data processing:* The raw mass spectrometry data of all samples of one experiment were processed using the MarkerLynx Application Manager for MassLynx 4.1 software, which

results in four data matrixes (one each for the polar extraction phase positively or negatively ionized, and for the unpolar extraction phase positively or negatively ionized). For further data processing like ranking and filtering of the data, adduct identification and correction of the raw masses, combining of the data matrixes as well as for clustering and visualization the toolbox MarVis (MarkerVisualization, <http://marvis.gobics.de>) has been used. The toolbox MarVis includes the routines MarVis Filter and MarVis Cluster. First a Kruskal-Wallis test was performed to extract markers with a p-value  $<10^{-4}$ . Next the masses of the selected high quality markers were adduct corrected according to the following rules:  $[M+H]^+$ ,  $[M+Na]^+$ ,  $[M+NH_4]^+$  for the positive and  $[M-H]^-$ ,  $[M+CH_2O_2-H]^-$ ,  $[M+CH_2O_2+Na-2H]^-$  for the negative ionisation mode. Afterwards data sets of both ionisation modes could be combined, used for cluster analysis (Kaefer et al, 2009) and automated database search (KEGG, LipidMaps, Aracyc, Knapsack and In-house-databases). The identity of selected markers was confirmed by coelution with identical standards and/or by quantitative RP-HPLC-DAD analysis.

#### **2.2.7.2 Determination of sinapate esters, flavonoids and indoles**

*Extraction:* 50 mg homogenized plant material was mixed with 0.5 ml 80 % methanol and shaken for 30 min at 60 °C. 7.5 µg fluoroindole carboxaldehyde and indole-3-propionic acid were added as internal standards prior to the extraction. The samples were centrifuged for 10 min at 16.000 x g and the supernatant was transferred into a new reaction tube. The pellet was reextracted with 0.5 ml 80 % methanol as described above. Combined supernatants were dried and solved in 200 µl 50 % methanol for HPLC analysis.

*Measurement:* Sinapate esters were separated by an Agilent 1100 HPLC system coupled to a diode array detector and equipped with a Nucleosil 120-5 C-18 column (EC250/2). The following gradient with solvent A (0.1 % acetic acid) and solvent B (98 % acetonitrile and 0.1 % acetic acid) was used: 0 min 100 % A, 4 min 80 % A, 8 min 76 % A, 44 min 37 % A, 46 min 0 % A. 20 µl of each sample was injected for the measurement. Sinapate esters and flavonoids were detected at 320 nm, indolic compounds at 229 nm. Peaks were identified and quantified by comparison with authentic standard substances.

#### **2.2.7.3 Determination of lignan glucosides and monolignol glucosides**

*Extraction and deglycosylation:* 50 mg homogenized plant tissue was mixed with 0.5 ml hot methanol (60 °C) and 1.5 µg deoxyrhapontin was added as internal standard. Samples were shaken for 15 min at 60 °C and afterwards centrifuged for 10 min at 16.000 x g. The supernatant was transferred into a new reaction tube and the pellet was

reextracted with hot methanol as described above. Combined supernatants were dried under a stream of N<sub>2</sub>. 0.5 ml β-glucosidase from almonds (1 mg ml<sup>-1</sup>) in Na-acetate buffer was added to the dried residue and the samples incubated at 37 °C for 24 h. The mixture was extracted three times with 0.5 ml ethyl acetate, the supernatants dried and solved in 50 µl 50 % methanol for HPLC measurements.

*Measurement:* HPLC separation was performed as described for sinapate ester analysis without the second step in the gradient. Lignans and monolignols were detected at 280 nm. Peaks were identified and quantified by comparison with authentic standards.

#### 2.2.7.4 Determination of residual bound lipids (suberin and cutin monomers)

*Extraction to remove soluble lipids:* Soluble lipids were extracted according to Molina et al (2006). 0.1 g homogenized root material (0.3 g in case of leaf material) was mixed with 4 ml (or 6 ml in case of leaves) 2-propanol in a glass vial and shaken for 4 h at 4 °C. The samples were centrifuged at 450 x g for 15 min and the supernatant was removed. The pellet was reextracted with 4 or 6 ml 2-propanol over night at 4 °C. The samples were centrifuged and the supernatant removed. The pellet was reextracted by shaking with 4 or 6 ml chloroform/methanol 2:1 for 8 h at 4 °C. After centrifugation the supernatant was again exchanged by 4 or 6 ml chloroform/methanol 1:2 and the samples were shaken over night at 4 °C. After centrifugation the supernatant was removed and the residue in the vials dried under a stream of nitrogen. The dried residue was then again extracted with different solutions each with a volume of 4 or 6 ml: methanol for 30 min, H<sub>2</sub>O for 30 min, 2 M NaCl for 1 h, H<sub>2</sub>O for 30 min, methanol for 30 min, chloroform/methanol 2:1 over night, chloroform/methanol 1:2 over night. After this extraction procedure the resulting residue was dried by lyophilization.

*Methanolysis:* Methanolysis was modified from Kurdyukov et al (2006b). The dried residue was methanolized with methanolic HCl. 4 mg root residue or 6 mg leaf residue was mixed with 4 ml methanolic HCl and internal standards were added (for roots 4 µg each: 17:0 fatty acid, 15:0 ω-OH fatty acid, und 15:0 fatty alcohol, for leaves 6 µg each: 17:0 fatty acid, 15:0 ω-OH fatty acid). The samples were incubated in a water bath at 60 °C for 2 h followed by three times extraction with 3 ml hexane. The hexane phases were combined and dried. The root residue was finally solved in 8 µl hexane and 2 µl Bis(trimethylsilyl)-trifluoroacetamid (BSTFA) and the leaf residue in 4 µl hexane with 2 µl BSTFA.

*Measurement:* GC-FID analysis was done using a capillary HP-5 column (30 m x 0.25 mm, 0.25 µm coating thickness). Helium was used as carrier gas with a flow of 1 ml min<sup>-1</sup>. The temperature gradient was as follows: 150 °C for 1 min, 150-200 °C at 4 °C min<sup>-1</sup>, 200-330 °C at 5 °C min<sup>-1</sup> and 330 °C hold for 6 min. 2 µl of each sample were injected with a split ratio of 5:1. Peaks were identified by authentic standards or by

fragmentation pattern of parallel GC/MS measurements and quantified according to the internal standards.

GC/MS measurement was carried out on an Agilent 5973 network mass selective detector connected to an Agilent 6890 gas chromatography equipped with a capillary HP-5 column. Mass range was set to 50-550 amu. Electron energy of 70 eV, an ion source temperature of 230 °C and a temperature of 330 °C for the transfer liner were used.

### 2.2.7.5 Determination of ceramides and glucosylceramides

These experiments were done together with Dr. Kirstin Feussner (Göttingen). The determination of ceramides and glucosylceramides was performed as described in Ternes et al (2011):

*Lipid extraction:* 1 g frozen and homogenized leave material was transferred to a glass vial and suspended in 12 ml chloroform/methanol, 1:2 (v/v). 5 nmol each of ceramide containing a C<sub>17</sub> fatty acid and glucosylceramide containing a C<sub>12</sub> fatty acid were added as internal standards to allow quantification of ceramide and glucosylceramide. After shaking at 4 °C for 4 h, the leaf tissue was sedimented by centrifugation, the supernatant was exchanged for 12 ml of chloroform/methanol, 2:1 (v/v) and the shaking was continued over night. The supernatant from the first extraction was evaporated under a stream of nitrogen and then combined with the supernatant from the second extraction. A phase separation was induced by adding 3 ml 0.45% NaCl (w/v), vortexing, and centrifugation. The lower phase was transferred to a glass tube, the upper phase was extracted a second time with 7 ml chloroform, and the solvent was evaporated under a stream of nitrogen.

*Mild alkaline hydrolysis:* To remove glycerolipids, the dried lipid extracts were dissolved in 1 ml 0.2 M NaOH in methanol and heated to 40 °C for 3 h. Phase separation was induced by adding 2 ml chloroform and 0.75 ml 0.75% NaCl (w/v), mixing, and centrifugation. The lower phase was transferred to a glass tube, the upper phase was extracted a second time with 2 ml chloroform, and the solvent was evaporated under a stream of nitrogen.

*Fractionation of the Lipid Extract:* Before first use, a 100 mg/1 ml Strata SI-1 silica cartridge was flushed with 4 ml chloroform, 4 ml acetone/2-propanol, 9:1 (v/v), and 2 ml methanol, and then equilibrated with 1 ml chloroform. The dried lipid extract was dissolved in 1 ml chloroform and loaded onto the cartridge. The lipids were eluted as three separate fractions with 2 ml chloroform, 4 ml acetone/2-propanol, 9:1 (v/v), and 2 ml methanol. The acetone/2-propanol fraction containing ceramide and glucosylceramide was evaporated under a stream of nitrogen, dissolved in chloroform/methanol, 5:1 (v/v), and stored at 4 °C until analysis by UPLC/MS.

*Analysis by UPLC/MS:* The molecular species of ceramide and glucosylceramide present in the acetone/2-propanol fraction were separated on an ACQUITY UPLC™ system

coupled to an LCT Premier™ ESI-TOF-MS analyzer. Chromatography was performed on an ACQUITY UPLC™ BEH SHIELD RP18 column at a temperature of 50 °C and a flow rate of 0.2 ml min<sup>-1</sup>. The ceramide and glucosylceramide species were eluted under the following conditions: 80 % solvent B for 0.5 min, followed by a gradient from 80 to 100 % solvent B in 6.5 min, and finally 100 % solvent B for 4 min. The column was re-equilibrated at 80 % solvent B for 4 min. Solvent A was water/methanol/acetonitrile, 90:5:5 (v/v/v), solvent B was acetonitrile. 0.1 % formic acid was added to both solvents to facilitate ionization.

Mass spectra in the range from 500 to 1000 Da with a mass resolution of > 10<sup>4</sup> were acquired by ESI-TOF-MS in positive ionization mode using 'W' optics and Dynamic Range Enhancement with a scan time of 0.5 s and an interscan delay of 0.1 s. The capillary and cone voltages were maintained at 2700 V and 30 V, and the desolvation and source temperatures at 250 °C and 80 °C, respectively. Nitrogen was used as cone (30 l h<sup>-1</sup>) and desolvation gas (600 l h<sup>-1</sup>). For exact mass measurement of > 5 ppm root mean squared, all analyses were monitored using leucine enkephaline (m/z = 556.2771) and its double <sup>13</sup>C isotopomer (m/z = 558.2828) as lock spray reference compound at a concentration of 0.5 µg ml<sup>-1</sup> in acetonitrile/water, 1:1 (v/v) at a flow rate of 30 µl min<sup>-1</sup>. Data were recorded in centroided format and analyzed using MassLynx software.

### 2.2.7.6 Determination of multiple phytohormones by HPLC-MS/MS

These experiments were done together with Dr. Tim Iven (Göttingen).

*Extraction:* In order to measure phytohormone concentrations plant material was extracted as previously described for lipids, with some modifications (Matyash et al, 2008). Plant material (200 mg) was extracted with 0.75 ml of methanol containing 10 ng D<sub>4</sub>-SA, 10 ng D<sub>6</sub>-ABA (both from CDN Isotopes, Quebec, Canada), 10 ng D<sub>6</sub>-JA, 30 ng D<sub>5</sub>-oPDA, 10 ng D<sub>3</sub>-jasmonic acid-leucine (D<sub>3</sub>-JA-Leu) (all three kindly provided by Otto Miersch, Halle/Saale, Germany), 20 ng D<sub>5</sub>-IAA (Eurisotop, Freising, Germany), 20 ng D<sub>5</sub>-tZeatin, 10 ng D<sub>3</sub>-GA<sub>3</sub> (OChemIm Ltd, Olomouc, Czech Republic), 100 ng 2-oxothiazolidine-4-carboxylic acid (OxoRA) each as internal standard. After mixing, 2.5 ml methyl-*tert*-butyl ether (MTBE) was added and the extract was shaken for 1 h at 4 °C. For phase separation, 0.6 ml water was added. The mixture was incubated for 10 min at room temperature and centrifuged at 450 x g for 15 min. The upper phase was collected and the lower phase was reextracted with 0.7 ml methanol/water (3:2.5 v/v) and 1.3 ml MTBE as described above. The combined upper phases were dried under streaming nitrogen and resuspended in 100 µl acetonitrile/water/acetic acid (20:80:0.1, v/v/v).

The analysis of constituents was performed using an Agilent 1100 HPLC system (Agilent, Waldbronn, Germany) coupled to an Applied Biosystems 3200 hybrid triple

quadrupole/linear ion trap mass spectrometer. Nanoelectrospray (nanoESI) analysis was achieved using a chip ion source. Reversed-phase HPLC separation was performed on an EC 50/2 Nucleodure C18 gravity 1.8  $\mu\text{m}$  column applying a column temperature of 30 °C. For analysis 10  $\mu\text{l}$  extract were injected. The binary gradient system consisted of solvent A, water/acetic acid (100:0.1, v/v) and solvent B, acetonitrile/acetic acid (100:0.1, v/v) with the following gradient program: 5 % solvent B for 1 min, followed by a linear increase of solvent B up to 95 % within 10 min and an isocratic run at 95 % solvent B for 4 min. To re-establish starting conditions a linear decrease to 5 % B within 2 min was performed, followed by 10 min isocratic equilibration at 5 % B. The flow rate was 0.3 ml min<sup>-1</sup>. For stable nanoESI, 130  $\mu\text{l}$  min<sup>-1</sup> of 2-propanol/acetonitrile/water/acetic acid (70:20:10:0.1, v/v/v/v) delivered by a 2150 HPLC pump (LKB, Bromma, Sweden) were added just after the column via a mixing tee valve. By using another post column splitter 790 nl min<sup>-1</sup> of the eluent were directed to the nanoESI chip. Ionization voltage was set to -1.7 kV. Phytohormones were negatively ionized and determined in a scheduled multiple reaction monitoring mode. For the scheduled mode the MRM detection window was set to 72 s and a target scan time of 1.2 s was applied. Mass transitions were as follows: 141/97 [declustering potential (DP) -45 V, entrance potential (EP) -7 V, collision energy (CE) -22 V] for D<sub>4</sub>-SA, 137/93 (DP -45 V, EP -7 V, CE -22 V) for SA, 299/137 (DP -45 V, EP -7 V, CE -22 V) for SA-Glucoside, 153/109 (DP -50 V, EP -4 V, CE -22 V) for DHBA, 179/135 (DP -40 V, EP -6.5 V, CE -22 V) for D<sub>5</sub>-IAA, 174/130 (DP -40 V, EP -6.5 V, CE -22 V) for IAA, 160/116 (DP -40 V, EP -6.5 V, CE -22 V) for ICA, 202/158 (DP -75 V, EP -10 V, CE -20 V) for IBA, 215/59 (DP -45 V, EP -9.5 V, CE -22 V) for D<sub>6</sub>-JA, 209/59 (DP -45 V, EP -9.5 V, CE -22 V) for JA, 325/133 (DP -80 V, EP -4 V, CE -30 V) for D<sub>4</sub>-JA-Leu, 322/130 (DP -80 V, EP -4 V, CE -30 V) for JA-IleLeu, 292/100 (DP -80 V, EP -4 V, CE -34 V) for JA-Acc, 308/116 (DP -80 V, EP -4 V, CE -30 V) for JA-Val, 356/164 (DP -80 V, EP -4 V, CE -30 V) for JA-Phe, 237/123 (DP -80 V, EP -10 V, CE -40 V) for OPC4, 265/151 (DP -80 V, EP -10 V, CE -35 V) for OPC6, 293/179 (DP -80 V, EP -10 V, CE -42 V) for OPC8, 269/159 (DP -55 V, EP -9 V, CE -16 V) for D<sub>6</sub>-ABA, 263/153 (DP -55 V, EP -9 V, CE -16 V) for ABA, 425/263 (DP -70 V, EP -3 V, CE -16 V) for ABA-GE, 296/170 (DP -70 V, EP -8.5 V, CE -28 V) for D<sub>5</sub>-oPDA, 291/165 (DP -70 V, EP -8.5 V, CE -28 V) for oPDA, 263/165 (DP -70 V, EP -8.5 V, CE -22 V) for dinor-oPDA, 146/103 (DP -40 V, EP -10 V, CE -14 V) for OxoRA, 162/58 (DP -45 V, EP -10 V, CE -14 V) for RA, 223/133 (DP -60 V, EP -4 V, CE -34 V) for D<sub>5</sub>-Zeatin, 218/133 (DP -70 V, EP -4 V, CE -32 V) for Zeatin, 220/134 (DP -80 V, EP -10 V, CE -32 V) for Dihydrozeatin, 202/134 (DP -70 V, EP -3 V, CE -22 V) for 6-Isopentenyladenine, 245/88 (DP -60 V, EP -4 V, CE -30 V) for IA-Ala, 273/116 (DP -50 V, EP -10 V, CE -50 V) for IA-Val, 287/130 (DP -60 V, EP -4 V, CE -30 V) for IA-IleLeu, 289/88 (DP -60 V, EP -4 V, CE -34 V) for IA-Asp, 303/146 (DP -60 V,

EP -4 V, CE -30 V) for IA-Glu, 321/164 (DP -60 V, EP -4 V, CE -30 V) for IA-Phe, 360/203 (DP -75 V, EP -4 V, CE -26 V) for IA-Trp, 347/143 (DP -55 V, EP -10 V, CE -40 V) for D<sub>2</sub>-GA<sub>3</sub>, 345/143 (DP -85 V, EP -10 V, CE -38 V) for GA<sub>3</sub>, 347/273 (DP -115 V, EP -10 V, CE -30 V) for GA<sub>1</sub>, 331/213 (DP -105 V, EP -10 V, CE -40 V) for GA<sub>4</sub>, 329/145 (DP -120 V, EP -10 V, CE -34 V) for GA<sub>5</sub>, 363/275 (DP -160 V, EP -10 V, CE -24 V) for GA<sub>8</sub>, 315/271 (DP -95 V, EP -10 V, CE -28 V) for GA<sub>9</sub>, 331/287 (DP -95 V, EP -10 V, CE -30 V) for GA<sub>20</sub>, 347/259 (DP -240 V, EP -10 V, CE -24 V) for GA<sub>34</sub>. The mass analyzers were adjusted to a resolution of 0.7 amu full width at half-height. The ion source temperature was 40 °C, and the curtain gas was set at 10 (given in arbitrary units). Quantification was carried out using a calibration curve of intensity (*m/z*) ratios of [unlabeled]/[deuterium-labeled] vs. molar amounts of unlabeled (0.3-1000 pmol).

#### **2.2.7.7 Synthesis of 4-methoxy-indol-3-ylmethyl-glucosinolate (4MI3G)**

The synthesis of 4MI3G was done by Dr. Matthias Bischoff in the group of Prof. Dr. Lutz F. Tietze (Göttingen) according to Viaud et al (1992).

#### **2.2.8 Molecular biological methods**

Molecular and microbiological methods in this chapter were performed according to Ausubel et al (1993) or Sambrook et al (1989) unless otherwise stated.

##### **2.2.8.1 DNA isolation from bacterial cultures, solutions and gel pieces**

For isolation of high pure plasmid DNA from bacterial liquid culture for transformation or sequencing, the NucleoSpin Plasmid Kit was used according to manufactures instructions. DNA clean up from PCR amplification or from agarose gel pieces for transformation or ligation was done using the NucleoSpin ExtractII Kit according to manufactures instructions.

##### **2.2.8.2 Extraction of genomic DNA of Arabidopsis leaves**

For isolation of plant genomic DNA the CTAB (Cetyltrimethylammoniumbromid) method was used. One single leaf per plant was pulverized in a 1.5 ml reaction tube in liquid nitrogen. 250 µl CTAB extraction solution (2 % (w/v) CTAB, 100 mM Tris-HCl, pH 8.0, 20 mM EDTA, 1.4 M NaCl) was added and the samples incubated at 65 °C for 15 min. An equal volume of chloroform/isoamylalcohol (24:1 (v/v)) was added and the samples were mixed. After centrifugation at 7500 x g for 3 min, 200 µl of the upper phase was transferred into a new reaction tube and 20 µl CTAB/NaCl solution (10 % CTAB, 0.7 %

NaCl) (preheated to 65 °C) was added. The samples were mixed well and incubated at room temperature for 2 min. Afterwards 220 µl 2-propanol was added and the samples mixed by inverting the tubes several times. After 2 min incubation time the samples were centrifuged at 16000 x g for 10 min. The supernatant was carefully removed and the pellet was washed with 100 µl 75 % ethanol. After removing the ethanol, the pellets were dried briefly and then dissolved in 70 µl sterile ddH<sub>2</sub>O.

### 2.2.8.3 Amplification of DNA fragments by polymerase chain reaction (PCR)

cDNA amplification for cloning purposes was performed using Phusion High Fidelity DNA Polymerase. PCR components were mixed as described in the manufacturer's recommendations (10 µl 5x HF buffer, 1 µl dNTPs (10 mM), 0.5 µM of each primer, 1 µl cDNA or genomic DNA, 1.5 µl DMSO, 0.5 µl polymerase and H<sub>2</sub>O to a final volume of 50 µl). PCR was run with the following program: 98 °C for 30 min, 30 cycles of 98 °C for 10 s, 60 °C for 20 s, 72 °C for 30 s. The final step was 5 min for 72 °C.

For PCR based analysis of plasmid DNA, Master Amp Tfl-Polymerase was used. The PCR components were mixed according to manufacturer's introductions (1.25 µl buffer, 1.5 µl dNTPs (10 mM), 2.5 µl MgCl<sub>2</sub> (25 mM), 1.5 µl of each primer, 0.25 µl polymerase and H<sub>2</sub>O to a final volume of 15 µl). The PCR was performed with the following temperature program: 94 °C for 3 min, 30 cycles of 94 °C for 30 s, 60 °C for 30 s, 72 °C for 1 min. The final extension step was at 72 °C for 10 min.

For PCR based genotyping of SALK-lines, Takara *Ex Taq* DNA Polymerase was used. The PCR mix was prepared according to manufacturer's recommendations (< 250 ng DNA, 2.5 µl 10x ExTaq buffer, 2 µl dNTPs (10 mM), 1 µl of each primer, 0.125 µl ExTaq and H<sub>2</sub>O to a final volume of 25 µl). The following PCR program was used: 2 min at 94 °C, 20-30 cycles of 94 °C for 30 s, 60 °C for 30 s, 72 °C for 2 min. The final extension step was 5 min at 72 °C. Alternatively the following program was used: 95 °C for 3 min, 30 cycles of 95 °C for 15 s, 58 °C for 30 s, 72 °C for 3 min. The final extension step was for 4 min at 72 °C.

### 2.2.8.4 PCR based genotyping of SALK-lines

To find homozygous SALK-lines, PCR of genomic DNA (isolated according to 2.2.8.2) with Takara *Ex Taq* DNA Polymerase was used. To identify the wild type allele, a combination of RP and LP primers was used. To identify the T-DNA insertion, a primer combination of LB and RP was used. Homozygous mutant plants finally produce only a PCR-fragment with LB and RP primers, heterozygous plants yield a PCR fragment with

both primer combinations and homozygous wild type plants only with LP and RP primers corresponding to the wild type allele.

#### **2.2.8.5 Quantification of *V. longisporum*-DNA in inoculated plants**

The analysis was performed in the group of Prof. Karlovsky (Göttingen). The preparation and densitometric analysis of the DNA standard was performed according to Brandfass et al, (2006) and the real time-PCR analysis was performed according to Eynck et al (2007).

#### **2.2.8.6 Separation of DNA by electrophoresis**

Electrophoretic separation of DNA fragments was performed in horizontal 1 % agarose gels (1 % agarose in TAE buffer (40 mM TRIS/HCl, pH 7.0, 20 mM acetic acid, 1 mM EDTA)). Before loading, the DNA samples were mixed with 1/6 volume loading dye (40 mM TRIS/acetate pH 8.5, 2 mM EDTA, 50 % glycerol, 0.4 % bromphenol blue). GeneRuler 1 kb DNA Ladder was used as size marker. The gel was run in TAE buffer for 20 min at 120 V and afterwards stained for 20 min in 2  $\mu\text{g ml}^{-1}$  ethidium bromide solution. DNA bands were visualized using UV light.

#### **2.2.8.7 Restriction and ligation of DNA**

Restriction of the *AtFAH2* gene out of the pJet vector was performed using 15  $\mu\text{l}$  plasmid DNA (3  $\mu\text{g}$ ), 150 U EcoRI and 150 U Sall in 4  $\mu\text{l}$  orange buffer in a total volume of 50  $\mu\text{l}$ . The mixture was incubated for 3 h at 37 °C. Restricted fragments were separated by gelelectrophoresis (2.2.8.5) and eluted from the gel (2.2.8.1) for ligation.

The T4 ligase was used for conventional cloning of a DNA fragment into the selected plasmid. The enzyme was used according to manufactures recommendations. For ligation of the pJet vector with the PCR amplification products the following ligation mixture was used: 0.5  $\mu\text{l}$  pJet Vector, 0.5  $\mu\text{l}$  T4 Ligase, 5  $\mu\text{l}$  2 x reaction buffer, 4  $\mu\text{l}$  DNA. Ligation was performed for 30 min at room temperature or at 4 °C over night.

For the ligation of DNA, restricted out of the pJet vector, with the pUC18entry vector the following ligation mixture was used: 1  $\mu\text{l}$  10x ligation buffer, 0.5  $\mu\text{l}$  T4 Ligase, 3.7  $\mu\text{l}$  DNA, 2.5  $\mu\text{l}$  pUC18entry vector, 2.5  $\mu\text{l}$  ddH<sub>2</sub>O.

#### **2.2.8.8 LR-Clonase reaction**

To get the desired DNA sequence in the pCambia vector, the gateway system was used. LR-Clonase was used according to the manufactures instructions. Clonase reaction was performed by mixing 1  $\mu\text{l}$  pUC18entry vector including the *FAH2*-construct, 1 ml pCambia

Gateway, 7.5 µl TE buffer (10 mM Tris/HCl, pH 8.0; 1 mM EDTA) and 0.5 µl LR-Clonase-mix. The mixture was incubated at room temperature over night. To stop the reaction 1 µl proteinase K was added and the mixture incubated for 10 min at 37 °C. This reaction was stopped by heating to 70 °C for 10 min. The mixture was used to transform *A. tumefaciens* cells.

#### **2.2.8.9 Sequencing reaction**

The sequence of the desired gene in the plasmids was analyzed by sequencing according to Sanger et al (1977).

The reaction mixture consisted of 200-400 ng plasmid (1 µl), 1 µl sequencing primer (0.5 µM), 1.5 µl sequencing mix and 1.5 µl sequencing buffer in a final volume of 10 µl. For the reaction the following temperature cycle was used: 2 min at 96 °C, 25 cycles of 10 s at 96 °C, 15 s at 55 °C and 4 min at 60 °C. The DNA was precipitated by addition of 1 µl 125 mM EDTA, 1 µl 3 M Na-acetate and 50 µl 100 % ethanol and sedimented by centrifugation for 15 min at 20,000 x g. The supernatant was removed and the pellet dried for 2-5 min at 65 °C. The DNA was solved in 15 µl formamide. The analysis of the sequencing reaction was done by Andreas Nolte (Georg-August University, Göttingen).

#### **2.2.8.10 Transformation of competent *E. coli* cells**

100 µl competent cells were mixed with 10 µl plasmid DNA and incubated for 20 min on ice. The cells were heat shocked in a 42 °C water bath for 50 s. Afterwards the cells were cooled on ice for 5 min. 900 µl LB medium was added and the cells were shaken for 1.5 h at 37 °C. After short centrifugation (3000 x g, 2 min) the supernatant was poured off and the cells were resuspended in the residual medium. The cells were plated onto LB agar plates with antibiotics and incubated for one day at 37 °C.

#### **2.2.8.11 Preparation of competent *A. tumefaciens* cells**

*A. tumefaciens* cells were precultured in 2 ml YEB containing 50 µg ml<sup>-1</sup> rifampicin over night at 28 °C. This culture was used to inoculate 50 ml YEB medium which was then shaken for 3-4 h at 28 °C until an OD<sub>600</sub> of 0.5 was reached. Cells were harvested by centrifugation at 5000 x g at 4 °C for 15 min. Cells were carefully suspended in 10 ml 0.15 M NaCl solution. Cells were again collected by centrifugation for 10 min and resuspended in 1 ml ice cold 75 mM CaCl<sub>2</sub> solution. Aliquots were frozen in liquid nitrogen and stored at – 80 °C.

#### **2.2.8.12 Transformation of *A. tumefaciens***

Competent cells were thawed and 3 µg plasmid DNA was added. The mixture was incubated 30 min on ice and then shock frozen at -80 °C for 2 min. Afterwards the mixture was thawed at 37 °C. After the addition of 800 µl YEB medium the cells were shaken at 28 °C for 3-4 h and plated on solid YEB media plates supplemented with 25 mg ml<sup>-1</sup> kanamycin and 50 mg ml<sup>-1</sup> rifampicin. Plates were incubated at 28 °C for 2 days.

#### **2.2.8.13 Transformation of Arabidopsis**

Arabidopsis plants were transformed via *A. tumefaciens* mediated gene transfer using the floral dip method (Clough und Bent, 1998). Cells were precultured in 20 ml YEB medium with 25 µg ml<sup>-1</sup> kanamycin and 50 µg ml<sup>-1</sup> rifampicin over night at 28 °C. This culture was used to inoculate 400 ml YEB medium which was again shaken over night at 28 °C. Cells were harvested by centrifugation (2000 x g, 20 min) and the resulting pellet was solved in 200 ml 5 % (w/v) saccharose solution. After solving the pellet, 100 µl SylWet was added and flowering inflorescences of Arabidopsis plants were dipped into the solution. Plants were kept under high humidity over night. Positive T1 transformed lines were selected by hygromycin (see 2.2.4.6) or BASTA selection (see 2.2.4.7).

#### **2.2.8.14 Cloning strategy for the complementation of *fah1xfah2***

cDNA of the *AtFAH2* gene was amplified with Phusion Polymerase using primers which generated a Sall restriction side at the 5' end of the gene and a EcoRI restriction side at the 3' end of the gene. First, the gene was cloned into the pJet vector by ligation. With the use of restriction enzymes, the gene was cut out of the vector and ligated into the pUC18entry vector, which can be used as entry vector in the gateway system. With the use of the LR-Clonase, the gene was transferred from the pUC18entry vector to the pCambia vector and integrated between a p35S Cauliflower mosaic virus (CaMV) promoter and a 35S polyA terminator.

#### **2.2.8.15 Cloning strategy for the promotor GUS fusions**

GUSplus DNA (Cambia, Brisbane, Australia) was amplified with Phusion Polymerase using primers which generate a NotI restriction side at the 5' end of the gene and a Sall restriction side at the 3' end of the gene and cloned into the pUC18 entry vector. For *AtFAH1* promoter cloning the region of 1500 bp in front of the ATG and the first two exons were amplified with generation of a Sall restriction side at the 5' end of the gene and a NotI restriction side at the 3' end of the gene. For *AtFAH2*, XhoI and NotI were used as

restriction sites. Each *AtFAH* promoter was cloned in front of the GUS gene in the pUC18entry vector. With the use of the LR-Clonase, the fusion constructs were transferred from the pUC18entry vector to the pCambia vector, which was used for *A. tumefaciens* transformation.

#### **2.2.8.16 Determination of transcript levels**

##### **2.2.8.16.1 RNA extraction**

Total RNA was extracted from 100 mg rosette leaf material using the TRIZOL method (Chomczynski & Mackey, 1995). 100 mg grinded leaf material was thawed in 1 ml TRIZOL buffer (38 % (v/v) Roti-Phenol, 0.8 M guanidinium thiocyanate, 0.4 M ammonium thiocyanate, 133.6 mM Na acetate pH 5.0, 5 % (v/v) glycerol) under extensive shaking. After 5 min incubation at room temperature the samples were centrifuged at 20,000 x g and 4 °C for 10 min and the supernatant was transferred into a new tube. After the addition of 200 µl chloroform samples were shaken by hand, incubated 3 min at room temperature and centrifuged at 20,000 x g and 4 °C for 15 min. The upper phase was transferred into a new tube and ½ volume 2-propanol and ½ volume high salt precipitation buffer (0.8 M sodium citrate, 1.2 M NaCl) were added. The samples were mixed by inverting the tubes several times. After 10 min incubation at room temperature and centrifugation as stated above, the supernatant was removed and the pellet washed twice with 75 % ethanol. The washed pellet was dried at room temperature and solved in 20 µl ddH<sub>2</sub>O at 65 °C for 5 min.

##### **2.2.8.16.2 cDNA synthesis**

RNA was treated with DNase I according to manufacturer's instructions. 1 µg RNA was mixed with 1 µl 10x reaction buffer and water to 9 µl and 1 µl DNase was added. After 30 min incubation at 37 °C, 1 µl 25 mM EDTA was added and the mixture was incubated for 10 min at 65 °C. The prepared RNA was reverse transcribed by RevertAid H Minus Reverse Transcriptase according to manufactures instructions. It was mixed with 1 µl oligo(dT)<sub>18</sub> primer and 1 µl H<sub>2</sub>O and incubated 5 min at 70 °C. Tubes were placed on ice and the following solutions were added: 4 ml 5x reaction buffer, 1 µl RiboLock Ribonuclease Inhibitor and 2 µl dNTP mix. The mixture was incubated 5 min at 37 °C. 1 µl RevertAid H Minus Reverse Transcriptase was added and the mixture incubated for 60 min at 42 °C. The reaction was stopped by heating to 70 °C for 10 min.

1 µl of cDNA was used for PCR with ExTakara Taq polymerase. PCR was run for 20, 23 and 26 cycles as described above.

## **2.2.9 Microscopy of *V. longisporum* infected plant material**

### **2.2.9.1 Paraffin embedding**

Hypocotyls and petioles from control and infected plants were harvested and stored in FAE (3.7 % formaldehyde, 5 % acetic acid and 50 % ethanol). For paraffin embedding the material was stepwise dehydrated in series of ethanol in the following concentrations: 65 %, 75 %, 85 %, 96 % and 100 %. The ethanol was exchanged by Roti-Histol by stepwise increasing Roti-Histol in the following concentrations: 25 %, 50 %, 75 % and 100 %. For the embedding, the samples were transferred into Roti-Histol saturated with paraplast at 42 °C for 1 h and the samples were then incubated in 100 % paraplast at 60 °C overnight. Samples were casted into forms of aluminum foil.

### **2.2.9.2 Lignin staining of embedded plant material**

Thin cuts of paraffin embedded material were made with a razorblade by hand. The cuts were dressed on a Polysine glass slide at 42 °C and the remaining paraffin was removed by exposing the cuts to 100 % Roti-Histol. The Roti-Histol was removed by washing the slides with ethanol. Staining was performed with 1 % phloroglucin in 90 % ethanol. Afterwards 10 % HCl was applied and the samples were covered with a cover glass. Microscopy was performed with an Olympus BX 51 microscope.

### **2.2.10 GUS staining**

For GUS staining, the tissue was placed into 90 % acetone on ice. Afterwards samples were incubated for 20 min at room temperature and were washed in freshly prepared cold staining buffer (0.5 M NaPi (pH 7.2), 10 % Triton X-100, 100 mM potassium ferrocyanide, 100 mM potassium ferricyanide). The buffer was exchanged for staining buffer including 2 mM X-gluc (5-bromo-4-chloro-3-indoxyl-beta-D-glucuronide cyclohexylammonium salt) in which the samples were infiltrated under vacuum on ice for 15-20 min. Infiltrated samples were incubated at room temperature until the blue color of the GUS staining appeared. The staining buffer was removed and the samples subjected to a series of ethanol: 20 %, 35 % and finally 50 %. The samples were fixed in FAE (3.7 % formaldehyde, 5 % acetic acid and 50 % ethanol) for at least 30 min and examined under the binocular.

### **2.2.11 Statistics**

To test the significance of obtained results, students t-test was performed using an internet tool ([www.physics.csbsju.edu/stats/t-test\\_bulk\\_form.html](http://www.physics.csbsju.edu/stats/t-test_bulk_form.html)). For  $p \leq 0.05$  the data were called significantly different and were marked with one asterisk. For  $p \leq 0.01$  data were marked with two asterisks and for  $p \leq 0.001$  data were marked with three asterisks.

### 3 RESULTS

The aim of this thesis was to identify the function of sinapate esters and long chain fatty acid derivatives during the infection of *Arabidopsis* with *V. longisporum*.

#### 3.1 Infection of *Arabidopsis* plants with *V. longisporum*

For the infection of *Arabidopsis* plants with *V. longisporum* two different infection procedures were applied in this work – the root cut and the root dip method.

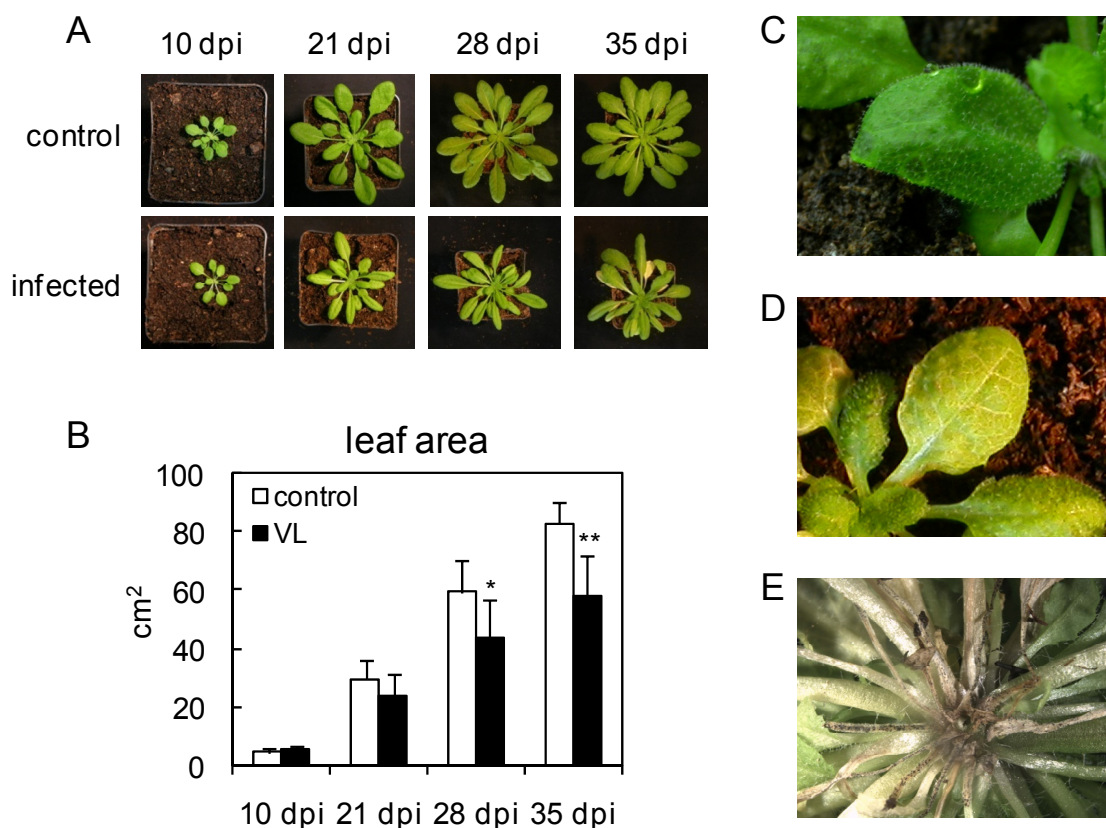


**Fig. 7: Symptoms of *Arabidopsis* plants infected with *V. longisporum* by root cut infection.** *Arabidopsis* plants grown under short day conditions were infected by root cut infection. A) Pictures of infected and control plants showing leaf area reduction from 21 dpi on and chlorosis and necrosis at 35 dpi. B) Time course of the leaf area of infected (black bars) and control (white bars) plants. Mean values were calculated from six independent experiments  $\pm$  standard deviation (SD). Asterisks indicate significant differences in the leaf area between control and infected plants according to student's t-test (\*  $p \leq 0.05$ , \*\*  $p \leq 0.01$ ). C) Water soaking of infected leaves at 14 dpi. D) Whitening of the leaf veins in infected plants at 14 dpi. E) Bottom of a rosette of an infected plant at 35 dpi showing microsclerotia development at petioles of senescent leaves.

In the root cut method plants were grown sterile on MS medium. For the infection they were pulled out of the agar and one centimeter of the root tip was cut off. Afterwards the plants were transferred into the soil by watering with spore solution. This infection method resulted in a slow and mild infection (Fig. 7). The most obvious phenotype of the infection was the stunting of the leaves which was visible at 21 dpi. Significant reduction of the leaf area could be determined at 28 dpi (Fig. 7B). At this stage a 27 % reduction could be detected, at 35 dpi the reduction was 30 %. At both time points also chlorotic and necrotic leaves were visible.

The second infection method used in this work was the root dip infection. Hereby plants were grown on a sand soil mixture. For infection, plants were uprooted and the roots were incubated in spore solution for 35 min before being transplanted into the soil. This infection led to a stronger and faster infection compared to root cut infection (Fig. 8). Already at 14 dpi a significant reduction of the leaf area could be detected. At 21 dpi stunting of the leaves was already at 63 % (Fig. 8B). The general infection symptoms of the plants were identical with both methods. Between 7 and 10 dpi first symptoms were visible. Infected leaves were soaked with water at the beginning of the light period (Fig. 7C), which is a common disease symptom in bacterial infections but also described for fungi (Katagiri et al, 2002; Lloyd et al, 2011). Sometimes water droplets coming out of the leaves were also visible. Additionally, whitening of the leaf veins could be noticed in infected leaves at this early time point of infection (Fig. 7D). At later stages the development of microsclerotia on dead and senescent plant material especially on the petioles was visible (Fig. 7E).

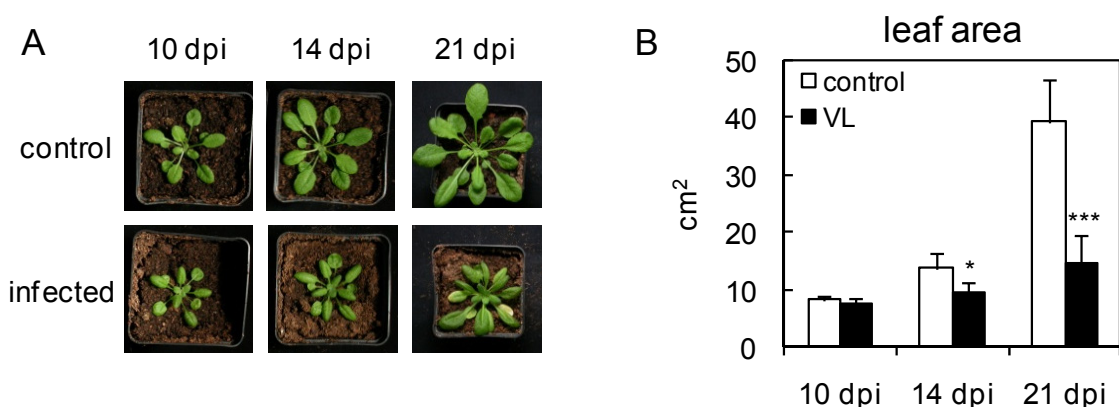


**Fig. 8: Leaf area reduction in Arabidopsis plants infected with *V. longisporum* by root dip infection.**

Plants were grown under short day conditions and infected by root dip infection. A) Pictures of infected and control plants at 10, 14 and 21 dpi, showing leaf area reduction from 14 dpi on and chlorotic and necrotic leaves at 21 dpi. B) Time course of the leaf area of infected (black bars) and control (white bars) plants. The data represent the mean values of five independent experiments  $\pm$ SD. Asterisks indicate significant differences in the leaf area between control and infected plants according to student's t-test (\*  $p \leq 0.05$ , \*\*\*  $p \leq 0.001$ ).

The root cut method was used for the initial experiments to analyze, if detected differences at the metabolic level change over the time course of infection. For infection studies of different mutant plants, the root dip method was used, which allowed to test more mutant lines in a given time range. To be sure that the infections with both methods resulted in the same metabolic changes, all metabolite analyses (except for suberin and cutin) done with root cut infected material were repeated with material from the root dip infections. But in this case only 21 dpi was used as time point for the analyses. These data, shown in the appendix, were comparable to those obtained with the root cut material.

### **3.2 Undirected metabolite fingerprinting in *V. longisporum* infected tissue using UPLC-MS(TOF)**

This work was based on preliminary data generated by UPLC-MS-based metabolic fingerprinting. The method was used to identify metabolic markers, which specifically accumulate in Arabidopsis leaf material infected with *V. longisporum*. For that, infected as well as uninfected plant material were extracted and analyzed by UPLC-MS(TOF). A data matrix with high quality marker candidates (mass/retention time pairs with the corresponding intensity profiles), which differ in their intensity between the chosen experimental conditions, was generated (see 2.2.7.1).

The data sets obtained were further analyzed by MarVis Cluster (Kaefer et al, 2009), which is an interactive software tool for clustering and visualization of intensity profiles by training an one-dimensional self-organizing maps (1D-SOMs) model. Intensity profiles of high similarity were clustered together into one prototype. This data mining process allows to overview all metabolite profiles of large data sets and supports the detection of infection related markers. The exact mass information of the selected marker candidates were used for the putative identification by searching public and In-house databases.

Despite an adduct correction routine has been achieved as data preprocessing step (for details see 2.2.7.1), the data sets still include a large number of adduct masses and masses derived from in-source-fragmentation, so that the true number of metabolite markers in one data set may be less than one-fifth to one-tenth of the calculated numbers. All the metabolic fingerprinting analyses described in this work were performed by Dr. Kirstin Feussner.

#### **3.2.1 Leaf material**

The undirected metabolite fingerprinting approach of leaf material was repeated to confirm the preliminary data (see 1.3) and to find additional markers especially in the

phenylpropanoid and hydroxy/dicarboxy fatty acid pathways. The same method as before was applied, but more biological replications and three different time points were chosen (10, 21 and 35 dpi) to analyze the time dependent changes of infection relevant metabolites. Samples were extracted in a two phase system leading to a polar and a non-polar phase. Both fractions of the samples were measured twice once in positive ionization mode and once in negative ionization mode.

The data generated from the polar phase resulted in 726 high quality markers in the positive ionization mode and 413 in the negative ionization mode. They were filtered by Kruskal-Wallis-Test with a cut off at  $p < 10^{-5}$ . The markers were grouped into 30 prototypes based on their normalized intensity profile and arranged on a 1D-SOM (Fig. 9A). Based on this 1D-SOM infection related markers and early infection markers could easily be detected. Using database searches (KEGG, AraCyc, Knapsack, LipidMaps and an In-house-database) the detected masses of infection relevant markers were compared with masses of known metabolites.

One prominent group of metabolites which could be detected with this tool was again the one of the phenylpropanoids (Fig. 9B, Tab. S1). One early marker was sinapoyl glucose detected in cluster 19. It was already enriched in infected samples at 10 dpi. The amount stayed at elevated levels in these samples over the whole observation time. The second detected sinapate ester was bis-sinapoyl glucose, which was also enriched in infected samples at all three time points.

Coniferin and syringin, which are the glucosylated forms of the precursors of lignin and lignan monomers, accumulated over the time of infection reaching the highest amounts at 35 dpi. With the same accumulation pattern also mono- and diglucosylated forms of pinoresinol and lariciresinol were detected. So far these lignans were only described in the roots of *Arabidopsis* (Nakatsubo et al, 2008). In addition to these known lignans, also the intensities of masses of so far not in *Arabidopsis* described lignans and structurally related compounds (phymarolin I, sesamolinal, sesamin, syringaresinol glucoside) were increased in infected leaves. These substances could not be further verified because standards are not commercially available and no MS/MS fragmentations have been performed until now.

Also part of the phenylpropanoid pathway are flavonoids. In the samples two kampferol glucosides were detected as markers. But in contrast to the sinapate esters, the monolignols and the lignans, their intensity profiles showed no strong differences between control and infected material (Fig. 10). Just at 35 dpi a minor decrease of these metabolites could be detected.

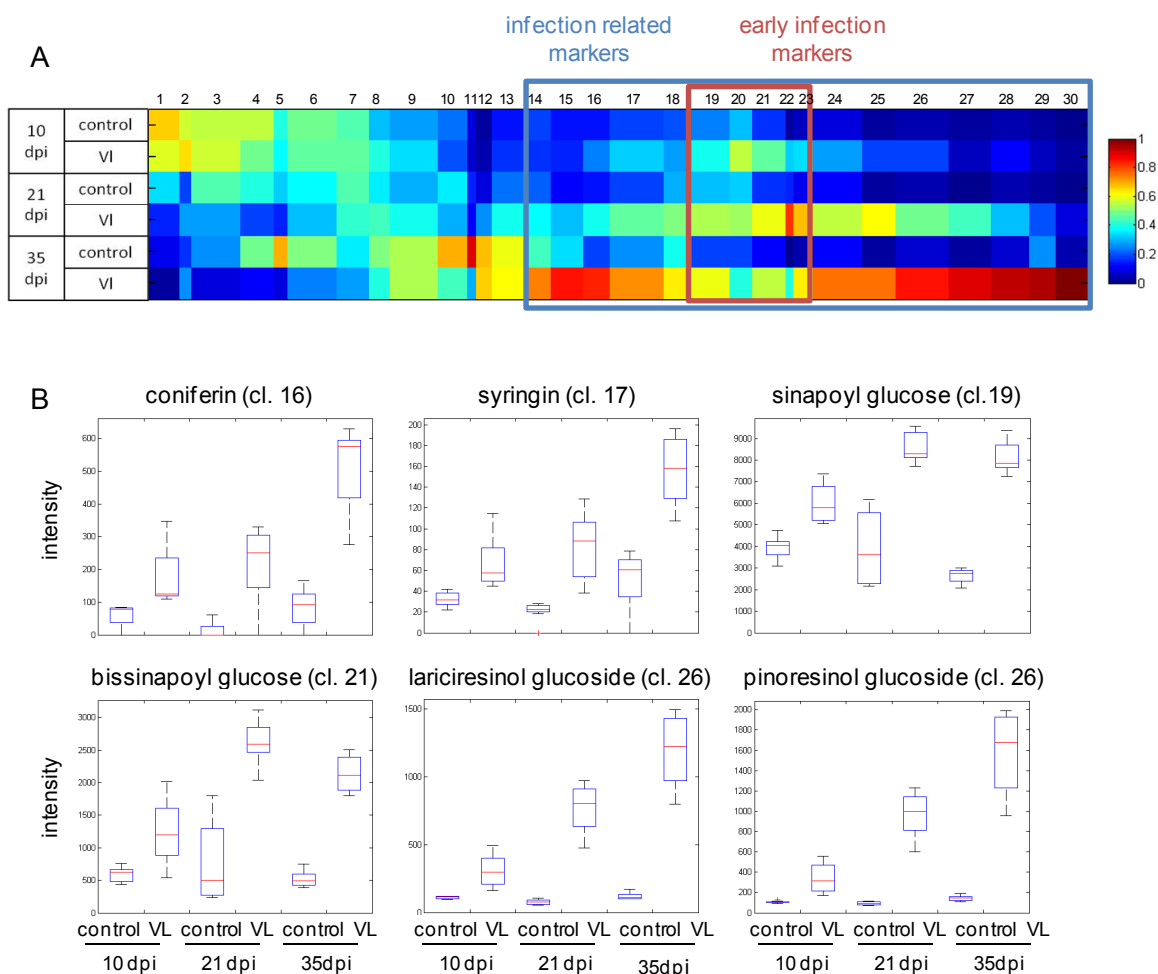


**Fig. 9: UPLC-MS(TOF) based metabolite fingerprinting of *V. longisporum* infected *Arabidopsis* leaves.**

Plants were infected by root cut infection and harvested at indicated time points. Leaf material was extracted by two phase partitioning, leading to a methanol phase with polar metabolites and a chloroform phase with non-polar metabolites. A) 1D-SOM of 726 markers of the methanol fraction of the extraction measured in positive ionization mode and 413 markers measured in negative ionization mode. Markers of different infection time points (10, 21 and 35 dpi) of infected (VL) and control plants were grouped into 30 clusters based on their intensity profile. B) Box plots of prominent markers from different clusters (cl.) which accumulate in *V. longisporum* infected plants (VL). Four samples per treatment from two independent experiments were analyzed.

Apart from the phenylpropanoids also indole glucosinolates were detected as markers. From these markers indol-3-ylmethyl glucosinolate (I3G) and 4-methoxy-indol-3-ylmethyl glucosinolate (4MI3G) could be unequivocally identified by comparison with standard substances. The third metabolite of this group could not be confirmed because of missing available standards. It had an identical exact mass, a similar UV spectrum and a comparable retention time like 4MI3G. Therefore it was assumed that this third compound from the group was 1MI3G. This putative 1MI3G showed an accumulation at 21 and at 35 dpi (Fig. 10). The amount of I3G was only slightly increased at 10 and 21 dpi whereas for 4MI3G no increase was visible.

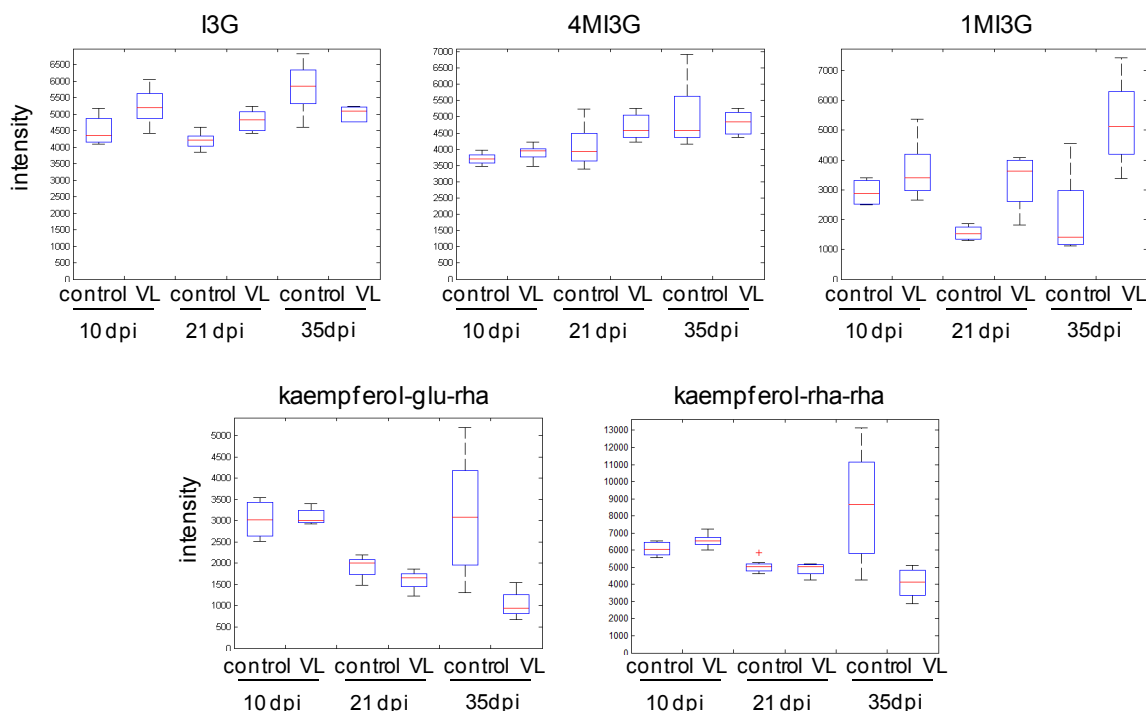


**Fig. 10: Flavonoid and indole glucosinolate markers in *V. longisporum* infected leaf material.** Plants were infected by root cut infection and harvested at the indicated time points of infection. Leaf material was extracted by two phase partitioning, leading to a methanol phase with polar substances and a chloroform phase with non-polar substances. Shown markers derived from the analysis of the methanol phase. Box plots of indole glucosinolates and of kaempferol derivatives (gluc-rha: 3-O-glucoside-7-O-rhamnoside, rha-rha: 3-O-rhamnoside-7-O-rhamnoside) are shown. Four samples per treatment from two independent experiments were analyzed.

Next to the described markers also other masses were detected that differ in their intensities between controls and infected samples. But for most of these masses no reliable database hit was found. They need to be further elucidated in the future.

Beside the polar phase described above, also the non-polar phase of extraction was measured and analyzed with the same method. It resulted in 267 markers in the positive ionization mode and 103 markers in the negative ionization mode with a cut off at  $p < 10^{-5}$ . No significant infection related markers were detected when analyzing these metabolites. Also the masses identified in the preliminary analysis of Dr. Kirstin Feussner could not be verified.

The analysis was additionally performed with material from root dip infections (21 dpi). The markers of the polar phase described above (root cut infection material), were nearly all also detected in the samples of the root dip infections (Tab. S2). With coniferylaldehyde glucoside and 4-hydroxy-indol-3-ylmethyl glucosinolate (4HI3G) also two additional markers, which were related to the already described markers, were determined. In the non-polar phase of these samples again no significant markers were detectable.

### 3.2.2 Root material

After measuring the leaf material, it was of interest if the identified infection markers were also detectable in the roots. The analysis of root material was performed as described for the leaves. But showing different basal levels of the metabolites both independent infection experiments could not be calculate together. Again only the polar phase of extraction is described here, because in the non-polar phase no infection related markers were detected.

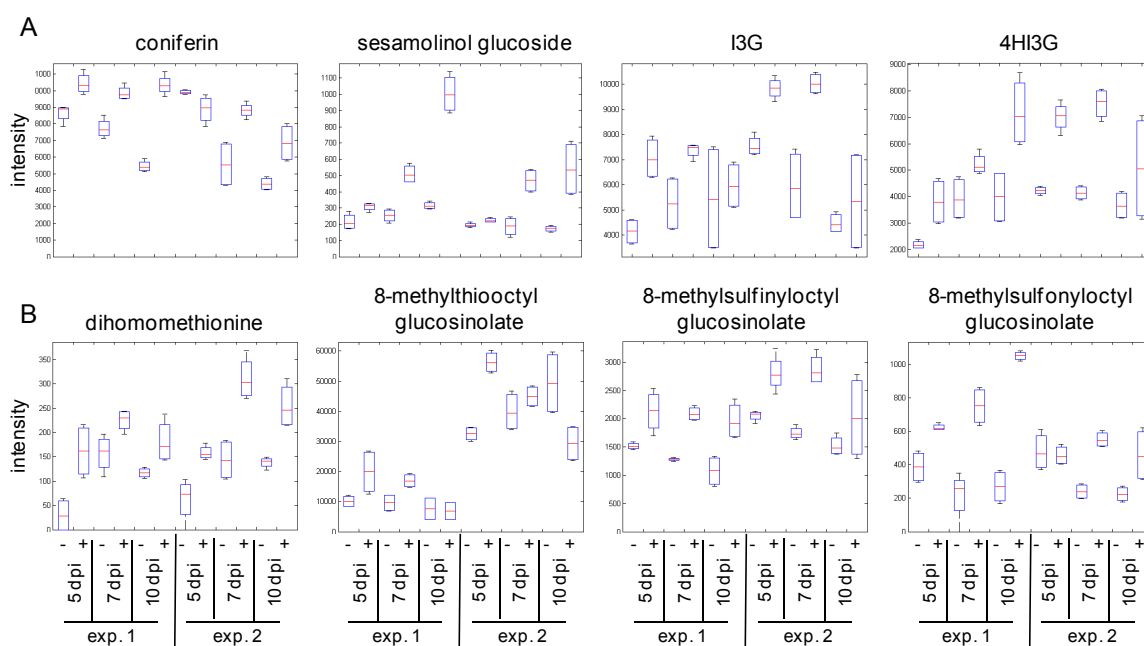


**Fig. 11: Markers of UPLC-MS(TOF) based metabolite fingerprinting of *V. longisporum* infected *Arabidopsis* roots.**

Plants were infected by root cut infection and harvested at 5, 7 and 10 dpi. Root material was extracted by two phase partitioning, leading to a methanol phase with the polar metabolites and a chloroform phase with the non-polar metabolites. A) Root infection markers related to markers detected in the leaves. B) Root infection markers representative for the aliphatic glucosinolates. Results of two independent experiments are shown separately. From each experiment four independent samples per treatment were analyzed. exp.: experiment, -: control material, +: *V. longisporum* infected material.

Only a few markers were affected in both experiments in the same way. Coniferin was one of those markers. It accumulated in infected plants already from 5 dpi in the first experiment and from 7 dpi in the second experiment (Fig. 11A). Also the mass of sesamolinal glucoside, which was detected as well in the leaves, showed a higher intensity in the roots upon infection at 7 and 10 dpi. From the indole glucosinolates I3G and 4HI3G were detected in the roots to accumulate. Both increased especially at early time points of infection at 5 and 7 dpi. In addition to those markers related to the leaf

markers, aliphatic glucosinolates were increased upon infection (Fig. 11B). 8-methylthiooctyl glucosinolate especially accumulated early at 5 dpi but its amount already decreased at 10 dpi in the infected samples. 8-methylsulinyloctyl glucosinolate accumulated in both experiments at 5 and 7 dpi but only in one experiment also at 10 dpi, whereas 8-methylsulfonyloctyl glucosinolates started to accumulate at 7 dpi in infected samples in both experiments and was also enriched at 10 dpi. Additionally, the mass of dihomomethionine was determined to accumulate over the whole time course of infection.

### 3.3 Phenylpropanoids and indoles in the interaction of *Arabidopsis* and *V. longisporum*

Because the undirected results only provided first indications for affected metabolites in response to *V. longisporum* infection, the phenylpropanoids and indole glucosinolates were verified and quantified by directed analyses. After quantification of the metabolites, also changes in the gene expression in the phenylpropanoid pathway were elucidated. Finally, the functional impact of this metabolic group for the infection process was further investigated by analyzing mutants of the pathway.

#### 3.3.1 Quantification of selected markers

To confirm the data generated by the undirected approach, selected metabolites were measured and quantified by RP-HPLC-DAD. The method used allowed the determination of sinapate esters, kaempferol derivatives and indole glucosinolates within one measurement.

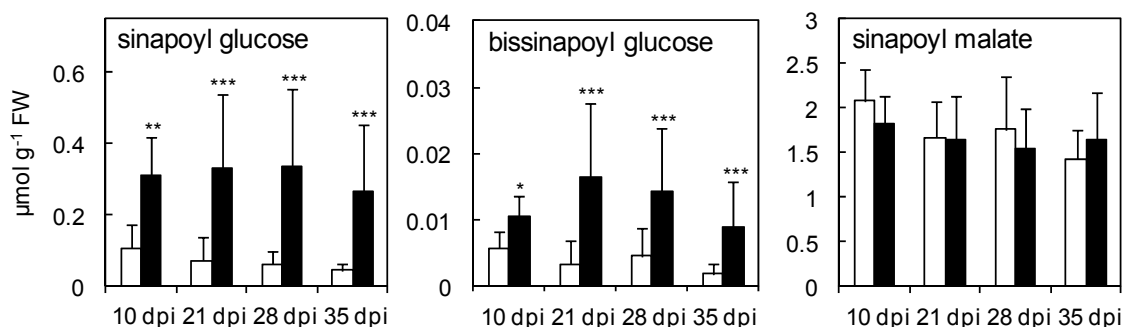


**Fig. 12: Quantification of sinapate esters in control and infected plants.**

Plants were infected by root cut infection and harvested at indicated time points. Methanol extracts of leaf material of control (white bars) and infected plants (black bars) were analyzed by RP-HPLC-DAD. Each data point represents the mean value of six (10 dpi) or 15 (21, 28 and 35 dpi) samples of three independent experiments  $\pm$ SD. Asterisks indicate significant differences between control and infected plants according to student's t-test (\*  $p < 0.05$ , \*\*  $p < 0.01$ , \*\*\*  $p < 0.001$ ).

For the sinapate esters a similar pattern could be detected as shown in the metabolite fingerprinting approach (Fig. 12). Sinapoyl glucose was already at high levels in infected leaves at 10 dpi and the amount stayed high over the time of infection at about  $0.3 \mu\text{mol g}^{-1}$  FW compared to  $0.05\text{-}0.1 \mu\text{mol g}^{-1}$  FW in the control samples. Bissinapoyl glucose showed a similar pattern but at lower amounts. The highest amount in infected plants was detected at 21 dpi with  $0.016 \mu\text{mol g}^{-1}$  FW compared to  $0.003 \mu\text{mol g}^{-1}$  FW in the controls. Sinapoyl malate, the most abundant sinapate ester in *Arabidopsis* leaves, did not change in its amount upon infection.

No significant changes upon infection were detected for the kaempferol glucosides (Fig. 13A). In all three analyzed kaempferol glucosides the amount was slightly lower in infected plants at 28 dpi and 35 dpi, but due to high standard deviations this was not significant.

For the indole glucosinolates significant higher amounts in the infected samples could be determined at 21 dpi for all three analyzed substances (Fig. 13B). But only for the putative 1MI3G a significant accumulation up to  $0.23 \mu\text{mol g}^{-1}$  FW in the samples of infected plants was detected at 28 and 35 dpi, compared to  $0.07$  and  $0.12 \mu\text{mol g}^{-1}$  FW, respectively, in the control samples.

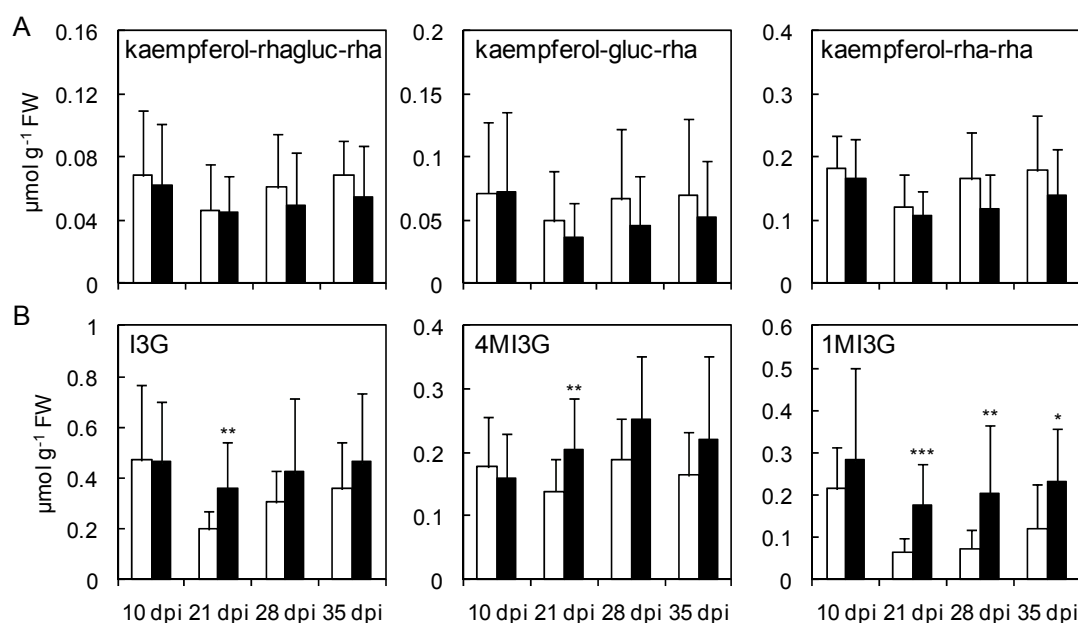


**Fig. 13: Quantification of flavonoids and indole glucosinolates in control and infected plants.**

Plants were infected by root cut infection and harvested at indicated time points. Methanol extracts of leaf material of control (white bars) and infected plants (black bars) were analyzed by RP-HPLC-DAD. A) Determination of the amount of kaempferol glucosides (rhaglug-rha: 3-O-rhamnosylglucoside-7-O-rhamnoside, gluc-rha: 3-O-glucoside-7-O-rhamnoside, rha-rha: 3-O-rhamnoside-7-O-rhamnoside). B) Determination of indole glucosinolates. Each data point represents the mean value of six (10 dpi) or 15 (21, 28 and 35 dpi) samples from three independent experiments  $\pm$ SD. Asterisks indicate significant differences between control and infected plants according to student's t-test (\*  $p \leq 0.05$ , \*\*  $p \leq 0.01$ , \*\*\*  $p \leq 0.001$ ).

For the lignan determination a different extraction method was used. In this method the methanol extractable metabolites in the samples were deglycosylated before the analysis. Thus only the total amount of lignan glucosides was measured and not the mono- and diglycosylated lignans itself. To exclude that the non-glucosylated forms were already in the samples before enzymatic treatment, control extractions without addition of the glucosidase were performed. But in those samples no significant amounts of lignans or monolignols were detected, showing that they were indeed all glucosylated.

In the RP-HPLC-chromatograms of the monolignol and lignan extractions coniferyl alcohol, lariciresinol and pinoresinol could be identified. The quantification confirmed the data of the metabolite fingerprinting approach. All three compounds accumulated in glucosylated form at high amounts over the time course of infection (Fig. 14). Lariciresinol glucosides were the most abundant ones of these three metabolites with 73-98 nmol g<sup>-1</sup> FW in infected plants at 21 and 28 dpi compared to 10-14 nmol g<sup>-1</sup> FW in control plants. Pinoresinol glucosides were around half of the amount of lariciresinol glucosides and coniferin was up to 26 nmol g<sup>-1</sup> FW in infected plants and about 5 nmol g<sup>-1</sup> FW in control plants concentrated. Syringin could not be detected in the samples.

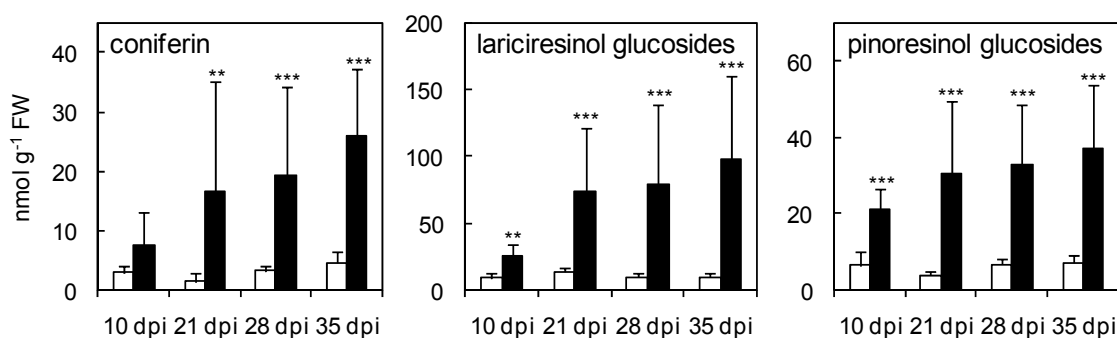


**Fig. 14: Quantification of coniferin and lignan glucosides in control and infected plants.**

Plants were infected by root cut infection and harvested at indicated time points. Methanol extracts of leaf material of control (white bars) and infected plants (black bars) were analyzed by RP-HPLC-DAD. Mono- and dilignols were analyzed after deglycosylation of the sample with  $\beta$ -glucosidase from almonds. Each data point represents the mean value of six (10 dpi) or 15 (21, 28 and 35 dpi) samples from three independent experiments  $\pm$ SD. Asterisks indicate significant differences between control and infected plants according to student's t-test (\*\*  $p \leq 0.01$ , \*\*\*  $p \leq 0.001$ ).

Beside these identified substances, comparison of RP-HPLC-chromatograms of infected leaf samples with the one of control leaf samples revealed differences in peaks of unknown identity (Fig. 15). These peaks were collected and analyzed with TOF-MS to obtain their exact masses. Peak 1 corresponded to a not identifiable metabolite with a mass of 407.171 Da. Peak 2 could be identified as secoisolariciresinol, which could be

further verified by comparison with an authentic standard. This metabolite belongs also to the group of lignans from the pathway of pinoresinol and lariciresinol. The mass of peak 3 was similar to the mass of pinoresinol. One known isomer of pinoresinol is mateiresinol but this could be excluded based on a different retention time of the standard of this substance. In peak 4 the mass of sesamolinol was detected but could not be further verified.

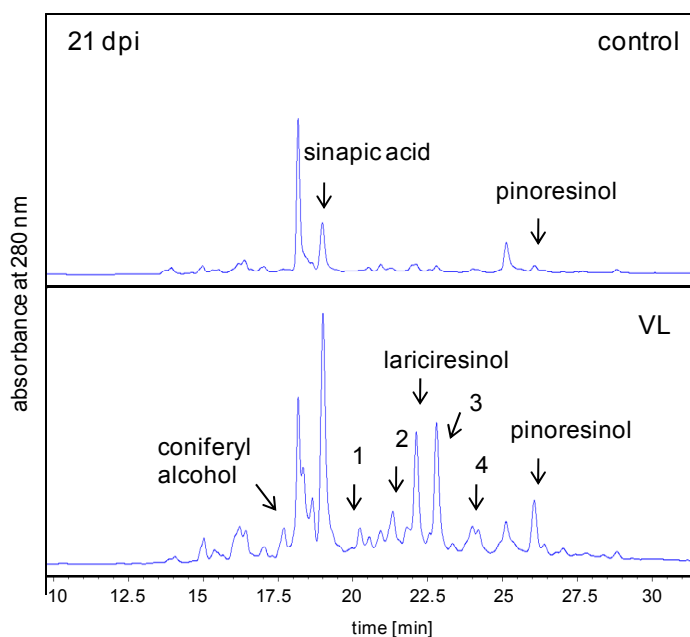


**Fig. 15: Lignan glucosides in *V. longisporum* infected *Arabidopsis* leaves.**

HPLC-chromatograms of deglycosylated methanolic leaf extracts of *V. longisporum* infected and control plants at 21 dpi. Peaks with numbers were collected from the HPLC and analyzed by UPLC-MS(TOF). Masses were measured in positive ionization mode: 1: 407.171, 2: 363.1798 (mass of secoisolariciresinol), 3: 359.1598 (mass of pinoresinol), 4: 373.1278 (mass of sesamolinol).

All these phenylpropanoid and indole glucosinolate quantifications were performed additionally with leaf material of root dip infected plants, to ensure that both methods resulted in the same reaction of the plants (Fig. S1). The results were comparable to those described here. Only a difference for the kaempferol derivatives was detected. Here a significant reduction at 21 dpi was visible.

### 3.3.2 Microscopic analysis of lignin accumulation in hypocotyls and petioles

As coniferin and also lignans accumulate in infected plants, it was of interest if also lignin was enriched in these plants. Recently, it was reported that in vascular tissue of

*V. longisporum* infected *Arabidopsis* plants transdifferentiation takes place (Michael Reusche, (Rg Dr. Teichmann, Göttingen), personal communication). In this study bundle sheath cells were shown to differentiate into new xylem vessels. This already indicated that lignification should be affected.

Cross sections of hypocotyls and petioles of control and infected plants were done and they were stained for lignin with Wiesner stain. As described before (Michael Reusche, personal communication) more but smaller vessels could be detected in infected plants in the petioles and additionally in the hypocotyls (Fig. 16). The total amount of stained lignin was indeed higher, which indicated that not only the synthesis of monolignols and lignans but also lignification is enhanced in infected plants.

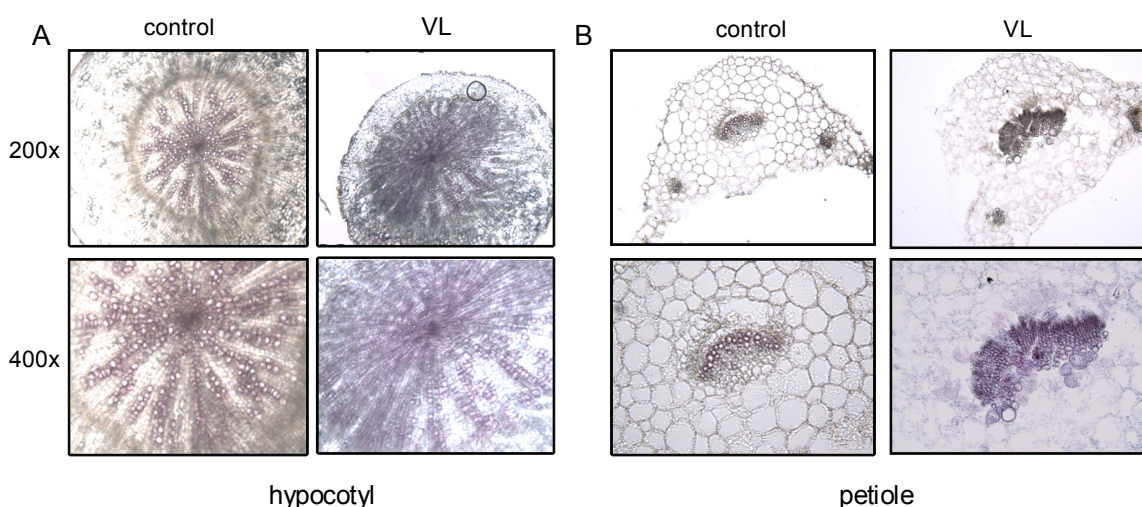


**Fig. 16: Lignin staining of hypocotyls and petioles from control and infected plants.**

Plants were infected by root cut infection and hypocotyls (A) and petioles (B) were harvested at 28 dpi. For easier cutting, the material was paraffin embedded before handsections were done. The cuts were stained with phloroglucin/HCl for lignified tissue and examined under the microscope with 200 and 400 times magnification. The pictures represent the results of at least three plants per condition.

### 3.3.3 Expression analysis of genes of the phenylpropanoid pathway

Beside the metabolite profiles, also the transcriptional level of genes of the phenylpropanoid pathway was of interest. Therefore, semiquantitative RT-PCR of several genes was performed (Fig. 17). The more general genes of this pathway were not affected in expression upon infection, like the phenylalanine ammonia lyase (*PAL*), cinnamate-4-hydroxylase (*C4H*), caffeoyl-CoA-O-methyl transferase (*CCoAOMT*) or the ferulate-5-hydroxylase (*F5H*). Differences were detected in two out of six tested cinnamoyl alcohol dehydrogenase (*CAD*) genes. *CAD5* and *CAD8* transcripts were both induced upon infection with *V. longisporum*. This is consistent with the metabolic data, because

these enzymes catalyze the synthesis of coniferyl alcohol and sinapyl alcohol, the precursors of lignin, lignans and coniferin/syringin. Also the gene of the glucosyltransferase *UGT84A3* was induced by the infection. The corresponding enzyme catalyzes the glucosylation of sinapic acid to sinapoyl glucose (Sinlapadech et al, 2007). The same activity is also described for *UGT84A2*, but the expression of this gene was not affected by the infection. Another induced gene was the dirigent protein 6 (*DIR6*) which might be responsible for stereospecific coupling of monolignols to lignans (Pickel et al, 2010), which is also in line with the accumulation of lignans in infected tissue. The observed repression of the glucosyltransferase *UGT72E1* was in contrast to our metabolic data. This gene is a member of the *UGT72E* gene family which is responsible for the synthesis of coniferin and syringin (Lanot et al, 2006). From this family *UGT72E3* was also tested, but no expression was detectable in the leaves. *UGT72E2* was not analyzed, because it is described to be especially expressed in the roots (Lanot et al, 2006).

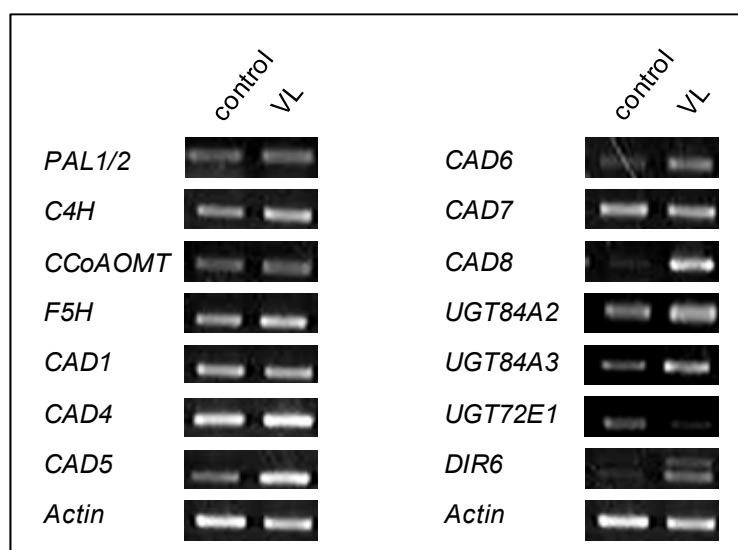


**Fig. 17: Expression analysis of genes of the phenylpropanoid pathway in control and infected plants.**

Plants were infected by root cut infection and leaf samples were harvested at 21 dpi. Analysis was done by semiquantitative RT-PCR, which was optimized for each gene. The analysis was performed with material of three independent experiments with comparable results.

### 3.3.4 Infection of mutant plants of the detected metabolic pathways

To analyze, whether the identified metabolites really have an impact on the infection, different mutant plants of the phenylpropanoid pathway were examined (Tab. S3). As stunting of the plants is one prominent infection symptom, the leaf area reduction was

analyzed as a parameter for the infection. Additionally the VL-DNA amount in infected plants was determined, to verify higher or lower susceptibility of the tested mutants.

Only in a few of the tested mutants differences in the infection compared to wild type could be observed. The results of the infection of these mutants will be further described in this chapter. For the other plant lines data concerning the infection are shown in Fig. S2.

#### 3.3.4.1 Infection of the indole mutant *cyp79b2/b3*

Indole mutants like the camalexin mutant *pad3-1* and the general indole mutant *cyp79b2/b3* (Fig. S3) were already tested in the PhD thesis of Tim Iven (Iven, 2009). It was shown that the *cyp79b2/b3* mutant but not the *pad3-1* is more susceptible against *V. longisporum*. *cyp79b2/b3* was therefore used as positive control in our infections to confirm that the infection worked properly. The results concerning this mutant are shown in Fig. S4 and Fig. S5. In both infection methods stronger leaf area reduction and a higher VL-DNA in the infected double mutant compared to wild type could be shown. These differences were more obvious in the root dip infection, which was used for most of the following pathogenicity tests.

#### 3.3.4.2 Infection of sinapate ester mutants

Three different sinapate ester mutants were chosen to examine the role of these metabolites for the infection. The *fah1-2* mutant (Chapple et al, 1992) is defective in the ferulate 5-hydroxylase and therefore unable to synthesize sinapates and its esters (Fig. S6, Fig. S8). Additionally it shows a changed lignin composition with no syringyl units. The *ref1-s* line shows reduced sinapate ester amounts with a normal lignin composition (Fig. S6, Fig. S8) (Nair et al, 2004). To analyze the importance of sinapoyl glucose itself, *sng1-1* mutant plants (Lorenzen et al, 1996) were used, which lack sinapoylglucose:malate sinapoyltransferase activity. This mutant accumulates high amounts of sinapoyl glucose in place of sinapoyl malate (Fig. S6, Fig. S8).

Pictures of the infected mutant and wild type plants are shown in Fig. 18A. All plants display similar symptom development, but in contrast to the other mutants the *fah1-2* was stronger stunted than the wild type. The leaf area of the infected plants of this mutant was more than 30 % stronger reduced than in wild type plants (Fig. 18B). This was consistent with the VL-DNA analysis in infected plants which revealed a 3.6 times higher VL-DNA content in the *fah1-2* mutant (76 pg mg<sup>-1</sup> FW) compared to wild type plants (21 pg mg<sup>-1</sup> FW) (Fig. 18C). For both other tested mutants no significant differences, neither in the relative leaf area nor in the fungal DNA amount, were detected.

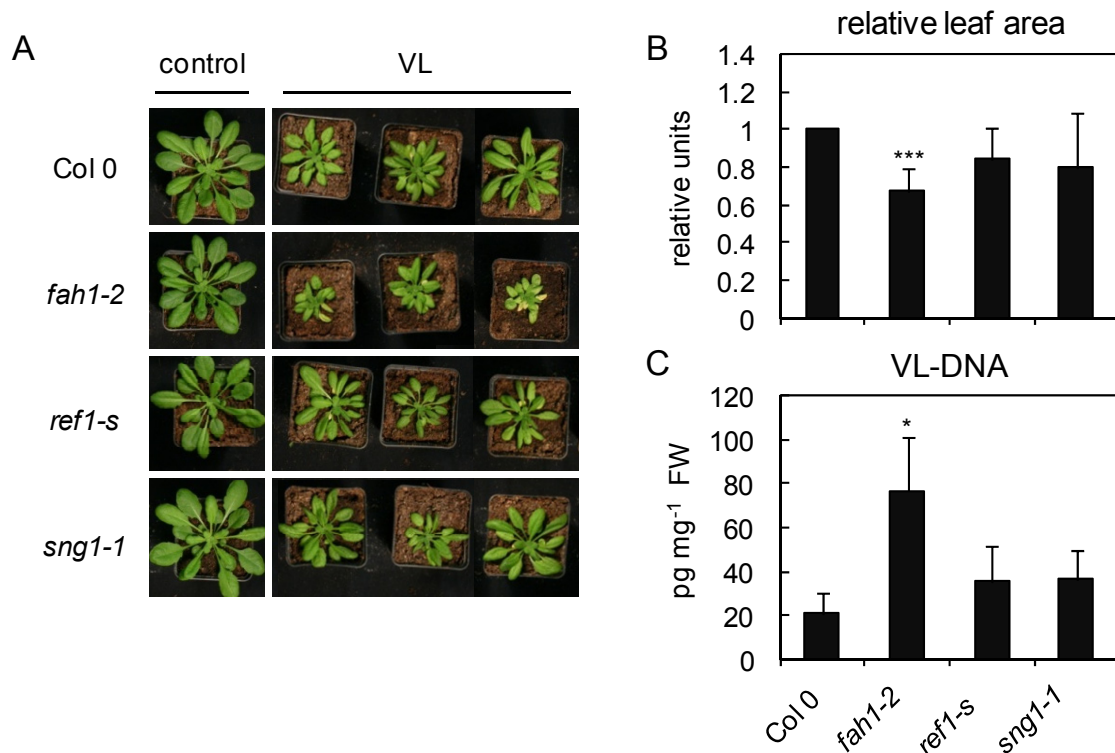


**Fig. 18: Infection of sinapate ester mutants with *V. longisporum*.**

Col 0, *fah1-2*, *ref1-s* and *sng1-1* plants were infected by root dip infection. A) Pictures of infected and control plants at 21 dpi. B) The leaf area was analyzed from the pictures of the plants and the relative leaf area was determined: The leaf area of infected plants was divided by the leaf area of control plants and the results of the mutant plants were set in relation to the value of the wild type. The data represent the mean values of five independent experiments  $\pm$ SD. C) VL-DNA analysis in infected leaves. Each data point represents the mean value of twelve samples of three independent experiments  $\pm$ standard error (SE). Asterisks indicate significant differences between control and infected plants according to student's t-test (\*  $p \leq 0.05$ , \*\*\*  $p \leq 0.001$ ). The VL-DNA analysis was performed by the group of Prof. Karlovsky (Göttingen).

Because the *fah1-2* plants showed a susceptible phenotype, an overexpressor line of this gene, the C4H:F5H line (Meyer et al, 1998), was also analyzed. This mutant was described in the literature to harbor especially syringyl lignin instead of guaiacyl lignin. After infection, the leaf area reduction of these plants was comparable to wild type plants, but differences in the VL-DNA amount were detected (Fig. 19). The VL-DNA content was 6.5 times lower than in wild type plants, although the difference was not significant ( $p=0.1$ ). In C4H:F5H plants an additional phenotype was detected during infection (Fig. S10). Especially at the end of the light period infected C4H:F5H plants showed symptoms related to water deficiency – the leaves were limp and without tension. It was tested, if changes in lignification in the vascular tissue of the hypocotyl or the petioles occur, which maybe the reason for hindrance in the water transport. It was assumed that less new vessels could be formed in these plants because of the missing guaiacyl lignin. Cross

sections of petioles and hypocotyl were analyzed, but in both tissues also new lignified vessels comparable to wild type could be detected in the infected plants (Fig. S11). So far the phenotype could not be explained.

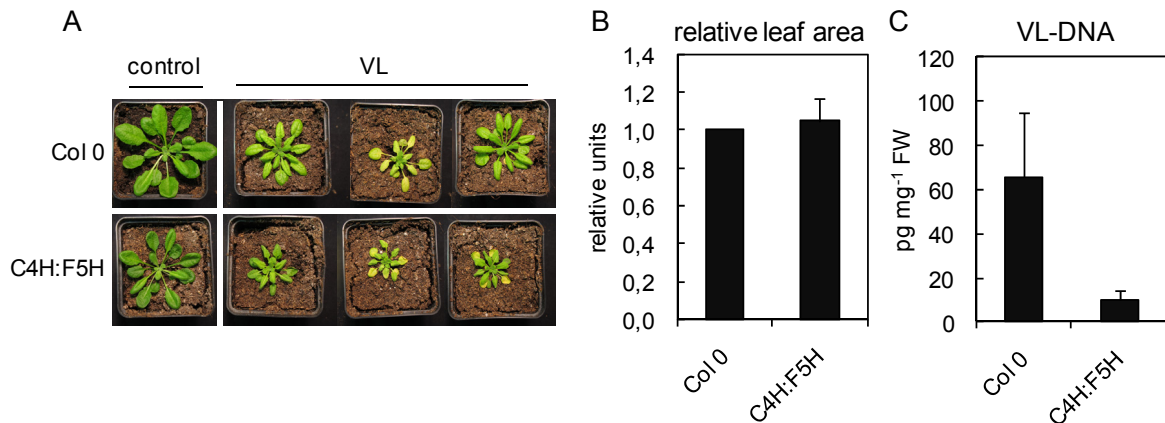


**Fig. 19: Infection of the C4H:F5H mutant with *V. longisporum*.**

Col 0 and C4H:F5H plants were infected by root dip infection and harvested at 21 dpi. A) Pictures of infected and control plants at 21 dpi. B) The relative leaf area was determined from pictures taken of the rosettes of the plants: The leaf area of infected plants was divided by the leaf area of control plants and the results of the mutant plants were set in relation to the value of the wild type. The data represent the mean values of five independent experiments  $\pm$ SD. C) Determination of VL-DNA in infected leaves. The mean values of ten samples of three independent experiments are shown  $\pm$ SE. The VL-DNA analysis was performed by the group of Prof. Karlovsky (Göttingen).

### 3.3.4.3 Coniferin and infection

To analyze whether apart from sinapate esters also coniferin and syringin have an influence on the infection and on fungal growth, UGT72E overexpressor (OE) plants were tested for their susceptibility against *V. longisporum*. *UGT72E* is a gene family of three genes (*E1*, *E2* and *E3*) which display glucosyltransferase activity for coniferyl alcohol and sinapyl alcohol leading to coniferin and syringin. The overexpressor plants of these genes were described to accumulate high amounts of syringin and especially coniferin (Lanot et al, 2006; Lanot et al, 2008).

These three different lines were examined in the infection with *V. longisporum* and in one of them (UGT72E2-OE) about 50 % less stunting compared to wildtype was observed (Fig. 20B). Also the VL-DNA in the leaves of these plants was much lower (5 pg mg<sup>-1</sup> FW) than in wild type plants (65.9 pg mg<sup>-1</sup> FW) (Fig. 20C). For both other lines no significant differences in the leaf area or the fungal DNA were detected.

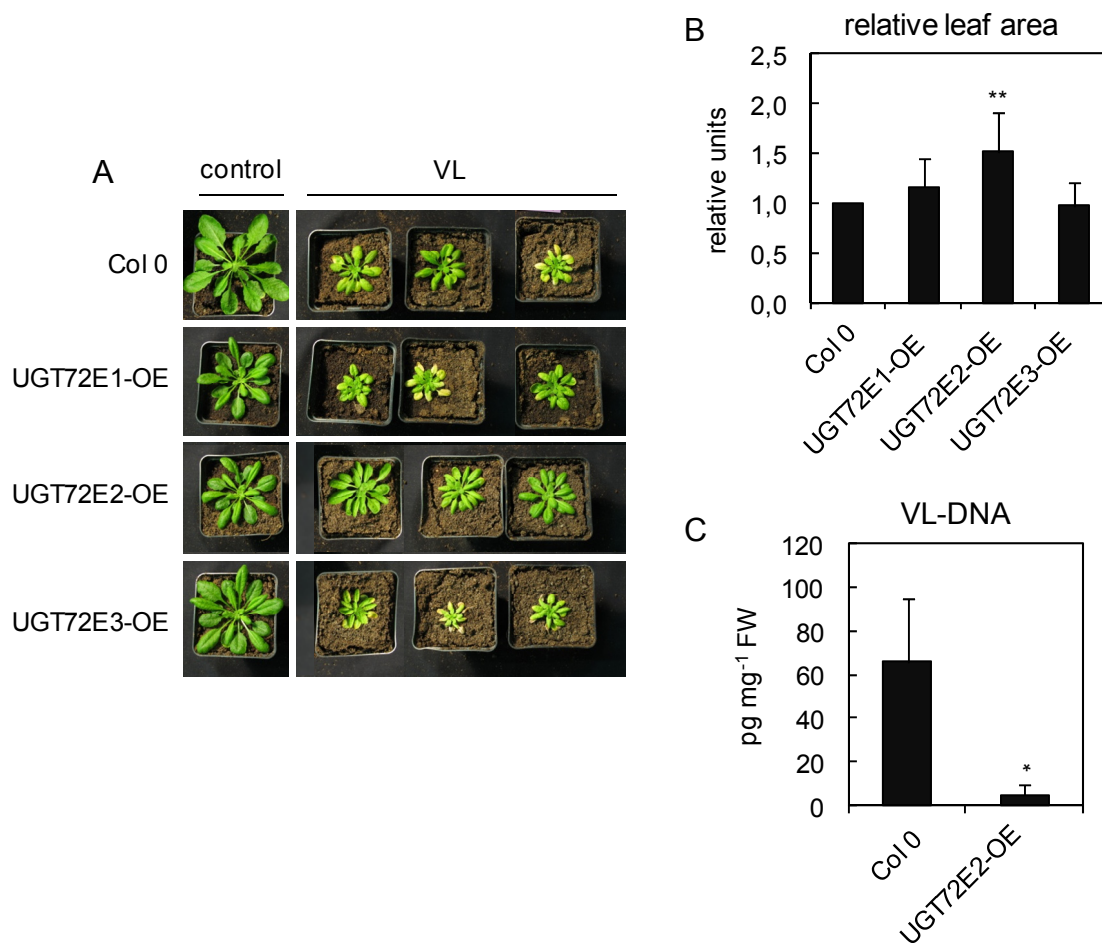


**Fig. 20: Infection of UGT72E-OE plants with *V. longisporum*.**

Col 0 and UGT72E-OE plants were infected by root dip infection and harvested at 21 dpi. A) Pictures of infected and control plants at 21 dpi. B) The leaf area was analyzed from the pictures of the plants and the relative leaf area was determined: The leaf area of infected plants was divided by the leaf area of control plants and the results of the mutant plants were set in relation to the value of the wild type. The data represent the mean values of five independent experiments. C) Determination of VL-DNA in infected leaves. The mean values of twelve samples of three independent experiments are shown  $\pm$ SE. Asterisks indicate significant differences between control and infected plants according to student's t-test (\*  $p \leq 0.05$ , \*\*  $p \leq 0.01$ ). The VL-DNA analysis was performed by the group of Prof. Karlovsky (Göttingen).

To elucidate, why overexpression of only one out of these three genes led to resistance, the monolignols glucosides in these plants were analyzed. As shown in Fig. 21, UGT72E1-OE did not accumulate those high amounts of coniferin and syringin that were observed in the other two mutants. UGT72E2-OE was especially enriched in coniferin, which was with  $13.4 \mu\text{mol g}^{-1}$  FW more than 400 times higher than in wild type plants during infection. In the UGT72E3-OE plants the factor of enrichment was approximately 90 compared to wild type, but in these plants also an additional increase in syringin up to  $2.5 \mu\text{mol g}^{-1}$  FW in infected plants compared to no detectable amounts in controls could be determined. In this context also lignan glucosides were analyzed but here the differences

were not that strong. The most obvious difference was that UGT72E1-OE showed higher enrichment in especially pinoresinol glucosides in infected plants compared to wild type.

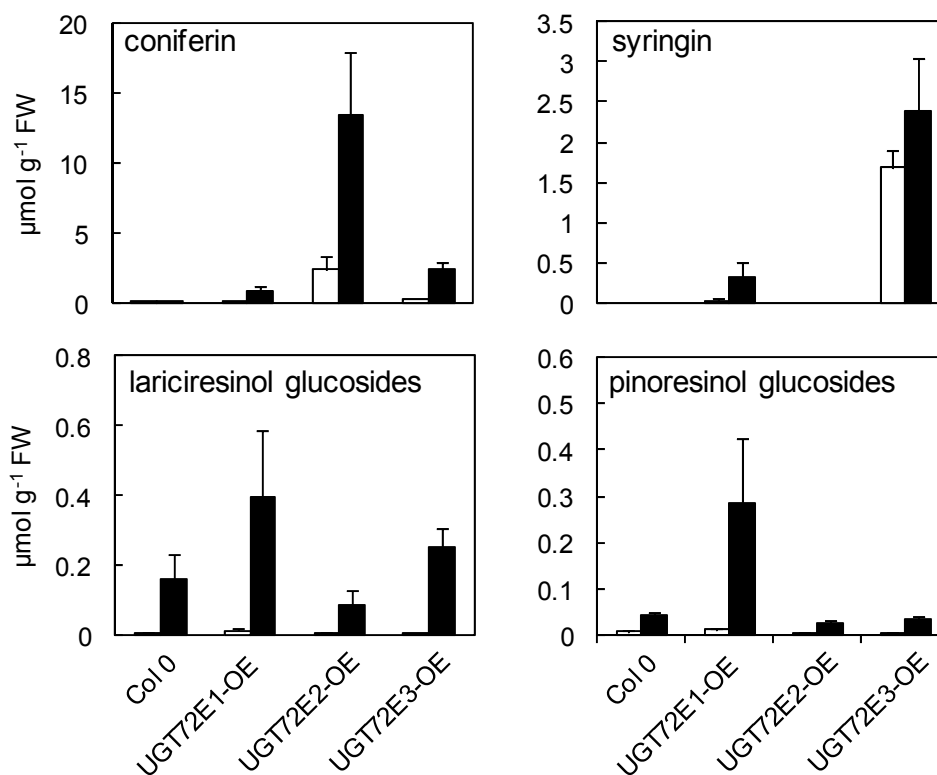


**Fig. 21: Quantification of coniferin, syringin and lignan glucosides in infected UGT72E-OE plants.**

Plants were infected by root dip inoculation and harvested at 21 dpi. Quantification of monolignols and lignans was done by RP-HPLC-DAD analysis of *V. longisporum*-infected (black bars) and control (white bars) plants. Monolignols and lignans were measured after deglycosylation of the sample. Each data point represents the mean value of eight biological replicates from two independent experiments  $\pm$ SD.

Because the mutants mainly differed in their enrichment in monolignol glucosides, it was examined if coniferin/coniferyl alcohol and syringin/sinapyl alcohol have an impact on the fungal growth. PDA plates were supplemented with these different metabolites and the colony area was determined after 17 days of growth.

Fig. 22A shows that coniferyl alcohol indeed inhibits fungal growth at a concentration of 10  $\mu$ M (20 % inhibition) and 100  $\mu$ M (30 % inhibition). This inhibitory effect could not be detected for sinapyl alcohol. Coniferin and syringin also did not show an inhibition of fungal growth in the concentrations used in this test.

When the fungus was grown for more than 21 days on the PDA plates it started to melanise and to generate microsclerotia. On the plates supplemented with 100  $\mu$ M

coniferin the melanization was delayed (Fig. 22C). Only minor black areas were detected at 28 days of growth. This effect could not be seen for the other three metabolites tested. In summary these results showed that coniferin and coniferyl alcohol but not syringin and sinapyl alcohol have an influence on fungal growth and development.

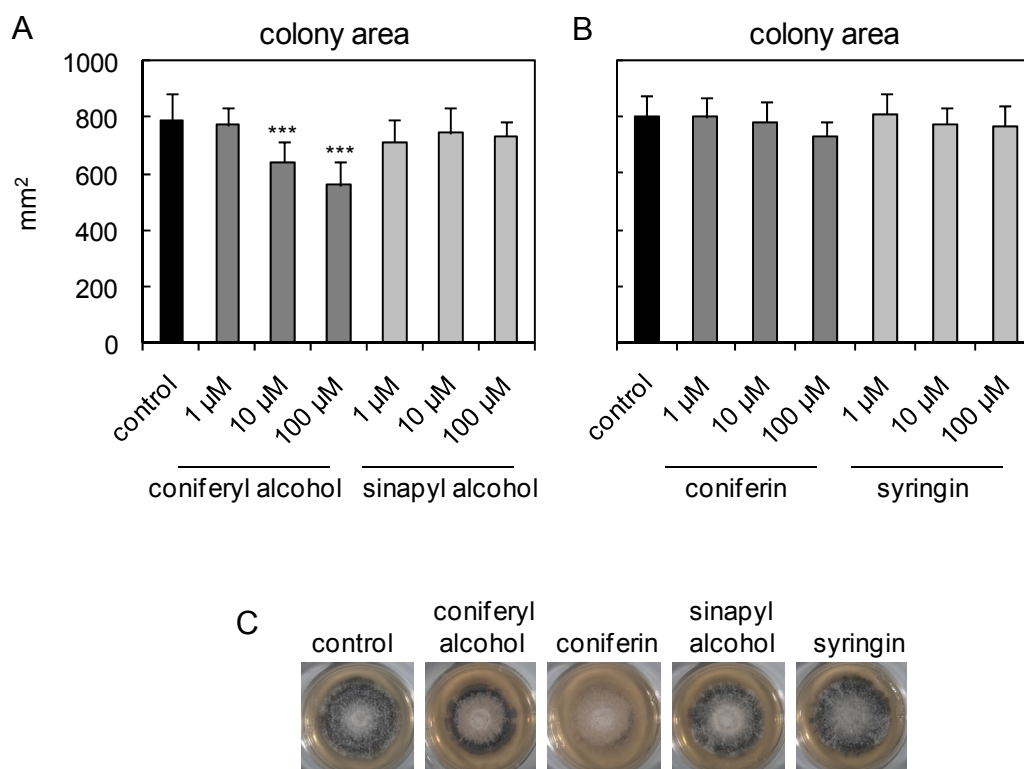


**Fig. 22: Influence of monolignols and their glucosides on *V. longisporum* growth.**

PDB plates were supplemented with coniferyl alcohol, sinapyl alcohol, coniferin and syringin in the indicated concentrations. A, B) After inoculation the fungus was grown for 17 days on these plates. Pictures of colonies were taken under a binocular and the colony area was determined. The data represent the mean values of at least eight different plates of three independent experiments (A) or of at least four different plates of two independent experiments (B). Asterisks indicate significant differences between control and supplemented plates according to student's t-test (\*\*\*)  $p \leq 0.001$ . C) The fungus was grown for 28 days on the PDB plates with 100 µM of the indicated substances. The experiment was performed on at least four plates per condition out of two independent experiments with similar results.

#### 3.3.4.4 Lignans and infection

For the lignans no mutant plants were available apart from a pinoresinol reductase double mutant (Nakatsubo et al, 2008). In this mutant the conversion of pinoresinol to lariciresinol is disturbed, thus no lariciresinol is synthesized but instead pinoresinol accumulates (Fig. S12). This mutant was analyzed for its susceptibility against *V. longisporum* infection, but no difference in the stunting was visible compared to wild type (Fig. S2).

In addition, the same fungal growth test, as for coniferin and syringin, was performed with different lignans (lariciresinol, pinoresinol, pinoresinol diglucoside (PDG)) to determine whether they influence fungal growth. But in the range of the tested concentrations (1, 10 and 100  $\mu\text{M}$ ) no reduction in fungal growth could be detected (Fig. S13).

### 3.3.5 Relevance of the phenylpropanoid and indole markers for the development of infection symptoms

In *Arabidopsis*, mutants are known that do not display symptoms after infection with *V. longisporum*, although they are infected (Anjali Ralhan, (Rg Prof. Gatz, Göttingen), personal communication). These *coi1* mutants are defective in the perception of the phytohormone jasmonic acid (Xie et al, 1998). Absent infection symptoms in infected *coi1* plants correlate with reduced fungal propagation after 10 dpi. (Anjali Ralhan, personal communication). In comparison to this JA perception mutant, mutants impaired in JA synthesis, like the allene oxide synthase knock out mutant (*dde2*, (von Malek et al, 2002)), behave like wild type. This phenomenon was also published for the infection of *Arabidopsis* with *Fusarium oxysporum* (Thatcher et al, 2009). How the fungus uses the COI1-perception system in the infection is not known so far.

The JA mutants were used to investigate, if the infection markers described here are correlated to symptom development. In this case changes in the amount of the markers should be visible in infected wild type and *dde2-2* plants but not in *coi1-t* mutant plants. Samples for these analyses were kindly provided by Anjali Ralhan. They were divided into petioles and lamina of the leaves. As petioles mainly consist of vascular tissue, a stronger response would be expected in these samples, if differences were not systemic but locally present at the fungal infection site.

From the phenylpropanoid markers sinapoyl glucose, coniferin and lariciresinol glucosides were analyzed (Fig. 23). No strong differences were observed between *coi1-t*, *dde2-2* and wild type plants for these metabolites. In all of them the markers were strongly induced upon infection. Differences could be observed in the comparison of lamina and petiole samples. In petioles of control plants sinapoyl glucose was in the same range as in the lamina, but upon infection the increase in amount was stronger in the petioles (up to  $1.1 \mu\text{mol g}^{-1} \text{FW}$ ) than in the lamina (up to  $0.5 \mu\text{mol g}^{-1} \text{FW}$ ). The coniferin amount in the petioles of control plants was eight times higher compared to the lamina. In both leaf parts an induction of coniferin biosynthesis occurred upon infection, which was slightly higher in the petiole. Also for lariciresinol glucosides the amount in the controls was slightly higher

in the petioles, but upon infection in both parts of the leaves the amount of lariciresinol reached comparable values between 0.13 and 0.19  $\mu\text{mol g}^{-1}$  FW.

In summary the phenylpropanoids were higher concentrated in the petioles than in the lamina, but in both tissues an accumulation of the metabolites occurred upon infection. No differences in this metabolic response could be detected in the JA mutants. Based on these data it could be concluded that the different infection symptoms are not directly related to different amounts of phenylpropanoid monomers.

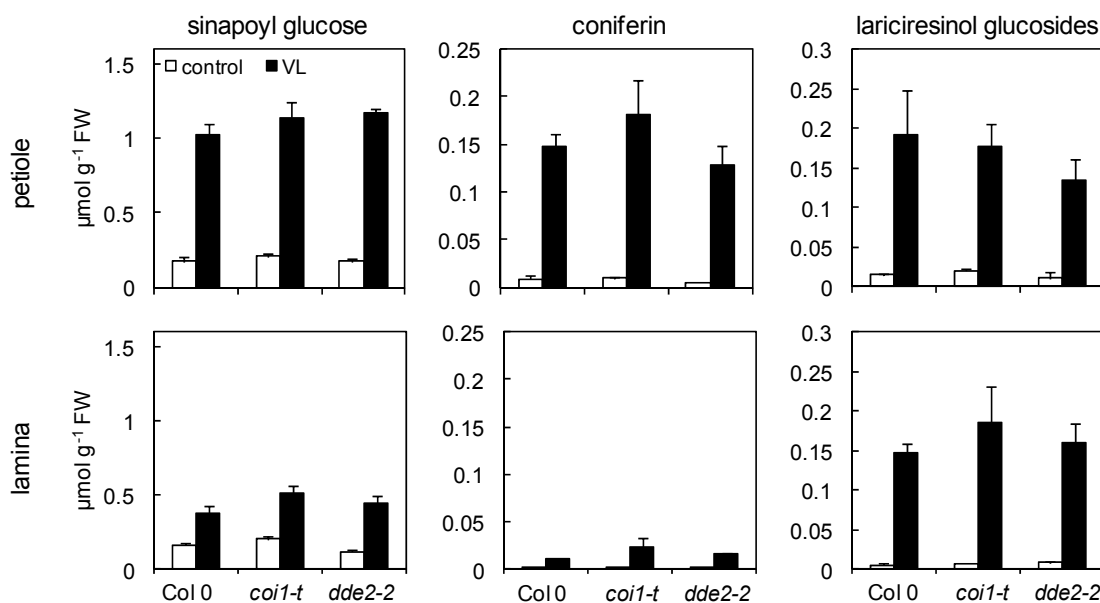


**Fig. 23: Determination of phenylpropanoid markers in lamina and petiole samples of *V. longisporum* infected JA mutants.**

Col 0, *coi1-t* and *dde2-2* plants were infected by root dip inoculation. Control (white bars) and infected plants (black bars) were harvested at 21 dpi and leaf samples were divided in lamina and petioles. The methanolic leaf extracts were analyzed by RP-HPLC-DAD. Coniferin and lariciresinol glucosides were measured after deglycosylation of the samples. The mean values of four biological replicates are shown  $\pm$ SD. Plant material for this analysis was received from Anjali Ralhan (Rg Prof. Gatz, Göttingen).

In addition to the phenylpropanoids, indole glucosinolates were analyzed in these samples (Fig. 24). In principle the accumulation of these metabolites in infected wild type plants was stronger compared to the *dde2-2* and *coi1-t* plants. For I3G differences between lamina and petiole samples were detected. In the petioles I3G was enriched in infected wild type plants, whereas in the lamina the amount was decreased upon infection. The amount in the petioles of control samples was around 75 % lower in *coi1-t* and 50 % in *dde2-2* mutant plants compared to wild type. In both mutants no change in the amount of this metabolite was detectable upon infection. Also in the lamina I3G amounts in the control samples of the mutants were lower than in wild type but upon infection it

decreased like in wild type plants. For 4MI3G similar amounts in control samples of petioles and lamina in all three plant lines were detected. Upon infection the amount increased mostly in the wild type petioles (2.6 times) but also in the lamina an increase was detectable (1.7 times). In *coi1-t* plants just a small increase was detected in the petioles (1.3 times) but no change in the lamina was observed. The increase of 4MI3G in *dde2-2* mutant plants was in-between wild type and *coi1-t* (1.8 times in the petioles, 1.2 times in the lamina). The most severe differences between the mutant and wild type plants occurred for 1MI3G. In wild type the amount was around 10 times less in the lamina compared to the petioles. Upon infection, a strong induction of this metabolite was detected in both parts of the leaves. In each mutant the amount was obviously lower than in the wild type. In the petioles of control plants it reached  $0.04 \mu\text{mol g}^{-1}$  FW in the *coi1-t* and  $0.1 \mu\text{mol g}^{-1}$  FW in the *dde2-2* compared with  $0.38 \mu\text{mol g}^{-1}$  FW in wild type. Only a small increase was detectable in petioles of *coi1-t* (1.3 times) and in *dde2-2* mutant plants (1.4 times) after infection. In the lamina 1MI3G could not be detected in both mutants.

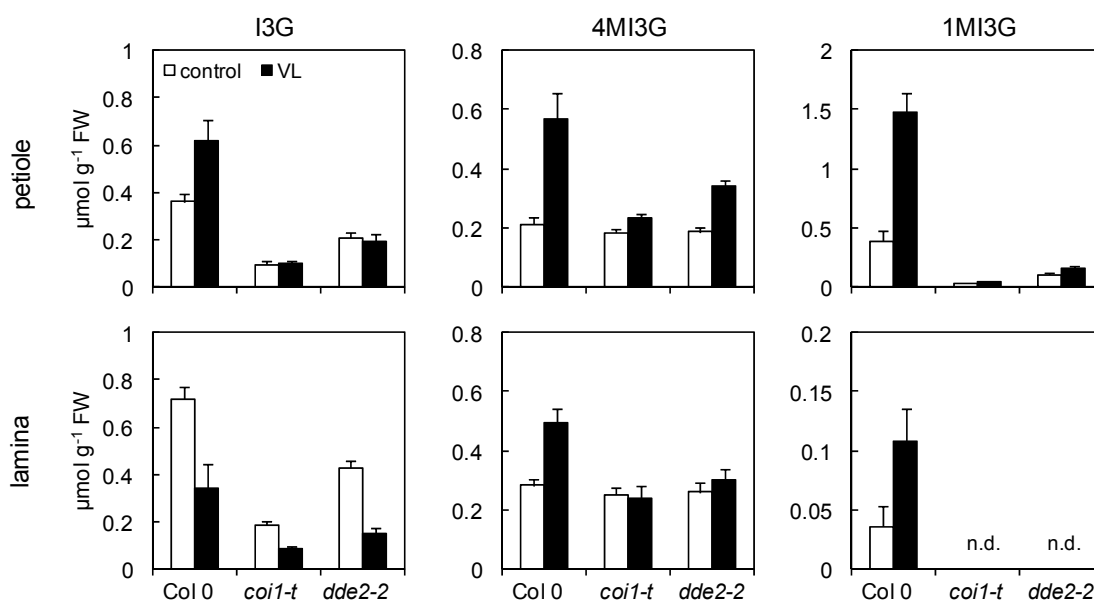


**Fig. 24: Determination of indolic markers in lamina and petiole samples of *V. longisporum* infected JA mutants.**

Col 0, *coi1-t* and *dde2-2* plants were infected by root dip inoculation. Control (white bars) and infected plants (black bars) were harvested at 21 dpi and leaf samples were divided in lamina and petioles. The methanolic leaf extracts were analyzed by RP-HPLC-DAD. The mean value of four biological replicates is shown  $\pm$ SD. Plant material was received from Anjali Ralhan (Rg Prof. Gatz, Göttingen). n.d.: not detectable.

In summary two of the three indole glucosinolates were reduced in the JA mutants and also the enrichment of the three metabolites in the petioles upon infection could not be detected in the mutants. But the differences were true for both mutants. Thus the indole

glucosinolates accumulate via the JA signaling machinery upon infection, but are not correlated to the infection symptoms.

### 3.3.6 Undirected metabolite fingerprinting to find markers involved in symptom development of Arabidopsis challenged with *V. longisporum*

As the phenylpropanoid and the indolic markers seem not to be involved in the symptom development, further analyses were performed to identify the responsible metabolites. For this purpose untargeted metabolite fingerprinting of Col 0, *coi1-t* and *dde2-2* infected plants was performed. The infection of these plants resulted in similar phenotypes as described by Anjali Ralhan for these mutants (personal communication): Infection of *dde2-2* led to symptoms comparable to wild type, but in the *coi1-t* mutant no symptoms were detectable (Fig. S14).

The undirected metabolite fingerprinting of the leaves of these plants was performed with samples of 10 and 14 dpi. It resulted in 2002 markers in positive ionization mode and 1803 markers in the negative ionization mode with a cut off at  $p < 10^{-5}$ . The already analyzed phenylpropanoid and indole markers showed a similar pattern like in the directed analysis. The lignans seemed to be delayed in their accumulation in the *coi1-t* mutant as the amount was lower in infected *coi1-t* plants than in Col 0/*dde2-2* ones, but also here the accumulation was obvious (Fig. S16).

In this experiment only the differences between Col 0/*dde2-2* and *coi1-t* have been of interest. Therefore reclustering of markers that were different in *coi1-t* compared to Col 0/*dde2-2* was performed based on the 1D-SOM in Fig. S15. Eleven clusters with 1044 markers were chosen for the reclustering. From the 1D-SOM of the reclustering process especially in clusters 1-4 and cluster 6 markers were detected which accumulate in Col 0/*dde2-2* plants upon infection but not in *coi1-t* (Fig. 25A). Representative box plots of metabolites from those clusters are shown in Fig. 25B. Using database searches the masses of different amino acids (glutamine, valine, asparagine, arginine, histidine and leucine) could be identified. All of them were enriched in infected Col 0 and *dde2-2* plants already at 10 dpi but not in *coi1-t* plants. Also the masses of malate and SAG could be detected in those clusters. Malate was not enriched at 10 dpi but at 14 dpi in Col 0 and *dde2-2* but not in *coi1-t* plants.

Additionally in the clusters 24-30 interesting intensity patterns could be detected, but for them as well as for many of the markers in cluster 1-4 and 6 so far no reliable database hit was received. Those markers need to be further analyzed with different analytical methods.

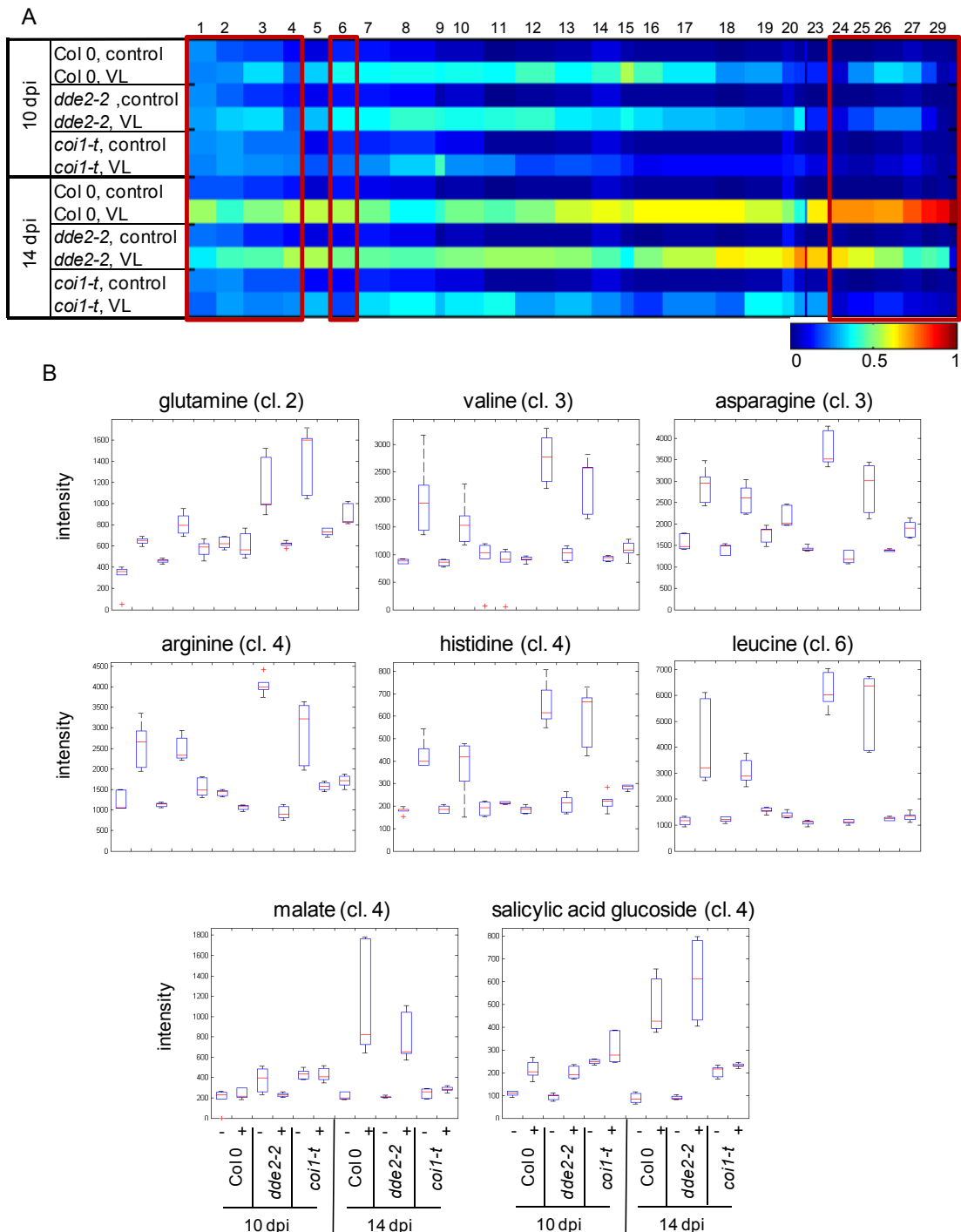


**Fig. 25: UPLC-MS(TOF) based undirected metabolite fingerprinting of *V. longisporum* infected Col 0, *dde2-2* and *coi1-t* Arabidopsis leaves.**

Col 0, *dde2-2* and *coi1-t* plants were infected by root dip infection and harvested at 10 and 14 dpi. Homozygous *coi1-t* plants were detected after harvest by PCR analysis. Leaf material of three samples per condition was extracted by two phase partitioning, leading to a methanol phase with polar substances and a chloroform phase with non-polar substances. Shown markers derived from analyses of the methanol phase. Each sample was measured twice. A) 1D-SOM of 1044 markers related to differences between Col 0 and *dde2-2* to *coi1-t*. Markers of different infection time points (10 and 14 dpi) of infected (+) and control (-) plants were grouped into 30 clusters based on their intensity profile. Interesting prototypes which include markers with no changes in *coi1-t* samples but changes in Col 0/*dde2-2* are marked in red. B) Box plots of markers induced in Col 0 and *dde2-2* plants but not in *coi1-t* plants. cl.: cluster. The analysis was performed together with Dr. Kirstin Feussner.

### **3.4 Analysis of hydroxy and dicarboxy fatty acids in the interaction of Arabidopsis and *V. longisporum***

In preliminary analyses dicarboxylic fatty acids and hydroxy fatty acids were detected to be affected in response to *V. longisporum* infection in Arabidopsis. The repetition of the undirected approach with material of both infection methods did not confirm these preliminary data (see section 3.2). Nevertheless analyses concerning these compounds were performed because both metabolic groups, where these substances belong to, were described to be involved in plant-pathogen interactions (see sections 1.5.3 and 1.6.3). Hydroxy and dicarboxy fatty acids may be monomers of suberin and cutin. Suberin is one barrier in the roots against invading pathogens, and even its involvement in different *Verticillium* interactions has been already described (Gold & Robb, 1995; Lee et al, 1992; Ranathunge et al, 2008). Therefore, it was of interest to investigate the impact of suberin and cutin on *V. longisporum* infection. Determination of suberin and cutin monomers in infected plants was done and different suberin mutants were analyzed for their susceptibility against *V. longisporum*.

Additionally,  $\alpha$ -hydroxy fatty acids which may be parts of sphingolipids (preferentially in glucosylceramides) in the plants were analyzed. Because also sphingolipids are described to be involved in plant pathogen interactions (Liang et al, 2003; Wang et al, 2008), this metabolic class was of interest for this thesis.  $\alpha$ -Hydroxylase mutants were generated and characterized and tested in infections.

#### **3.4.1 Suberin and cutin**

##### **3.4.1.1 Composition of cutin and suberin monomers in infected plants**

Suberin in the roots and cutin in the leaves were analyzed at early time points of infection (5, 7 and 10 dpi). These infections were performed under long day conditions because more root material was available than under short day conditions. For analyzing these polymers, first all extractable lipids were removed by longsome extractions with different solvents. The resulting cell wall residue was methanolized and the monomers analyzed by GC-FID.

In Fig. 26 the amounts of suberin and cutin monomers detected at 10 dpi are shown. Controls and samples of the infected plants did not reveal any differences, neither in the amount nor in the composition of cutin and suberin monomers. The other time points (5 and 7 dpi) are not shown in the figure because the results were similar with those obtained at 10 dpi.

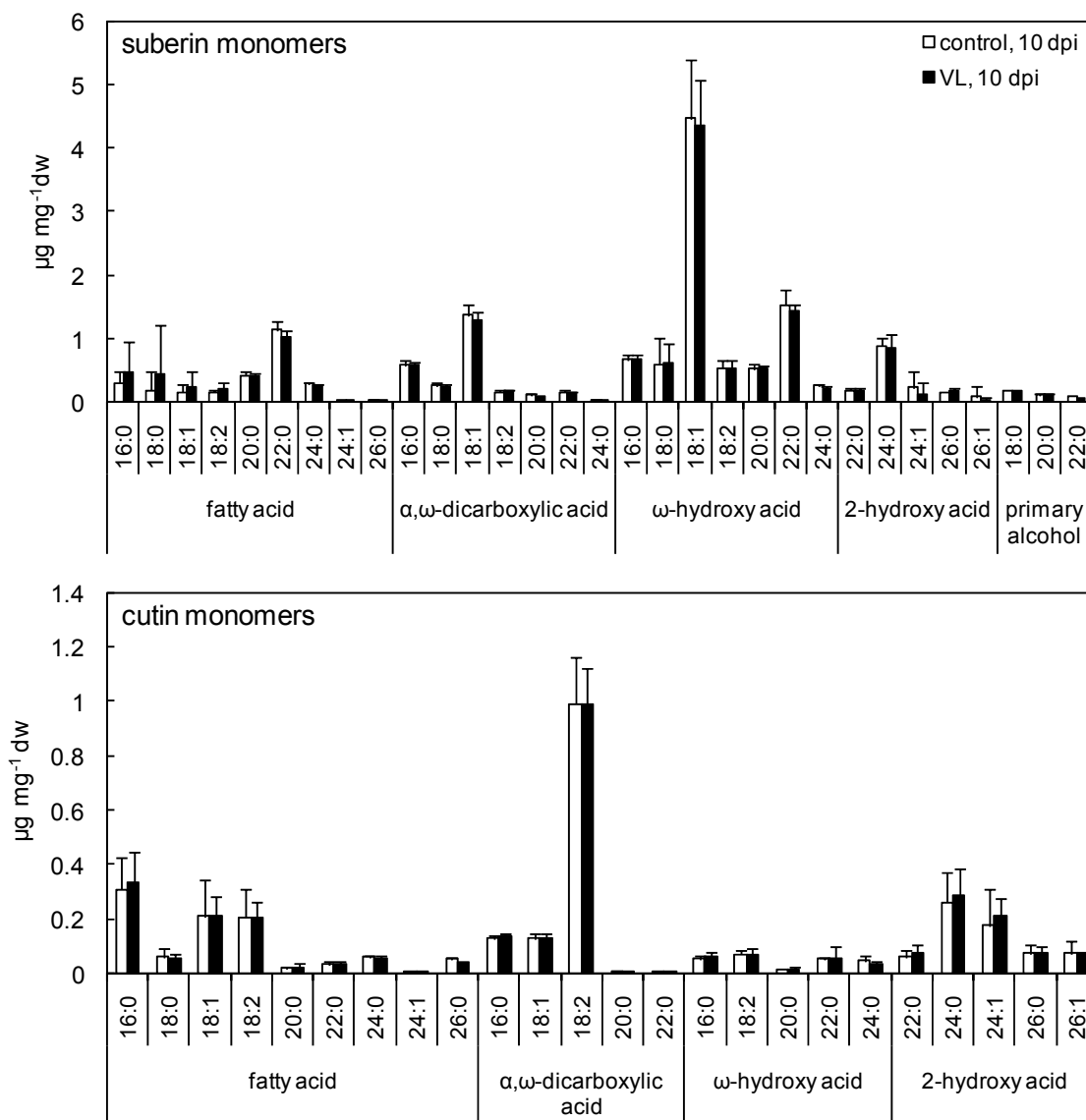


**Fig. 26: Determination of cutin and suberin monomers in *V. longisporum* infected plants.**

Plants were grown under long day conditions and infected by root cut infection. Root and leaf material was harvested at 10 dpi. The material was extracted by extensive treatment with different solvents and the resulting residue was methanolized by methanolic HCl. Monomers were analyzed using GC-FID. The data represent the mean values of at least six biological replicates from two independent experiments  $\pm$ SD.

### 3.4.1.2 Infection of suberin mutants with different infection methods

Although no differences in suberin and cutin monomers were detectable, different suberin mutants were analyzed, to determine the influence of a reduction of distinct monomers or of total suberin on the susceptibility of the plants against *V. longisporum*. Mutations in two different enzyme classes were examined. One class was the CYP86 family, which is described to be involved in the  $\omega$ -hydroxylation of fatty acids. Here, *cyp86a1-2* is described to have reduced amounts of dicarboxylic acids and  $\omega$ -hydroxy fatty acids in a

chain length of C16 to C20 and a reduction of 60 % of total suberin (Compagnon et al, 2009). In *cyp86b1-2* plants instead, reductions especially in monomers with chain length of C22 and C24 and no reduction in total suberin are described (Höfer et al, 2008). The third mutant tested was the *gpat5-1*. Here a defect in an acyl-CoA:glycerol-3-phosphate acyltransferase also results in a monomer reduction in the longer chain length monomers and a total reduction of suberin to 50 % in young roots (Beisson et al, 2007).

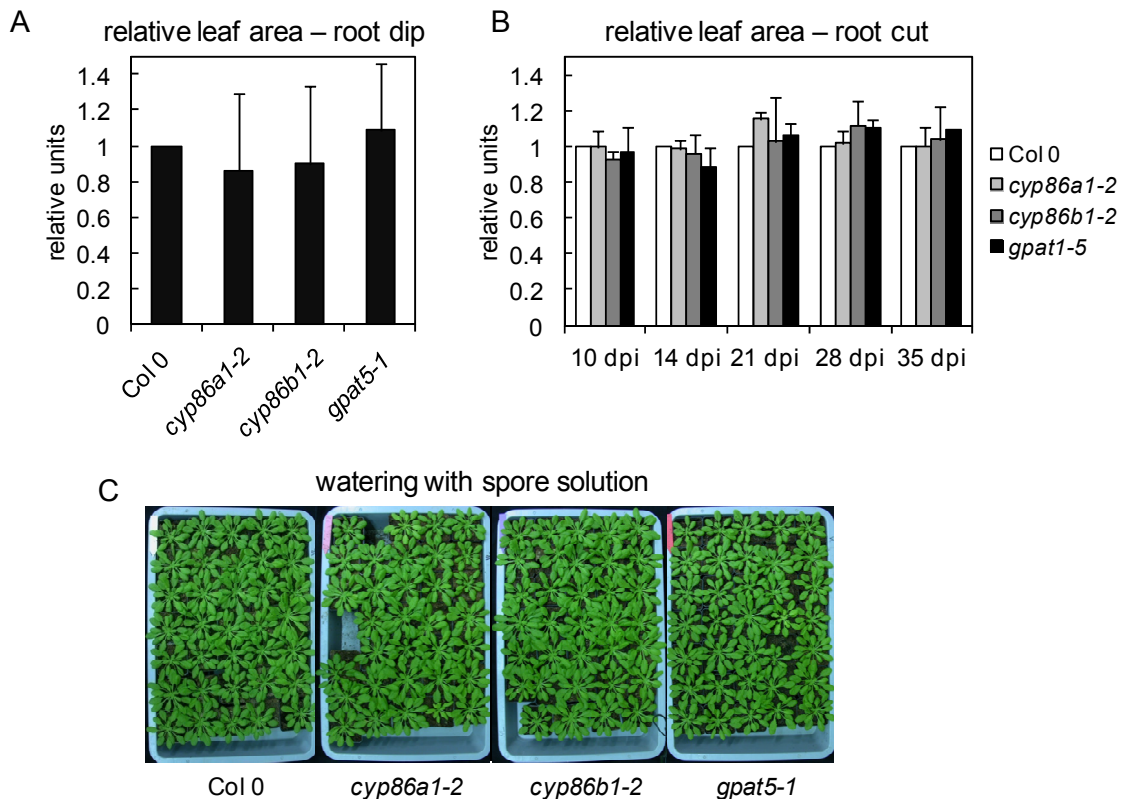


**Fig. 27: Infection of suberin mutants with different infection methods.**

A) Col 0, *cyp86a1-2*, *cyp86b1-2* and *gpat5-1* were infected by root dip infection and the relative leaf area was determined at 21 dpi: The leaf area of infected plants was divided by the leaf area of control plants and the results of the mutant plants were set in relation to the value of the wild type. The mean values of two independent experiments are shown  $\pm$ SD. B) Col 0 (white bars), *cyp86a1-2* (bright gray bars), *cyp86b1-2* (dark grey bars) and *gpat5-1* (black bars) were infected by root cut infection method and the leaf area was determined at indicated time points. The mean values of three independent experiments are shown  $\pm$ SD. C) Plants were infected without root damage by watering soil grown plants with spore solution. Displayed are only the inoculated plants at 21 dpi.

The mutants were tested with different infection methods to analyze their susceptibility against the fungus. As shown in Fig. 27 no significant differences compared to wild type in stunting of the leaves were visible, neither with the root cut nor with the root dip infection method. As the roots get damaged with both infection methods and therefore the suberin

layer may also be already impaired before the infection, an infection method without damaging the roots was tried. Plants grown on soil were directly inoculated with spore solution, but this treatment did not result in any infection symptom.

### 3.4.2 $\alpha$ -Hydroxy fatty acids

In this section, mutants of the *AtFAH1* and *FAH2* genes in *Arabidopsis* were further characterized. They are described in the literature to be  $\alpha$ -hydroxylases of the sphingolipid fatty acid moiety in *Arabidopsis* (Nagano et al. 2009). But this was not shown directly in plants so far. T-DNA insertion lines of these genes were obtained from the Nottingham *Arabidopsis* Stock Centre (NASC) and a double mutant was generated. The mutants were examined for their changes on the metabolic level and for their behavior against biotic stress, including *V. longisporum* infection.

#### 3.4.2.1 Characterization of T-DNA insertion lines of *AtFAH1* and *AtFAH2*

For each gene one T-DNA insertion line was available at the stock centre. Homozygous plants were generated of these lines by selfing and gene expression analysis was performed. The result of the RT-PCR analysis showed that the insertion in the *fah1* line did not lead to a total knock out – still residual gene expression was detectable (Fig. 28A). This is in agreement with the prediction of the insertion side which is in the promoter of the gene ([http://atensembl.arabidopsis.info/Arabidopsis\\_thaliana\\_TAIR/index.html](http://atensembl.arabidopsis.info/Arabidopsis_thaliana_TAIR/index.html)). The *fah2* mutant was determined to be a total knock out with no detectable RNA of the gene left. The prediction of the insertion side by NASC is in the fifth exon of the gene. Because both lines did not display a growth phenotype, they were also crossed to obtain a double mutant. This double mutant showed a phenotype with smaller, curled and wrinkled leaves when grown under long day conditions (Fig. 28B, C). This phenotype was not detectable under short day conditions.

The reduced leaf area of the double mutant was also quantified. In 24-day-old plants, grown under long day conditions, leaves were 25 % smaller than in wild type plants (Fig. 28E). Additionally, the root length was determined in plants vertically grown on agar plates. It was around 25 % reduced in 14-day-old double mutants (Fig. 28D, F). As a third parameter, the flowering time point was determined to elucidate, if the growth reductions were due to developmental changes or to growth reductions. The flowering time point was determined by counting the rosette leaves at the time point where the plants exhibit an inflorescence stem of one centimeter. For this parameter no difference could be detected between double mutant and wild type (Fig. 28G).

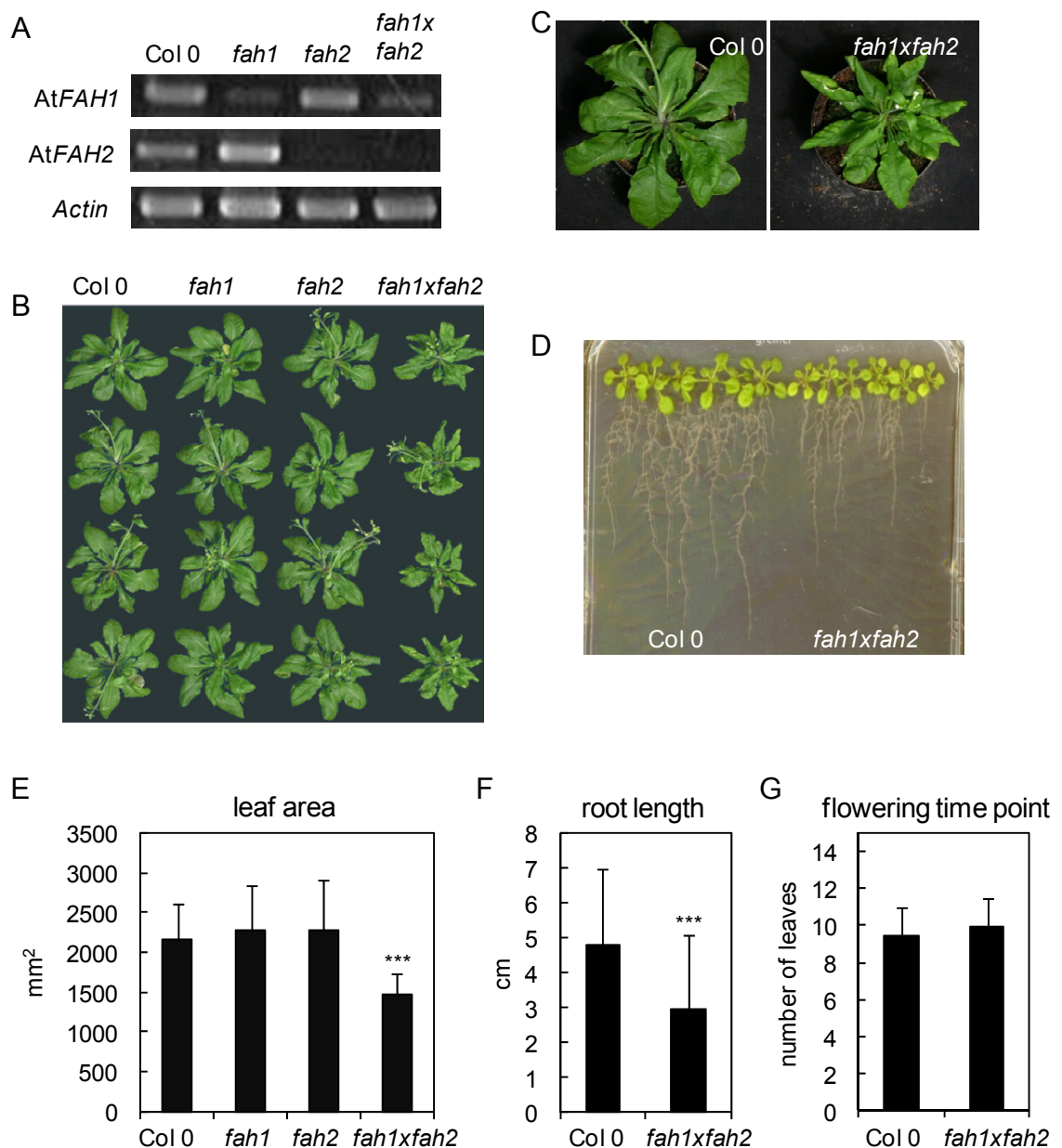


**Fig. 28: T-DNA insertion lines of *AtFAH1* and *AtFAH2* in Arabidopsis.**

A) The transcript levels of the *AtFAH1* and *AtFAH2* genes in Col 0, *fah1* (SALK\_140660), *fah2* (SAIL\_862\_H01) and *fah1xfah2* were analyzed by semiquantitative RT-PCR of leaf material. B, C) Pictures of the single and double mutant plants grown for 31 days under long day conditions. D) Root growth of Col 0 and *fah1xfah2* plants grown vertically on MS agar plates E) Leaf area quantification of plants grown for 24 days under long day conditions on soil. The data represent the mean values of 16 plants out of three independent experiments  $\pm$ SD. F) Root growth quantification of plants grown for 14 days under long day conditions on vertical MS agar plates. The mean values of 72 plants per line out of three independent experiments are shown  $\pm$ SD. G) Determination of the flowering time point of long day grown plants. The numbers of leaves were determined when the inflorescence stem of the plants had a height of 1 cm. The mean values of 24 plants per line out of three independent experiments are shown  $\pm$ SD. Asterisks indicate significant differences between control and infected plants according to student's t-test (\*\*\*)  $p \leq 0.001$ .

In order to confirm that the indicated mutations are the reason for the growth phenotype, the double mutant was complemented by introducing the *AtFAH2* gene behind a 35S promoter into the double mutant by *Agrobacterium tumefaciens* mediated transformation. The transformation resulted in the T3 generation in hygromycin resistant lines with mutant phenotype and lines with wild type phenotype (Fig. 29). No expression of the introduced *FAH2* gene was detectable in the lines with the mutant phenotype, but in the lines with the wild type phenotype low amounts of mRNA were detectable.

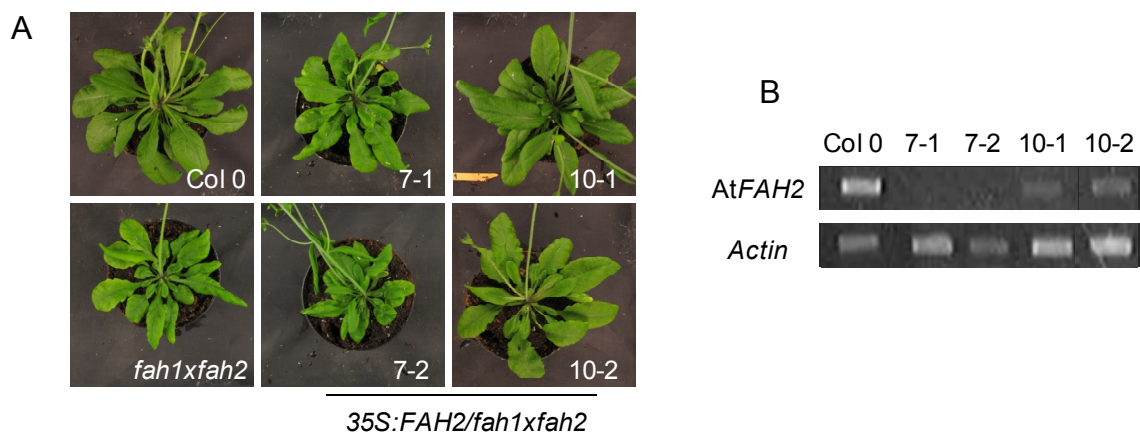


**Fig. 29: Complementation of the *fah1xfah2* double mutant.**

The *fah1xfah2* double mutant was transformed with *AtFAH2* under the 35S promoter. Resulting T3 plants were analyzed by RT-PCR. A) Wild type, double mutant and two transformed lines grown for 35 days under long day conditions are shown. B) Semiquantitative RT-PCR was performed to analyze the expression of the introduced gene.

#### 3.4.2.2 Expression analysis of *AtFAH1* and *AtFAH2* by GUS staining

To compare the expression of both *FAH* genes in different tissues, promoter:GUS fusions were generated and introduced in Col 0 Arabidopsis plants by *Agrobacterium tumefaciens* mediated transformation. For GUS expression analyses of the transformed plants, tissue of different age was used. For both genes the staining was similar (Fig. 30). In 14-day-old seedlings expression was visible in the whole seedling – in the roots and in the shoots. Also in young rosette leaves of 28-day-old plants expression was detectable but not in old leaves of the same plant. Also in floral buds including the young part of the inflorescence stem and the young leaves at the stem blue coloration of the staining was detected. In the open flower expression was restricted to the pollen.

In summary the expression of both genes was detected in young growing tissue and in the pollen.

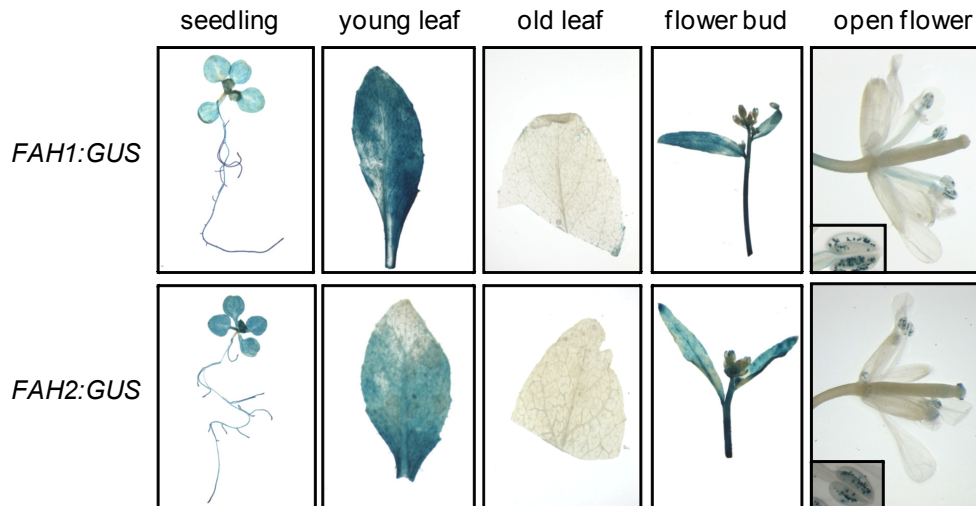


**Fig. 30: Gene expression of *AtFAH1* and *AtFAH2* in different tissues.**

Localization of GUS activity in *Arabidopsis* plants transformed with *AtFAH* promoter GUS fusions. Transformed plants were grown under long day conditions on soil, except the seedlings were grown on MS agar plates. Staining was performed with three independent plant lines of each construct with comparable results.

### 3.4.2.3 Ceramide and glucosylceramide analysis

To analyze the metabolic consequences of the T-DNA insertion in the *FAH* genes, two classes of sphingolipids in these mutants were determined.

Long chain bases, ceramides, glucosylceramides and glycosylinositolphosphoryl ceramides are the main sphingolipid species in *Arabidopsis*. Till now only ceramides and glucosylceramides were measured in the mutant plants (Fig. 31). These metabolites harbor hydroxy groups which can be present in different positions in the molecule. Dihydroxy ceramides harbor two hydroxy groups at position C-1 and C-2 in the long chain base. Trihydroxy- $\alpha$  ceramides contain an additional hydroxy group in the fatty acid moiety at the  $\alpha$  position, whereas in trihydroxy-phyto ceramides the third hydroxy group is in C-4 position at the long chain base. Tetrahydroxy ceramides contain both additional hydroxy groups. It was expected that in the double mutant the trihydroxy- $\alpha$  and the tetrahydroxy ceramides and glucosylceramides were reduced.

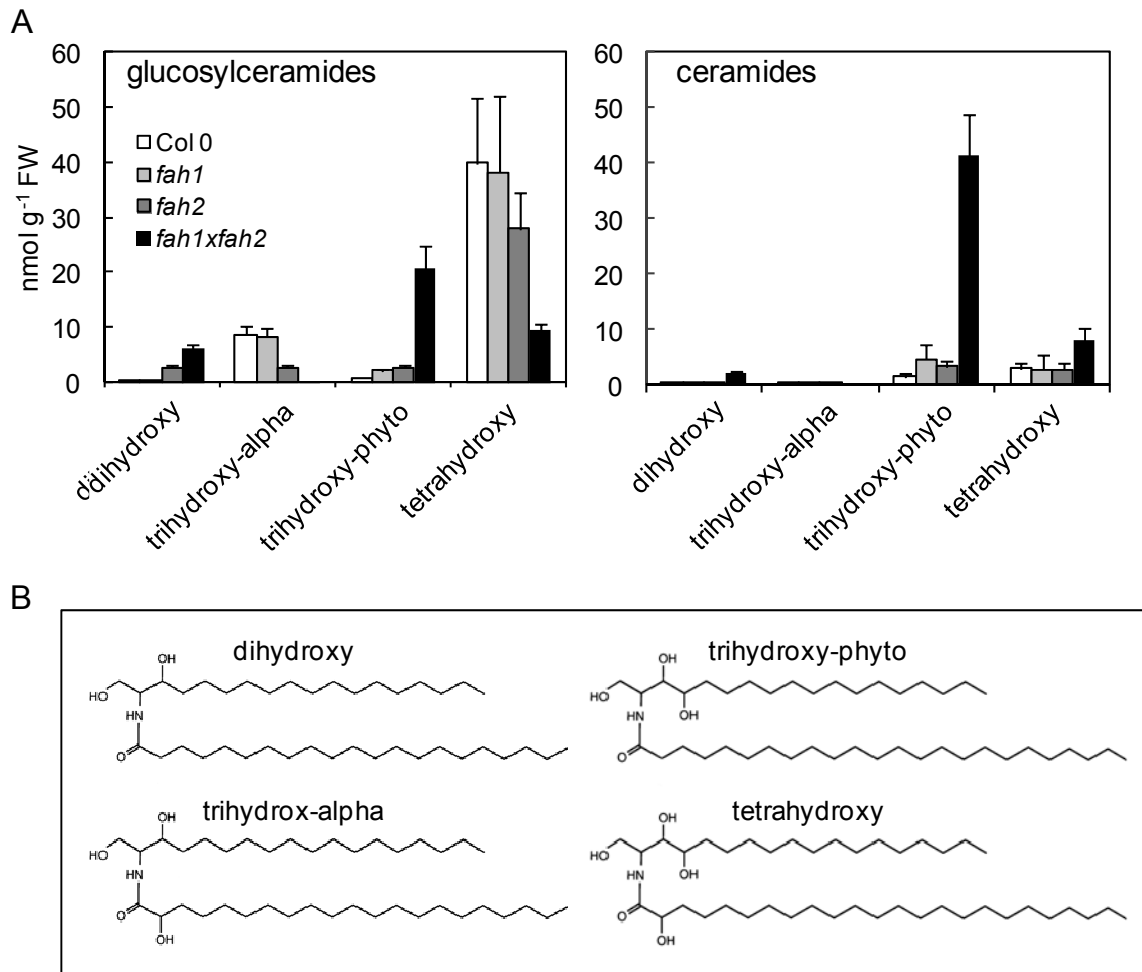


**Fig. 31: Determination of ceramides and glucosylceramides in  $\alpha$ -hydroxylase mutant plants.** Col 0 (white bars), *fah1* (bright grey bars), *fah2* (dark grey bars) and *fah1xfah2* (black bars) plants were grown for 35 days under long day conditions. Ceramides and glucosylceramides were extracted from leaf material by chloroform:methanol extraction, SPE-separation and alkaline hydrolysis. The mean values of six biological replicates out of two independent experiments are shown  $\pm$ SD. Extracted ceramides and glucosylceramides were analyzed by Dr. Kirstin Feussner. B) Different possibilities of the hydroxylation of the ceramides.

In general the analysis showed that  $\alpha$ -hydroxylated ceramides could be detected especially in the glucosylceramide pool and only in trace amounts in the ceramide pool as it is also described in the literature (Pata et al, 2010). For the glucosylceramide analysis the changes in the double mutant were as expected (Fig. 31). The amount of trihydroxy-alpha was much lower in the double mutant ( $0.1 \text{ nmol g}^{-1} \text{ FW}$ ) than in the wild type ( $10 \text{ nmol g}^{-1} \text{ FW}$ ). Also the amount of the tetrahydroxy species was with  $10 \text{ nmol g}^{-1} \text{ FW}$  lower compared to wild type plants with  $40 \text{ nmol g}^{-1} \text{ FW}$ . In contrast to this, the dihydroxy and the trihydroxy-phyto glucosylceramides were ten times higher in the double mutant than in the wild type.

In the ceramide pool both species also accumulated in large amounts in the double mutant. The trihydroxy-phyto ceramides were ten times higher (4 nmol g<sup>-1</sup> FW in the wild type, 40 nmol g<sup>-1</sup> FW in the double mutant) than in wild type plants. Trihydroxy-alpha ceramides were only detectable in trace amounts and not detectable in the double mutants. The tetrahydroxy ceramide amount in the double mutant was enriched from 3 nmol to 8 nmol g<sup>-1</sup> FW compared to wild type.

For the single mutants only minor differences could be detected, which were in general slightly stronger in the *fah2* mutant than in the *fah1* mutant.

The data shown and described here were only the sums of the different ceramide and glycosyl ceramide species analyzed. Also determination of the different chain lengths and desaturation of these species was performed. In total, the differences between mutants and wild type plants were quite equally distributed to all the different species of one group (Fig. S17, Fig. S18).

#### 3.4.2.4 Metabolite fingerprinting of the *fah1xfah2* mutant

To elucidate, if the changes in the ceramide pools have a further influence on the metabolism of the plants, metabolite fingerprinting was performed to compare the *fah1xfah2* double mutant with wild type plants. Plants of three different ages (14, 24 and 35 days) were chosen for the analysis to determine the differences in a growth and developmental dependent time course. 14-day-old plants were chosen because no differences in the growth phenotype of the double mutant compared to wild type could be detected at this time point, at 24 days the leaves started to differ and at 35 days the differences were obvious.

1689 markers were detected in the methanol phase measured in positive ionization mode and 1560 in negative ionization mode with a p-value < 10<sup>-3</sup>. The 1D-SOM shows that most of the markers were correlated to developmental changes (Fig. 32A). Differences between double mutant and wild type plants were detected in six out of the 30 clusters. The most obvious markers were related to SA, which was detected in cluster 23 (Fig. 32B). It accumulated in young double mutant plants where no phenotypic differences were yet visible. In older plants this accumulation was reduced to nearly wild type levels in the 35-day-old plants. In comparison to this, SAG detected in cluster 15, was stronger enriched in the older plants than in the 14-day-old plants. Also the structurally related protocatechuate glucoside (a dihydroxy benzoic acid) was detected to accumulate in the *fah1xfah2* plants and showed enrichment over the time period in the double mutant plants. Next to these obvious markers also different other markers with database hits from different secondary metabolite pathways like indolics, aliphatic glucosinolates or flavonoids were detected, but so far they have not been verified.

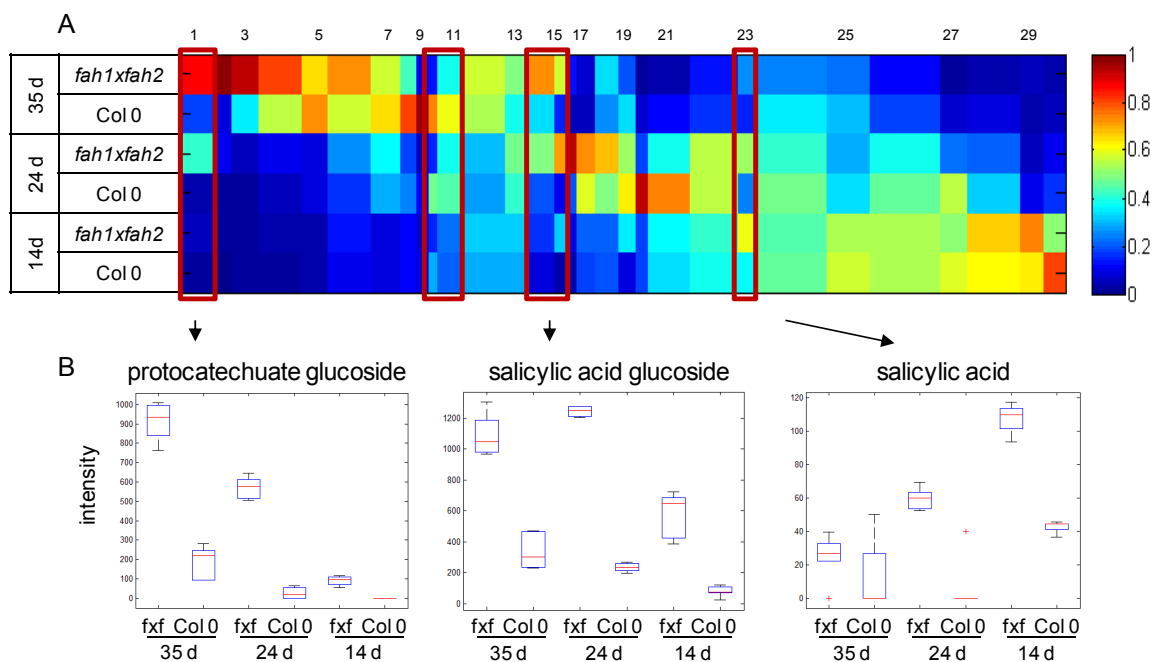


**Fig. 32: Metabolite fingerprinting of *fah1xfah2* leaves (polar phase).**

Plants were grown under long day conditions for 14, 24 and 35 days (d). Leaf material was extracted by two phase partitioning, leading to a methanol phase with polar metabolites and a MTBE phase with unpolar metabolites. A) 1D-SOM of 1689 markers from the methanol fraction of the extraction measured in positive ionization mode and 1560 from the measurement in negative ionization mode. Markers of different growth time points were grouped into 30 clusters based on their intensity profile. In the red boxes the cluster are marked which are dependent on the mutation. B) Box plots of prominent markers from different clusters which accumulate in the double mutant plants. For the analysis four biological replicates per treatment were measured twice. fxf: *fah1xfah2* mutant plants.

In the unpolar phase 1064 markers were detected in the positive ionization mode and 802 markers in the negative ionization mode. Here as well, most of the markers were developmental dependent and 10 out of 30 clusters could be related to the mutation (Fig. 33A). In the positive ionization mode some ceramides and glucosylceramides were detected that have been already described in the directed analysis (Fig. 33B). In the undirected approach it could not be distinguished between trihydroxy- $\alpha$  and trihydroxy-phyto, but in principle the results were in line with the directed measurements. Interestingly, apparently shorter chain length trihydroxy-phyto ceramides (C16-C22) accumulate only in older *fah1xfah2* plants and not like the ceramides with longer chain length or the glucosylceramides already in 14-day-old plants.

In addition also in this unpolar phase different markers could still not be assigned to distinct metabolites. A group of markers received database hits for different phospholipids but these hits need to be further verified by directed measurements.

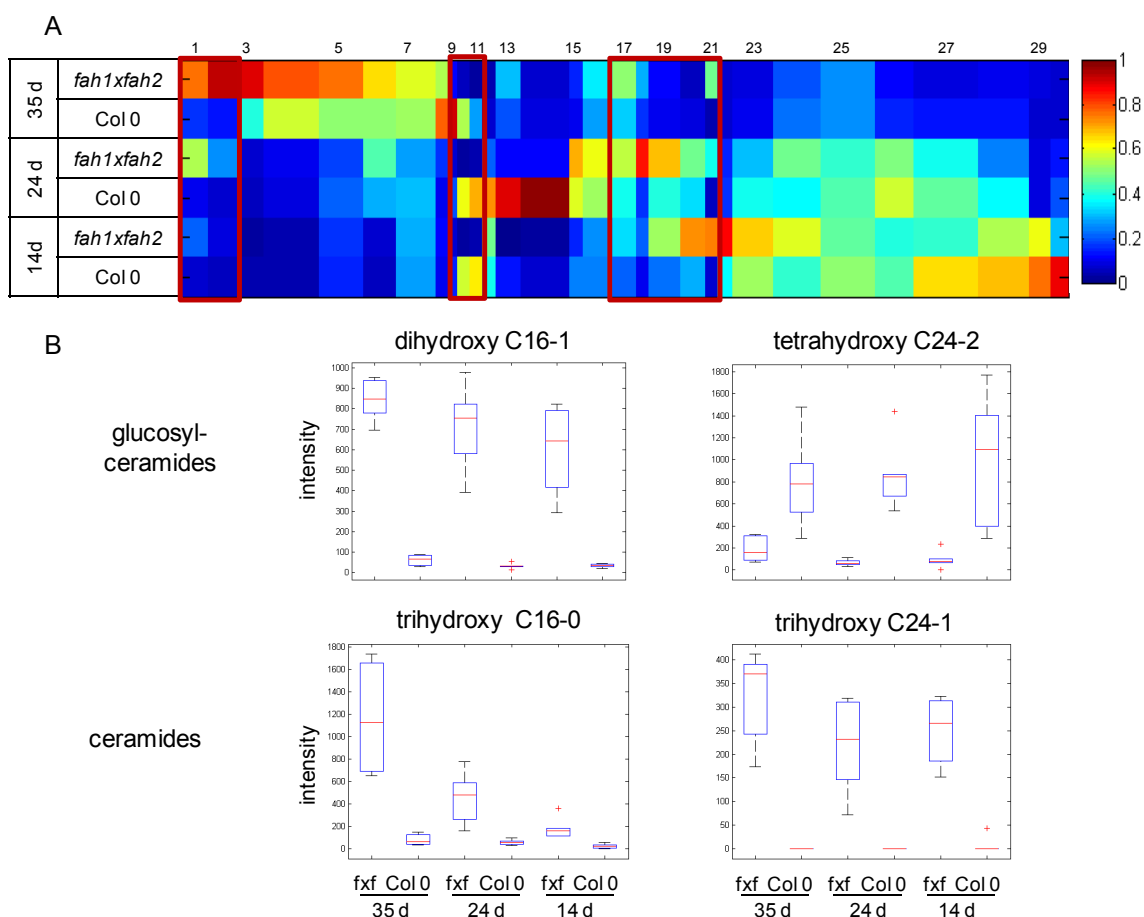


**Fig. 33: Metabolite fingerprinting of *fah1xfah2* leaves (non-polar phase).**

Plants were grown under long day conditions for 14, 24 and 35 days (d). Leaf material was extracted by two phase partitioning, leading to a methanol phase with polar metabolites and a MTBE phase with unpolar metabolites. A) 1D-SOM of 1064 markers from the MTBE fraction of the extraction measured in positive ionization mode and 802 from the analysis in negative ionization mode. Markers of different growth time points were grouped into 30 clusters based on their intensity profile. In the red boxes the cluster are marked which are dependent on the mutation. B) Box plots of selected glucosylceramides and ceramides. Nomenclature: the first number represents the chain length of the fatty acid moiety, the second number represents the number of double bonds in the molecule. For the analysis four biological replicates per treatment were measured twice. fxf: *fah1xfah2* mutant plants.

### 3.4.2.5 Phytohormone analysis in the *fah1xfah2* mutant

Because the most obvious markers in the undirected approach were related to SA we focused on these metabolites. To verify these markers, the phytohormone levels in the double mutant were determined. The analysis was performed by Dr. Tim Iven.

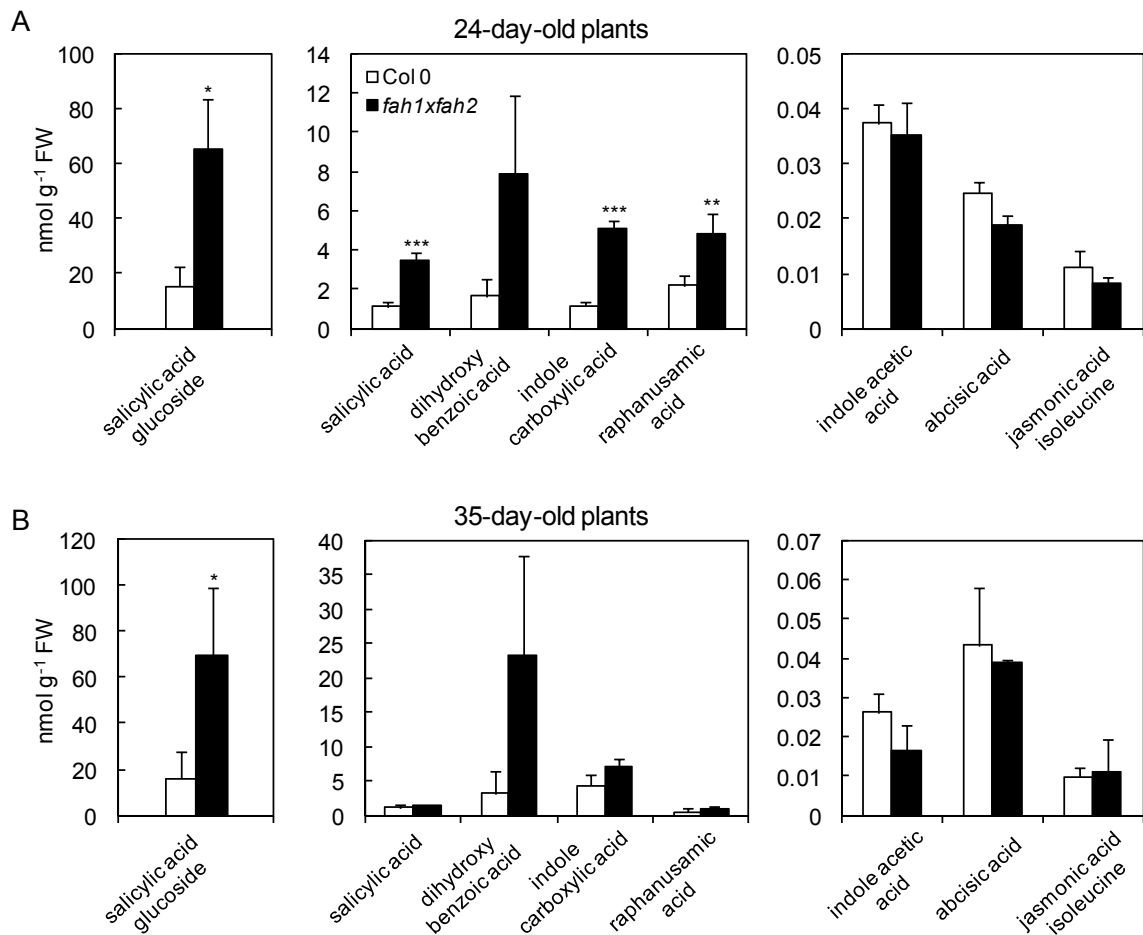


**Fig. 34: Determination of phytohormone levels in the *fah1xfah2* mutant.**

Plants were grown for 24 days (A) or 35 days (B) in long day conditions. Leaf material of Col 0 (white bars) and *fah1xfah2* (black bars) was extracted with MTBE and phytohormone levels were determined by HPLC-MS/MS analysis. The mean values of three biological replicates are shown  $\pm$ SD. Asterisks indicate significant differences between control and infected plants according to student's t-test (\*  $p \leq 0.05$ , \*\*  $p \leq 0.01$ , \*\*\*  $p \leq 0.001$ ). The analysis was performed by Dr. Tim Iven.

Samples of 24 and 35-day-old plants were used for the analysis. For SA and SAG the analysis confirmed the data of the undirected approach (Fig. 34). SA was enriched from 1.1 nmol g<sup>-1</sup> FW in wild type to 3.5 nmol g<sup>-1</sup> FW in the 24-day-old mutant plants while no enrichment was detectable in 35-day-old plants. For SAG the enrichment was equal in both growth stages - the amount in the double mutant was 4.3 times higher (65-69 nmol g<sup>-1</sup> FW) than in wild type plants. Also for dihydroxy benzoic acid the enrichment was detectable. It was highest in 35-day-old plants, where it was 7.7 times higher (23.3 nmol g<sup>-1</sup> FW) than in wild type plants. In addition to these phytohormones also an enrichment of indole carboxylic acid and raphanusamic acid was detected. Both were strongly enriched in 24-day-old plants but not in the 35-day-old plants. For the different

other phytohormones analyzed, like auxin, abscisic acid and the jasmonic acid isoleucine conjugate no significant differences were detected compared to wild type plants.

### 3.4.2.6 Biotic stress response

Because the *fah1xfah2* double mutant displayed enrichment of SAG and other phytohormones, infections with two different pathogens were performed. One was the obligate biotrophic leaf pathogen *G. cichoracearum* and secondly infection with *V. longisporum* as hemibiotrophic root pathogen was examined.

#### 3.4.2.6.1 Infection of *fah* mutants with powdery mildew (*G. cichoracearum*)

The infection with *G. cichoracearum* was performed by Marnie Schwarz (Rg Prof. Lipka, Göttingen). Next to the single and the double mutant plants of the AtFAH genes, *edr1* (*enhanced disease resistance1*, Frye & Innes, 1998) was included as control for a resistant plant and Col 0 wild type and *pen2/pad4/sag101* as control for susceptible and hypersusceptible plants, respectively (Lipka et al, 2005).

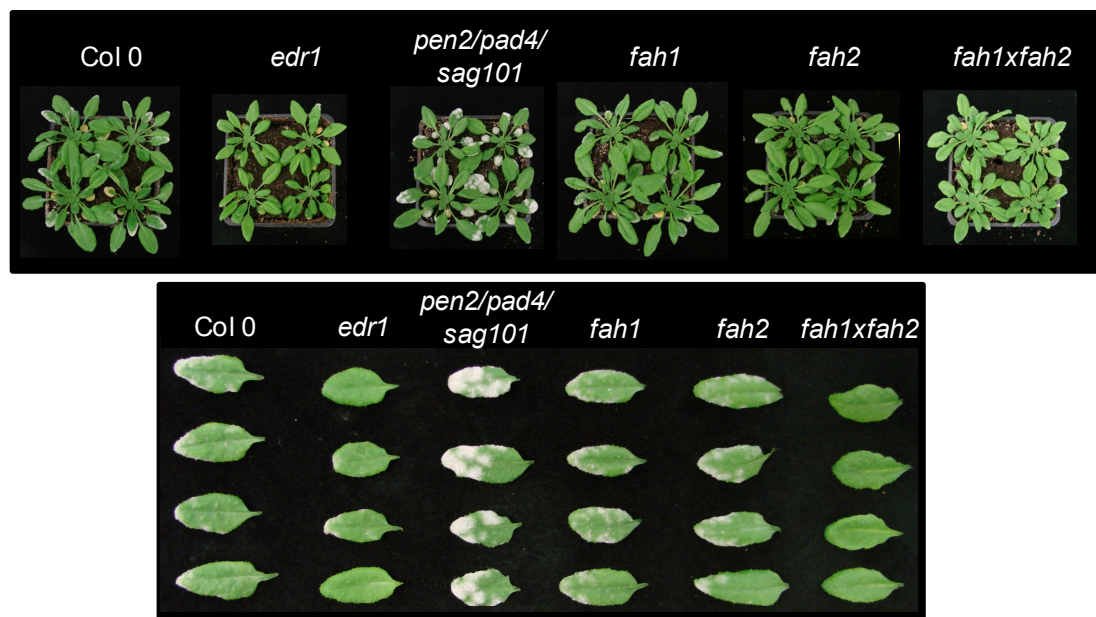


**Fig. 35: Infection of Arabidopsis *fah* mutants with *G. cichoracearum*.**

Plants were grown four weeks under short day conditions and infected by dusting with fungal spores. The *edr1* mutant was used as a control for a resistant plant and the *pen2/pad4/sag101* as control for a hypersusceptible line. The upper panel shows whole infected plants, whereas the lower panel shows infected single leaves of those plants. Infections were repeated three times with comparable results. (*edr*: enhanced disease resistance, *pen*: penetration mutant, *pad*: phytoalexin deficient, *sag*: senescence associated gene). Infection was performed by Marnie Schwarz (Rg Prof. Lipka, Göttingen).

The pictures of the single leaves shown in the lower panel of Fig. 35 allow a direct comparison of the fungal colonization success. As expected, wild type plants were normally susceptible, *edr1* mutants fully resistant and *pen2/pad4/sag101* strongly infected. The infection phenotype of both single *fah*-mutants was comparable to wild type, whereas double mutant plants did not show any macroscopic disease symptoms and were comparable to the resistant *edr1* mutant.

#### 3.4.2.6.2 Infection of the *fah1xfah2* mutant with *V. longisporum*

Finally also infection with *V. longisporum* was performed to analyze the influence of the metabolic changes in the *fah1xfah2* double mutant on the susceptibility of the plants.

Infection with *V. longisporum* resulted in 20 % stronger stunting of the infected leaves of the double mutant compared to wild type (Fig. 36). Additionally, the VL-DNA amount was slightly increased from 21 pg mg<sup>-1</sup> FW to 36 pg mg<sup>-1</sup> FW in these plants, but this was not significant.

In general it was shown that the infections with both fungal pathogens were affected by the mutations in different ways.

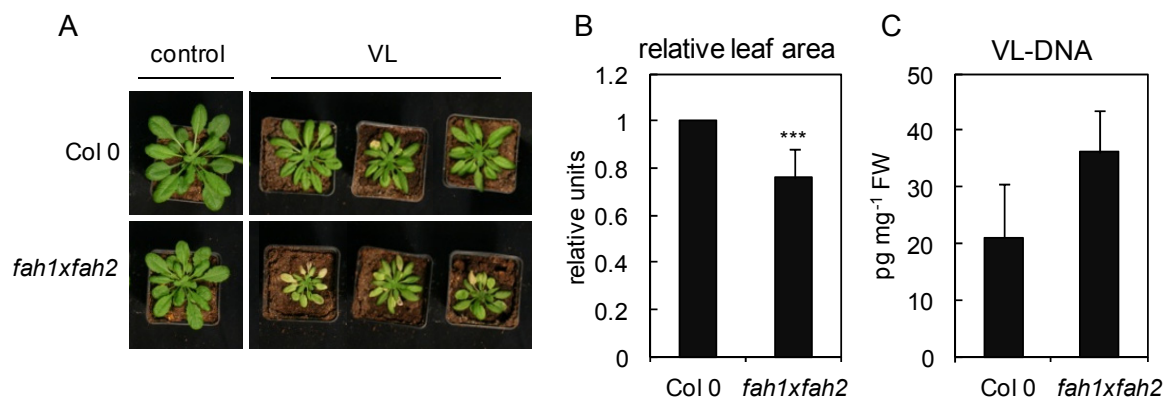


**Fig. 36: Infection of the *fah1xfah2* mutant with *V. longisporum*.**

Col 0 and *fah1xfah2* plants were infected by root dip infection A) Pictures of infected and control plants at 21 dpi. B) The leaf area was measured from the pictures of the plants and the relative leaf area was determined: The leaf area of infected plants was divided by the leaf area of control plants and the results of the mutant plants were set in relation to the value of the wild type. The data represent the mean values of five independent experiments  $\pm$ SD. C) Determination of VL-DNA in infected leaves. The mean values of twelve biological replicates out of three independent experiments were shown  $\pm$ SD. Asterisks indicate significant differences between control and infected plants according to student's t-test (\*\*\*)  $p \leq 0.001$ ). The VL-DNA analysis was performed by the group of Prof. Karlovsky (Göttingen).

## 4 Discussion

This work focused on the analysis of the metabolic response of *Arabidopsis* upon infection with *V. longisporum*. The phenylpropanoid pathway and fatty acid derivatives from the sphingolipid pathway as well as the suberin/cutin pathway have been of special interest, as previous studies showed that these metabolic classes are influenced by *V. longisporum* infection (Tab. 1). To prove these metabolic changes and to determine the role of the involved pathways was the special goal of this work.

### 4.1 Undirected metabolite fingerprinting

To identify metabolites which are affected by the infection with *V. longisporum*, a metabolite fingerprinting approach in leaves and roots was performed. In both parts of the plants different infection related markers were detectable, but only in the polar phase of extraction.

In the polar phase of leaf extracts the previously identified phenylpropanoid markers sinapoyl glucose and bispinapoyl glucose could be verified. Additionally, different lignans and coniferin were detected (Fig. 9, Tab. S1). These markers are further discussed in the following sections. Different other markers with database hits for metabolites of the phenylpropanoid pathway like phrymarolin I, sesamolol, sesamin or syringaresinol glucoside (Tab. S1) were also detected, but could not be verified so far. It has to be kept in mind that the undirected analysis only provides putative assignments of metabolites. If no standard substance is available to be compared to or no fragmentations have been generated by MS/MS measurements, the defined metabolites can not be further confirmed. Thus markers remain, whose identity has only been putatively predicted by relating the measured masses to metabolites.

In the unpolar phase no significant infection related markers were detected. Thus the fatty acid derivatives detected in previous experiments (Tab. 1) could not be verified. The reasons for this could be on the one hand that the previous work was done with only one highly infected sample per condition. Therefore it might be possible that these markers were lost in later experiments due to biological variation. On the other hand, those markers were very low concentrated and may not be identified in every analysis. The quality of the analysis always depends on the extraction and on the conditions of the UPLC-MS, and therefore variations between different analyses are possible. The free fatty acid derivatives were also tried to analyze directly by GC-MS, but this failed because of the low amount of these compounds and too much background in higher concentrated samples.

Although soluble monomers of cutin and suberin and sphingolipid derived fatty acids could not be further determined in metabolite fingerprinting analyses, both metabolic groups were analyzed in this thesis because of their general implications in plant defense also described for fungal pathogens.

#### 4.1.1 Root metabolites

This work focused on the leaf metabolites, nevertheless also root analyses were performed to compare markers in both parts of the plant. Compared to the leaves, only few infection related markers were detected in root samples (Fig. 11). This might not be due to the fact that roots respond less than leaves but to the infection and preparation of the roots. Both independent experiments showed different intensities and differed also in the intensity profiles of many markers. Root material needs to be extensively washed from the soil, which may lead to damages of the roots and to further metabolic changes that may interfere with the analysis.

In a recent study, gene expression analysis was performed in the roots and it was demonstrated that many genes involved in synthesis of infection markers are already affected in early stages of infection (Iven, 2009). For example the induction of genes of the camalexin pathway was very prominent and camalexin was shown to increase already from 2 dpi on. This increase could not be shown in the undirected analysis of the root samples in this thesis which could be due to different reasons. Iven (2009) used an infection system on MS plates which is not comparable to infection on soil. Additionally, the extraction and the analysis methods differed, which could lead to the fact that camalexin could not be identified in this approach.

With coniferin and indole glucosinolates some markers already determined in the leaves could also be identified to be induced in response to infection in the roots (Fig. 11). Additionally, masses of aliphatic glucosinolates were detected in higher intensities in infected roots compared to controls (Fig. 11). Only few studies related to metabolic changes in response to root pathogens were published so far. Pedras et al (2008) infected Canola with the biotroph *Plasmodiphora brassicaceae* and in contrast to the data shown in this thesis coniferin and indole glucosinolates were reduced upon infection. These differences might be due to the use of a biotrophic pathogen in contrast to the hemibiotrophic *V. longisporum* in this thesis. Bednarek et al (2005) also showed an influence on the indole and the phenylpropanoid pathway in Arabidopsis root cell cultures infected with *Phytium sylvaticum*. This, in combination with the data presented here, demonstrates that also in the roots both pathways are important in response to pathogens. The enrichment of coniferin (Fig. 11) is in agreement with data of gene expression analyses performed by Iven (2009), where it was shown that *CCoAOMT* and

one putative *CAD* gene were induced upon infection. This might lead to enhanced coniferin and phenylpropanoid synthesis. Next to the phenylpropanoids an accumulation of I3G and 4HI3G as well as aliphatic glucosinolates could be demonstrated in this thesis (Fig. 11). Glucosinolates are phytoanticipins which are preformed in healthy plants and can also accumulate upon pathogen challenge (VanEtten et al, 1994). It was shown that glucosinolates especially indolic ones are important against fungal pathogens (Bednarek et al, 2009). Brader et al (2006) showed that alterations in specific glucosinolates are important for resistance to different pathogens. It might therefore be possible that in the roots these aliphatic glucosinolates play a specific role apart from the indolic ones in the *V. longisporum* infection.

## 4.2 Phenylpropanoids

Sinapoyl glucose esters, monolignol glucosides and lignan glucosides were detected by untargeted as well as by targeted analyses to accumulate in *V. longisporum* infected *Arabidopsis* leaves (summarized in Fig. 37).

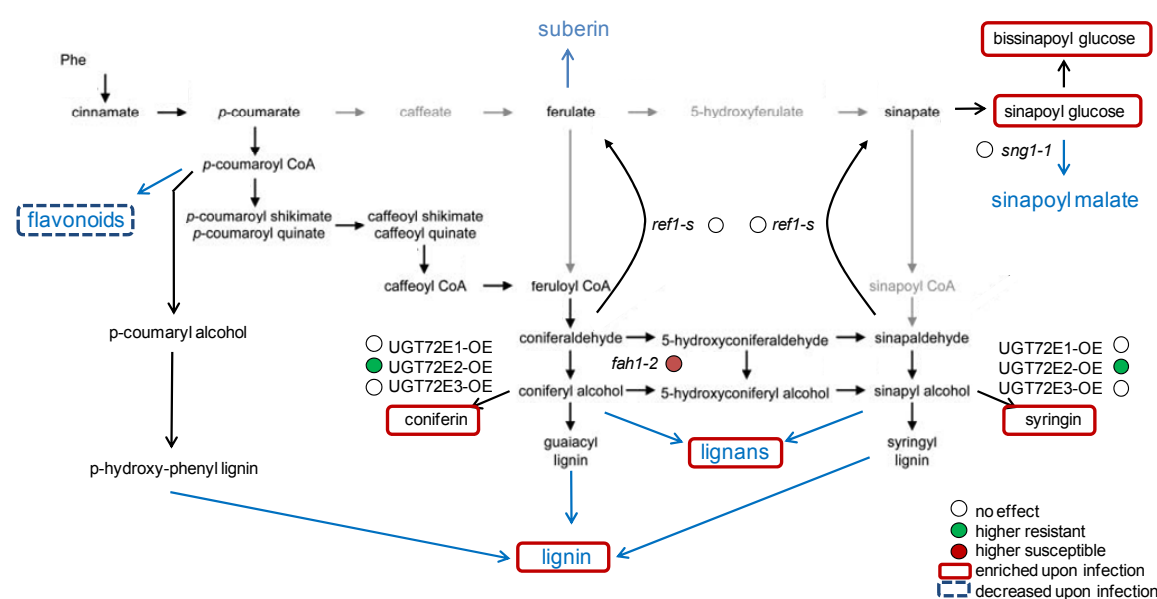


**Fig. 37: Affected phenylpropanoids in *Arabidopsis* in response to *V. longisporum* infection and susceptibility of tested mutants of the pathway.**

The implication of the phenylpropanoid pathway in *V. longisporum* infections was already demonstrated in the infection of *B. napus* (Eynck et al, 2009). It was shown in this study that soluble and wall bound-phenolic compounds accumulate upon infection as well as lignification is enhanced, which leads to reinforcement of the tracheary elements. By comparison of a susceptible with a resistant line, it was shown that these responses are

involved in resistance. But the specific compounds were not further elucidated in this study. Also in different *V. dahliae* and *F. oxysporum* infections affection of the phenylpropanoid pathway was described showing a general function of this pathway in hemibiotrophic root pathogen infections (Gayoso et al, 2010; Hano et al, 2006; Njoroge et al, 2011).

#### 4.2.1 Sinapate esters in the defense response of Arabidopsis

Sinapoyl glucose and bissinapoyl glucose are the markers already identified in the previous work (Tab. 1). They could be verified and quantified in this thesis by RP-HPLC analyses (Fig. 12). In contrast to sinapoyl glucose, the sinapoyl malate content was not affected in infected plants. Additionally it was shown that sinapoyl glucose enrichment takes place especially in the petioles of the leaves (Fig. 23), which leads to the assumption that this enrichment is a direct effect to the fungal infection.

Consistent with the accumulation of sinapoyl glucose, expression of *UGT84A3* was induced, shown by semiquantitative RT-PCR (Fig. 17). The homologue gene *UGT84A2* was not induced. Both genes are described to be involved in sinapoyl glucose synthesis (Lim et al, 2001; Sinlapadech et al, 2007). It was shown that *UGT84A2* has a high basal activity of 95 % of the total sinapic acid glucosylating activity in the leaves (Sinlapadech et al, 2007), which might be the reason why only an induction for the *UGT84A3* gene could be observed.

Sinapate esters are a special feature of the *Brassicaceae* family and they have an important UV-B light protective function (Landry, 1995), but no function in defense was described so far. Also no study showed an enrichment of sinapoyl glucose after pathogen challenge. Most of the studies focus on sinapoyl malate, which is described to be affected in plant-pathogen interactions in different ways. Hagemeyer et al (2001) showed that sinapoyl malate is decreasing in *P. syringae* infection of *Arabidopsis* and it was also shown that at lesion site sinapoyl malate amount is decreasing in *B. cinerea* infections (Kliebenstein et al, 2005). In contrast to this, in *Fusarium oxysporum* infected *B. rapa* an accumulation of sinapoyl-, feruloyl and 5-hydroxy feruloyl malate was detected (Abdel-Farid et al, 2009).

To further elucidate the role of the sinapoyl glucose accumulation for the *V. longisporum* infection, different mutants in the pathway were tested in this thesis (Fig. 18). The *fah1-2* mutant, which has no sinapates and its esters, could be shown to be more susceptible, whereas *ref1-s*, which has only reduced amount of the esters, was not more susceptible. To test if sinapoyl glucose itself is responsible for differences in susceptibility, the *sng1-1* mutant with high amounts of sinapoyl glucose but no sinapoyl malate was analyzed. But this mutant also did not show differences in the infection. These results lead to the

assumption that the susceptibility does not depend on sinapoyl glucose itself, but on the total amount of sinapate esters.

The function of these esters in the infection could not be addressed so far, but different roles are conceivable. Abdel-Farid et al (2009) suggested an antifungal role of sinapoyl, feruloyl and 5-hydroxyferuloyl malate, which accumulated in *F. oxysporum* infected *B. rapa*. This was not further elucidated, but different phenolic compounds and phenylpropanoids were tested in the literature for fungal toxicity. Due to the lack of commercially available sinapoyl glucose and sinapoyl malate, these compounds have not been tested so far, but sinapic acid was shown to reduce growth of *Fusarium gramineum*, which causes Fusarium head blight in barley, to 50 % at a concentration of 1.7 mM (Bollina et al, 2010). Another function of hydroxycinnamate esters was described by Quentin et al (2009). Here it was shown that 5-hydroxyferuloyl malate, which accumulates in specific phenylpropanoid mutants, promotes sexual reproduction of the downy mildew pathogen *Hyaloperonospora arabidopsidis*. This result is not applicable to *V. longisporum* because it propagates asexually. But this example shows that possible functions of the hydroxycinnamate esters could be rather broad.

Next to the absent sinapate esters a possible explanation for the higher susceptibility of the *fah1-2* mutant could be the crosstalk between the phenylpropanoid pathway and the indole pathway described by Huang et al (2009). They showed that the *fah1-2* mutant possess lower amounts of indole glucosinolates, which leads to higher susceptibility against *Sclerotia sclerotiorum* infection. But the authors only analyzed these compounds in the seeds of the mutants. In this thesis no changes in indole glucosinolate amounts in leaves of the mutant could be determined (Fig. S9) and therefore it could be excluded that indolic compounds were responsible for the higher susceptibility of the *fah1-2* mutants.

Another possibility for the higher susceptibility of the *fah1-2* mutant is the changed lignin composition in these plants. They only contain guaiacyl lignin and no syringyl lignin (Meyer et al, 1998). The possible impact of this alteration will be discussed in the following section.

#### **4.2.2 Lignin and lignans in the defense response of Arabidopsis**

In this thesis, lignan glucosides have been detected to be strongly enriched in Arabidopsis leaves in response to infection with *V. longisporum* in undirected measurements and in quantification by RP-HPLC (Fig. 14). In cross sections of hypocotyls and petioles it was additionally detected that lignin accumulated (Fig. 16).

Semiquantitative RT-PCR studies revealed that two *CAD* genes are induced upon infection, *CAD5* and *CAD8* (Fig. 17). This is in line with the accumulation of lignans and lignin because these enzymes catalyze the synthesis of coniferyl alcohol and sinapyl

alcohol – the precursors of lignin and lignans. Out of nine putative CADs in Arabidopsis these both genes are also described to be induced in *P. syringae* infection in Arabidopsis (Tronchet et al, 2010). The authors demonstrated by infecting knock out mutants of *CAD5* and *CAD8*, that both genes are involved in the basal resistance of Arabidopsis against *P. syringae*. Based on this study a *cad5* SALK-line was tested in this thesis for its susceptibility against *V. longisporum*, but no difference compared to the wild type could be determined (Fig. S2). This may be due to a redundant function to *CAD4*, as Tronchet et al (2010) also showed that in their infection system the double mutant of *CAD4* and *CAD5* was more susceptible than both single mutants. Another possibility of the unaltered susceptibility of *cad5* might be based on the fact that the mutant is not a total knock out of the gene but has only reduced levels of *cad5* mRNA.

Lignification is a common reaction of plants in response to infection with different pathogens. In the work of Michael Reusche (Rg Dr. Teichmann, Göttingen; personal communication) and in this thesis it could be shown that more lignified cells in *V. longisporum* infected Arabidopsis petioles and hypocotyls are present (Fig. 16). Also Floerl (2007) detected that lignin is enriched in *V. longisporum* infected Arabidopsis leaves.

In different studies it was shown that upon infection with different pathogens plants synthesize 'defense lignin', which can differ in the composition from the normal lignin (Zhang et al, 2007; Lloyd et al, 2011; Wuyts et al, 2006; Pomar et al, 2004). These defense lignins can not only have the function to reinforce the cell wall but also an antimicrobial one (De Ascensano et al, 2003).

The higher susceptibility of the *fah1-2* mutant in the *V. longisporum*–Arabidopsis interaction shown in this thesis (Fig. 18), could therefore also be due to the different lignin composition of the mutant, which is due to a defect in the syringyl lignin synthesis (Meyer et al, 1998). There are several examples where syringyl lignin is highly enriched at the infection site, for example in *Puccinia graminis* infected wheat (Menden et al, 2007), in *F. oxysporum* elicited flax cells (Hano et al, 2006) and in *B. cinerea* infected Arabidopsis plants (Lloyd et al, 2011). Also in the *B. cinerea* interaction it was shown that the *fah1-2* mutant was stronger infected than the wild type (Lloyd et al, 2011). The authors suggested that this is due to less defense related lignin locally deposited on the infection site. Lignin composition cannot only have an impact on the stability of the polymer but also on the degradability for pathogens. Syringyl lignin is a more linear polymer than coniferyl lignin and therefore better protects large areas of secondary cell walls from degradation (Jung & Deetz, 1993). Degradability of the cell wall in *fah1-2* mutants was tested in different systems. For rumen microorganisms it was not shown to be higher degradable

(Jung et al, 1999), but in tobacco the cell wall of mutants with lower amounts of syringyl units was better degradable for fungal enzymes (Vailhé et al, 1996). So it is conceivable that the type of lignin found in the *fah1-2* mutant results in a higher susceptibility.

In addition to the *fah1-2* mutant also an overexpressor mutant (C4H:F5H) of the gene was analyzed in infections (Fig. 19). This mutant was described in the literature to harbor especially syringyl lignin instead of guaiacyl lignin (Meyer et al, 1998). Consistent with the theory of the importance of defense lignin in the interaction, fungal growth was reduced in the C4H:F5H mutants (Fig. 19). The VL-DNA amounts in infected plants were lower compared to wild type plants, although the reduction of the leaf area was comparable. This leaf area reduction might be a secondary effect due to water deficiency symptoms in infected C4H:F5H plants at the end of the light period (Fig. S10). The reason for this symptom could not be elucidated so far.

Next to lignin, also lignans were shown in this thesis to be affected in Arabidopsis upon infection with *V. longisporum*. Lignans are widely distributed in different plant species. In Arabidopsis they were so far only described in the roots (Nakatsubo et al, 2008). But in this thesis, it could be shown that lignans like pinoresinol and lariciresinol are also abundant in the leaves of Arabidopsis and that they accumulate as glucosides in high amounts upon infection with *V. longisporum* (Fig. 14). In line with this, an induction of *DIR6*, which is involved in lignan synthesis, could be shown by semiquantitative RT-PCR analysis (Fig. 17). The induction of dirigent proteins was described to be active in conifer resistance against insects (Ralph et al, 2007) and may also imply a possible function in fungal defense of plants.

Next to the identified lignans pinoresinol and lariciresinol, also masses of related metabolites were found by the HPLC analyses of *V. longisporum* infected Arabidopsis leaves, but their identity could not be proven so far (Fig. 15). Due to the high variety between different plant species it may well be that Arabidopsis possess other lignans apart from pinoresinol and lariciresinol that are not yet identified.

Due to the lack of mutants the impact of lignans on the infection could not be analyzed in this thesis. The pinoresinol-reductase double mutant (Nakatsubo et al, 2008) was examined but in this mutant only the ratio of lariciresinol to pinoresinol is changed (Fig S12). Therefore it was not surprising that no differences compared to wild type could be detected (Fig. S2). In wheat plants it was described that overexpression of the pinoresinol reductase led to an increase in total amount of secoisolariciresinol diglucoside which is the final lignan in wheat (Ayella et al, 2007). Maybe also in Arabidopsis an overexpression of the gene could lead to higher amounts of lignans and therefore, to a valuable tool to test the importance of these compounds for infections.

Different functions of lignans in defense are conceivable, one is the function as an antifungal compound. Carpinella et al (2003) showed that pinoresinol has antifungal activity against different phytopathogenic fungi, for example *F. verticillioides*. The minimal inhibitory concentration in the study was determined to be 1 mg ml<sup>-1</sup> for pinoresinol. In this thesis, an inhibition of lariciresinol or pinoresinol on *V. longisporum* growth could not be shown, but this may be due to lower concentrations (up to 100 µM, approximately 0.035 mg ml<sup>-1</sup>) used in the analysis (Fig. S13). Because the concentrations of the lignans at infection sites could not be estimated, the possibility of fungal growth inhibition upon higher concentrations of lignans cannot be ruled out. Additionally, the synergistic effects of different lignans, lignans with coniferin or other upregulated phenylpropanoids were not tested so far. Synergistic effects can lead to higher toxicity compared to single compounds and are widely described (Osbourn 1999, Carpinella 2005).

Another function of lignans in defense could be the generation of vascular obstructions to block the fungal spread. In woody plants lignans are described to be highly abundant in heartwood as antioxidant and to shut of non-productive water and nutrient transport to protect the sapwood and to tighten the longevity against wood rotting fungi (Naoumkina et al, 2010). Eynck et al (2009) could also show that phenolic compounds play a role in *V. longisporum* infected *B. napus* to build up occlusion in the vessels against the fungus. This function could also be related to lignan accumulation. But the fact that the lignan accumulation is equally distributed in petiole and lamina (Fig. 23), does not favor this explanation.

#### **4.2.3 Monolignols and its glucosides in the defense response of Arabidopsis**

The metabolite fingerprinting approach of Arabidopsis showed an enrichment of coniferin and syringin in infected leaves. Also direct measurements could confirm the accumulation of coniferin over the time of infection (Fig. 14), especially in the petioles (Fig. 23). Syringin could not be detected in wild type plants, which was possibly due to low amounts that were below the detection limit.

The function of coniferin and syringin in plants is still not known. It is debated if coniferin and syringin might be transport or storage forms of lignin precursors (Boerjan et al, 2003). The fact that mutants defect in glucosylation of coniferyl alcohol and sinapyl alcohol do not show changes in lignin content does not promote this widespread theory (Lanot et al, 2006; Vanholme et al, 2010).

Because high amounts of coniferin were detected in infected plants, glucosidase overexpressor plants of the UGT72E-family, involved in coniferin and syringin synthesis,

were tested for their susceptibility against fungal infection. In the infection experiments only the UGT72E2-OE with the highest amounts of coniferin showed elevated resistance to the fungus compared to wild type, while UGT72E1-OE and E3-OE were as susceptible as wild type plants (Fig. 20, Fig. 21). Because the coniferin accumulating overexpressors did not accumulate lignans (Fig. 21) and probably not more lignin (Lanot et al, 2006; Vanholme et al, 2010), the toxicity of coniferin and syringin itself was analyzed, to determine the possible direct effect on fungal growth of these compounds (Fig. 22). In addition to coniferin and syringin also the non glucosylated forms coniferyl alcohol and sinapyl alcohol were included in the toxicity assays. Of the investigated metabolites only coniferyl alcohol showed fungal growth inhibition. This was surprising as coniferyl alcohol differs only by one additional methoxy group from sinapyl alcohol (Fig. 3). In the literature coniferyl alcohol was shown to accumulate in flax infected with *Melampsora lini* (Keen & Littlefield, 1979). The authors also tested coniferyl alcohol to be fungal toxic. In this thesis, not coniferyl alcohol but the glucoside was found to be enriched upon infection; but this compound showed no fungal inhibition at the tested concentrations. This is not surprising because glucosylation is also described to be a detoxification mechanism (Jones & Vogt, 2001). A possible explanation for the situation in the plant would be that the plants possess high amounts of coniferin and just at the infection sites the coniferin becomes deglucosylated, which results in only local accumulation of coniferyl alcohol not measurable with the applied method.

After a distinct time of growth on PDB plates of the toxicity assay, *V. longisporum* started to melanize. Coniferin treatment resulted in a delayed melanization of the fungus, whereas none of the other three substances induced the same result (Fig. 22C). This shows that coniferin might also interact with the development of the fungus. To elucidate if the fungus can convert or consume the different metabolites, treatment of liquid cultures with these substances and analysis of the products shall be performed in further studies. In summary it was shown that coniferin and coniferyl alcohol influences fungal growth and development, while no effect of syringin and sinapyl alcohol could be observed.

To summarize the phenylpropanoids part of the work, the data support that the phenylpropanoid metabolism is affected in the infection with *V. longisporum*, and that some of the detected markers play a functional role in the defense response of the plants. The data further show, that the metabolite fingerprinting approach is suitable to find metabolic markers in infected plants that are important in the infection process.

### 4.3 Indole glucosinolates in the defense response of Arabidopsis

Next to the phenylpropanoids also the second common defense pathway in Arabidopsis – the indole pathway was shown to be affected by *V. longisporum* (Fig. 13). Especially in root dip infections indole glucosinolates were enriched in infected plants (Fig. S1). Indole glucosinolates are one of the main phytoanticipins of Arabidopsis. They are involved in defense against insects, fungal and bacterial pathogens (Bednarek et al, 2009; Brader et al, 2001). Iven (2009) could already show in his thesis that the *cyp79b2/b3* mutant is more susceptible against *V. longisporum* infection. In this mutant no indole glucosinolates and no camalexin is synthesized due to a defect early in the indole pathway (Fig. S3). The higher susceptibility of the *cyp79b2/b3* double mutant led to the assumption that indole glucosinolates play an important role in the plant defense against the fungus. So far the degradation products of indole glucosinolates raphanusamic acid and indole-3-ylmethylamine, which have been proposed to be the fungicidal compounds (Bednarek et al, 2009), were not detected as markers in the *V. longisporum* infected plants. Therefore, it is uncertain if the degradation of indole glucosinolates takes place in this interaction. The defect of the *cyp79b2/b3* mutant is early in the indole pathway. It can therefore not be excluded that also other indolic substances apart from indole glucosinolates are involved in the infection response.

### 4.4 Polar metabolites involved in symptom development

To analyze the relevance of the detected metabolic markers for their induction in symptom development in *V. longisporum* infection, infections with *coi1-t* plants have been performed. This JA perception mutant was shown not to develop any symptoms upon infection, which correlates with less fungal propagation in these plants at time points later than 10 dpi (Anjali Ralhan, Rg Prof. Gatz (Göttingen), personal communication). *dde2-2* mutants were included in these experiments because they are defect in JA biosynthesis but show normal infection symptoms and fungal propagation comparable to wild type. The infection markers detected in this thesis, like the phenylpropanoids or the indole glucosinolates seem not to be involved in the COI1-mediated response of the plant. The phenylpropanoids accumulated in all three plant lines, although delayed in *coi1-t* plants (Fig. 23, Fig. S16). Indole glucosinolates instead were less abundant (I3G and 1MI3G) in both JA mutants and were also less induced (Fig. 24). This is in agreement with different studies which showed that the genes of the indole pathway are JA regulated and that JA mutants display reduced amounts of these metabolites (Brader et al, 2001; Sasaki-Sekimoto et al, 2005).

To find markers included in symptom development, metabolite fingerprinting of the infected JA mutants was performed. In different clusters masses were determined that accumulated in infected wild type and *dde2-2* plants, but not in *coi1-t* plants (Fig. 25). Most of the metabolites corresponding to the detected masses could not be identified yet. They need to be fragmented by MS/MS experiments to obtain indications about their structure. Apart from these unidentified metabolites, masses of different amino acids could be detected, especially those with an additional nitrogen group in the side chain (glutamine, asparagine, arginine and histidine), but also valine and leucine (Fig. 25B). Amino acids are proposed to be the main carbon and nitrogen sources for the fungus in the xylem of the plant (Pegg & Brady, 2002). Therefore, the low amounts in the *coi1-t* plants could be the cause of reduced fungal growth in these plants after 10 dpi. As part of the primary metabolism and precursors of different secondary metabolites, changes in amino acids amounts in different infection studies were shown (Dixon & Pegg, 1972; Parker et al, 2009; Ward et al, 2010). Dixon & Pegg (1972) demonstrated a change in the amount of different amino acids in tomato xylem sap of different *V. dahliae* infected cultivars. But a specific role in resistance or susceptibility could not be addressed to them. In other infection studies aromatic amino acids have been shown to accumulate upon infection as in *Arabidopsis* treated with *P. syringae* (Ward et al, 2010). In this case the aromatic amino acids are affected due to the induced phenylpropanoid and indolic pathways. Whether in our experiments the accumulation is defense related or a secondary effect could not be elucidated so far. Asparagine and glutamine are also involved in remobilization of nitrogen in senescent leaves. Therefore it seems also possible that the accumulation of amino acids is an indicator for senescence abundant in the plants with infection symptoms, but not in the ones without.

Apart from the amino acids also the mass of malate was detected as a marker in this experiment (Fig. 25B). Malate can have different functions in plants, like in carbon storage, pH regulation, nutrient uptake, stomatal function and support of efficient photosynthesis (Ferne & Martinoia, 2009). Also a role of malate in facilitating apoplastic NADH production for stimulating production of hydrogen peroxide needed to sustain lignin production and for defense responses is discussed (Ferne & Martinoia, 2009). The role in the *Arabidopsis* - *V. longisporum* interaction needs to be further elucidated.

A third detected marker, which was not enriched in *coi1-t* upon infection but in Col 0 and *dde2-2*, was SAG (Fig. 25B). In contrast to this result, an enrichment of SAG could be shown in petioles of infected *coi1* plants at 15 dpi in the Rg of Prof. Gatz (personal communication). Therefore SAG accumulation seems not to be part of the COI1-mediated plant response.

So far it could just be shown that there are indeed metabolic differences in infected *coi1-t* plants compared to wild type, But probably by further analysis of the detected masses and by comparison with transcriptional data generated by Anjali Ralhan more information could be derived from these data.

#### 4.5 Cutin and suberin

One aim of this work was to analyze if suberin or cutin monomers are implicated in defense against *V. longisporum*. The analysis of suberin and cutin related monomers in early infection time points did not reveal any differences in infected plants compared to controls (Fig. 26). Therefore it seemed that these barriers are not affected upon infection. But it was still possible that suberin was only locally enhanced at infection sites and that these minor changes in suberin amounts were undetectable in the analysis. Also a possible signaling effect of the monomers could not be excluded. Therefore different suberin mutants: *cyp86a1-2*, *cyp86b1-2* and *gpat5-1* were analyzed. *cyp86a1-2* and *gpat5-1* were both described to possess at least 50 % reduced amounts of suberin, whereas in *cyp86b1-2* just the composition of the monomers is changed (Beisson et al, 2007; Compagnon et al, 2009; Höfer et al, 2008). With both applied infection methods all three mutants did not show any differences compared to wild type infected plants (Fig. 27). Because the roots and probably also the suberin layer get damaged before the inoculation with the fungus in both infection methods, an infection by watering intact soil grown plants with spore solution was tried. But in this infection with non-damaged roots no difference to wild type plants was visible, none of the plants was infected (Fig. 27). This experiment needs to be considered with caution, because it is not known, if just watering the plants with spore solution brings enough spores in contact to the root to really initiate infection. What also needs to be considered is that a possible signaling effect could still not be excluded because these mutants lack only monomers of specific chain length. In studies with cutin mutants describing higher or lower susceptibility, the mutants were defect in synthesis of all chain length monomers (Tang et al, 2007; Xiao et al, 2004). Maybe crossing *cyp84a1-2* and *cyp84b1-2* would help to elucidate this situation in the roots. But based on these studies it seems that suberinization, as described for example in tomato plants in response to *V. dahliae* infection (Robb et al, 1991), is not induced and not important in *V. longisporum* infection in *Arabidopsis*.

## 4.6 Sphingolipids

Another special focus of this work was on  $\alpha$ -hydroxylated fatty acids, which are part of sphingolipids. Because the function of putative Arabidopsis genes involved in the synthesis of  $\alpha$ -hydroxylated fatty acids was not shown *in planta* so far, analysis of T-DNA insertion mutants of the two assigned  $\alpha$ -hydroxylase genes in Arabidopsis was performed and double mutants (*fah1xfah2*) of the two genes were generated. The further purpose was to test the impact of  $\alpha$ -hydroxy fatty acids in plants growth and especially to test the function in plant defense against *V. longisporum*.

### 4.6.1 Changes in sphingolipid metabolism of the *fah1xfah2* mutant

It could be demonstrated in this thesis that *fah1xfah2* double mutants of the putative AtFAH genes show strongly reduced amounts of ceramides and glucosylceramides with  $\alpha$ -hydroxy fatty acids (Fig. 31). This confirmed the prediction that the AtFAH genes indeed act as  $\alpha$ -hydroxylases in Arabidopsis. So far this was just shown by expression of the genes in yeast cells (Mitchell & Martin, 1997; Nagano et al, 2009). The fact that the amount of ceramides and glucosylceramides with  $\alpha$ -hydroxy fatty acids decreased but were still present in minor amounts, could be explained by the residual expression of FAH1 in single and double mutants shown by semiquantitative RT-PCR analyses (Fig. 28). Surprisingly, the analysis revealed that tetrahydroxy ceramides did not decrease in the double mutant but rather increased. So far no reason for this effect could be elucidated. Maybe this is also due to the residual activity of FAH1, although it is not very plausible. Another possible explanation would be that there are more genes in Arabidopsis that are able to introduce hydroxy groups in  $\alpha$ -position in fatty acids. In mammals another activity, apart from the AtFAH homologue FA2H, is known. This PHYH gene product, which is an  $\alpha$ -ketoglutarate dependent acyl-CoA  $\alpha$ -hydroxylase in the peroxisomal  $\alpha$ -oxidation pathway, is assumed to be involved in sphingolipid  $\alpha$ -hydroxylation in the absence of FA2H activity (Hama, 2010). Possible candidates in Arabidopsis would be the  $\alpha$ -dioxygenases 1 and 2 ( $\alpha$ -DOX1 and 2) (Bannenberg et al, 2009; Hamberg et al, 1999). These enzymes oxygenate fatty acids *in vitro* of different chain length resulting in  $\alpha$ -hydroxy fatty acids, aldehydes and fatty acids both shortened by one C atom (Hamberg et al, 1999). The At $\alpha$ -DOX1 gene was shown to be involved in protection against oxidative stress and cell death (De Leon et al, 2002). Deletion of At $\alpha$ -DOX1 or 2 in Arabidopsis did not lead to any phenotype, but in tomato plants defect in Sl $\alpha$ -DOX2 induced early dwarfing and anthocyanin synthesis (Bannenberg et al, 2009). The analysis of ceramides and glucosylceramides in  *$\alpha$ -dox1* and  *$\alpha$ -dox2* mutants as well

as crossing *fah1xfah2* double mutants with  $\alpha$ -*dox* mutants could reveal the implication of the  $\alpha$ -*DOX* genes in ceramide dependent  $\alpha$ -hydroxy fatty acid synthesis.

Surprising in the ceramide analysis was the strong accumulation of ceramides in the double mutant (Fig. 31). For the glucosylceramides as well as for the ceramides a strong reduction in species with  $\alpha$ -hydroxy fatty acids was shown and an increase in non- $\alpha$ -hydroxylated species, respectively. While in total the amount of glucosylceramides decreased about 25 %, the total amount of ceramides instead increased about ten times. One possible explanation would be that  $\alpha$ -hydroxylation occurs preferentially at the level of the ceramides. This general assumption is based on the fact that the ceramide synthase was shown to be inhibited by  $\alpha$ -hydroxy fatty acids (Kaya et al, 1984; Lynch & Dunn, 2004) and that this  $\alpha$ -hydroxylation should therefore take place after ceramide synthesis. In this case ceramides would be synthesized in the *fah1xfah2* mutant but not further converted to their  $\alpha$ -hydroxylated forms and subsequently not further converted to  $\alpha$ -hydroxylated glucosylceramides and  $\alpha$ -hydroxylated inositolphosphoryl ceramides. At least for the IPC synthase in wax bean it was shown that it prefers ceramides with  $\alpha$ -hydroxy fatty acids (Bromley et al, 2003). Analysis of free LCBs in the double mutant will further provide information about this situation. If they do not accumulate it would support this theory.

#### 4.6.2 Growth phenotype of the *fah1xfah2* plants

The growth phenotype of *fah1* and *fah2* plants was comparable to wild type, but the *fah1xfah2* double mutant plants showed reduction in leaf and root growth (Fig. 28). The leaves were more wrinkled and curled than wild type leaves. This phenotype was visible under long day but not under short day conditions and it got visible after 2.5 weeks of growth. It could be shown by complementing the plants with the *35S:AtFAH2* construct that this phenotype is due to the mutations in the *FAH* genes (Fig. 29).

Different reasons for the leaf phenotype of the double mutants are possible: One possibility might be the direct consequence of the missing sphingolipids with  $\alpha$ -hydroxylated acyl chains. Because of their hydrogen bonding capacity, the hydroxy group can have an important effect on the lipid organization within membranes (Löfgren & Pascher, 1977; Pascher & Sundell, 1977; Boggs et al, 1988). Also for a mutant with a defect in long chain base C-4 hydroxylation a strong influence on plant growth and viability was shown (Tab. 2) (Chen et al, 2008). But also in this case the direct effect of the absent hydroxy group could not be proven. A second possible reason for the phenotype could be the secondary alteration in the sphingolipid profile. In the double mutants a strong enrichment of ceramides occurred. In the literature it was also shown in other mutants (*acd5* and *erh1*) that accumulation of ceramides can lead to altered leaf and growth

phenotypes in Arabidopsis as well as to the induction of cell death (Tab. 2) (Liang et al, 2003; Wang et al, 2008). The third possible reason for the phenotype could be the secondary effect of metabolites apart from sphingolipids. In this thesis it could be shown by a metabolite fingerprinting approach that the *fah1xfah2* double mutant accumulates SA and its glucoside as well as dihydroxybenzoic acid (Fig. 32). Additionally, other masses with accumulation over the growth periods were detected in the double mutant but so far not verified. SAG or other accumulating compounds could as well be the reason for the reduced growth and changes in leaf morphology. The fact that the symptoms in the plant start to evolve after 2.5 weeks of growth, but the ceramide and glucosylceramide changes are already abundant at 14 days of growth renders the third possibility the most convincing. This would also be in agreement with the expression data showing that *AtFAH1* and *AtFAH2* are expressed especially in young growing tissue (Fig. 30) and therefore might not be directly involved in the phenotype of older plants.

Accumulation of SA and its glucoside is quite common in sphingolipid mutant plants (Tab. 2) (Brodersen et al, 2002; Liang et al, 2003; Wang et al, 2008). Also above mentioned ceramide accumulation mutants (*acd5* and *erh1*) are enriched in SA, but in these mutants SA accumulation results in formation of PCD like lesions (Liang et al, 2003; Wang et al, 2008). SA is an important inducer of PCD dependent HR and it was shown that after crossing these ceramide mutants with SA mutants the lesion phenotype disappeared (Brodersen et al, 2005). The fact that in the *fah1xfah2* mutant no lesions occurred although the increase as well as the total amounts of SA and SA metabolites of the double mutant is comparable to the mutants with SA dependent lesions (Tab. 2) (Brodersen et al, 2002; Greenberg et al, 2000; Wang et al, 2008) could not be explained so far. But the comparison of the SA amounts of the different mutants is rather difficult because different growth conditions and plants of different age were used in the diverse studies. In the *fah1xfah2* a time dependent decrease in SA and an increase in SAG was shown (Fig. 32), which might be less active in inducing PCD. In addition to the SA accumulation the results of Townley et al (2005) and Nagano et al (2009) would promote the hypothesis of PCD in *fah1xfah2* plants. Townley et al (2005) showed that ceramides were able to induce cell death in Arabidopsis cell culture but  $\alpha$ -hydroxy ceramides are not. Nagano et al (2009) further speculated that  $\alpha$ -hydroxy fatty acids are involved in suppression of cell death. It was shown that *AtFAH* interacts with the cell death suppressor *AtBI-1* via *Cytb5*. As an inhibitor of cell death *AtBI-1* should regulate the activity of *AtFAH* under stress reaction to induce  $\alpha$ -hydroxy fatty acids as pro survival signal. This leads to the assumption that PCD should be promoted in the *fah1xfah2* mutant. These mentioned theories show that the whole differences, which are present

upon mutation in the sphingolipid metabolism, are rather complex and that phenotypes are not easy to predict.

**Tab. 2: Comparison of different sphingolipid mutants.**

mutant	gene	sphingolipid enrichment	phenotype	SA	infection	reference
<i>accelerated cell death 5 (acd5)</i>	ceramide kinase	ceramide enrichment	lesions/PCD, reduced height	3x	resistant to infection with <i>G. cichoracearum</i> , higher susceptible against <i>P. syringae</i>	Liang et al, 2003 Greenberg et al, 2000
<i>accelerated cell death 11 (acd11)</i>	sphingosine transporter		lesions/PCD, growth reduction, chlorosis	80x	n.d.	Brodersen et al, 2002 Brodersen et al, 2005
<i>enhancing RPW8-mediated HR-like cell death (erh1)</i>	IPC synthase	ceramide enrichment	lesions/PCD	3x	resistant to infection with <i>G. cichoracearum</i> ,	Wang et al, 2008
<i>sphingoid base hydroxylase (sbh1/2)</i>	LCB C-4 hydroxylase	enrichment of sphingolipids with C16-fatty acids	lesions/PCD, severe growth reduction	n.d.	n.d.	Chen et al, 2008
<i>fatty acid <math>\alpha</math>-hydroxylase (fah1xfah2)</i>	fatty acid $\alpha$ -hydroxylase	ceramide enrichment	growth reductions, changes in leaf morphology	4x	resistant to infection with <i>G. cichoracearum</i> , slightly higher susceptible against <i>V. longisporum</i>	this thesis

n.d.: not determined, SA: salicylic acid enrichment, LCB: long chain base. IPC: inositol phosphoryl ceramide

#### 4.6.3 Response of the *fah1xfah2* mutant to infection with different fungi

In order to examine the response of the double mutant to biotic stress those plants were infected with the *G. cichoracearum* and with *V. longisporum* (Fig. 35, Fig. 36). The powdery mildew infection resulted in the *fah1* and *fah2* single mutants in symptoms comparable to wild type, whereas the double mutant showed an enhanced disease resistant phenotype (Fig. 35). This is in agreement with the increase in SA in these mutants. It is well established that SA is important for the defense against biotrophic pathogens including powdery mildew (Glazebrook, 2005). Enhanced resistance to powdery mildew has also been shown in other sphingolipids mutants that accumulate SA (Wang et al, 2008).

Infection with *V. longisporum* resulted in 20 % stronger stunting of the leaves but only in a non-significant increase in VL-DNA amounts (Fig. 36). These different reactions compared to powdery mildew infection are in agreement with the theory that SA mediated defense is especially effective against biotrophs but not against hemibiotrophs and necrotrophs (Glazebrook, 2005). Differences in the infection response to different pathogens were also

shown in another sphingolipid mutant. Against *P. syringae* a stronger susceptibility was shown in the *acd5* mutant, whereas against powdery mildew higher resistance was observed (Tab. 2) (Greenberg et al, 2000; Wang et al, 2008).

For the involvement of the phytohormone SA in response to *V. longisporum* in Arabidopsis different results were shown in the literature. Ratzinger et al (2009) detected a strong increase in SA and SAG in infected xylem sap of *B. napus*. Tappe (2008) described SA accumulation in Arabidopsis late in the infection with *V. longisporum*. It was also shown in this study that SA, JA and ethylene are not involved in early infection responses and that mutants of these pathways do not act differently than wild type plants. This underlines that the differences in SA content may not have a strong influence on the infection with *V. longisporum*. The slightly stronger susceptibility might be due to direct effects of the changes in sphingolipid pools or to the enriched substances not verified so far.

In summary it could be shown, that AtFAH1 and AtFAH2 act indeed as  $\alpha$ -hydroxylases in Arabidopsis and that this hydroxylation is important for the balance of the ceramide and glucosylceramide pool which is subsequently important for SA metabolism. The accumulation of SA metabolites promotes resistance in *G. cichoracearum* infections but for *V. longisporum* infections the metabolic differences in the mutant seems to have only minor effects.

Further studies have to be performed to really solve the consequences of reduced amounts of  $\alpha$ -hydroxy fatty acids in Arabidopsis. The *fah1xfah2* mutant needs to be crossed with SA mutants to examine which effect in the mutant is due to the accumulation of the phytohormone. Further, LCBs and glycosylinositolphosphoryl ceramides have to be measured to see how these sphingolipid species are affected by the  $\alpha$ -hydroxylation defect. Additionally, sphingolipids in *V. longisporum* infected plants need to be measured to determine if they are affected and if they could have an impact on the infection.

## 5 Summary

*Verticillium longisporum* is a soil borne pathogen which infects plants of the *Brassicaceae* family. The fungus enters through the roots and spreads within the plant through the xylem. Using the model plant *Arabidopsis thaliana* this thesis focused on metabolic changes accompanying the plant-fungus interaction. A metabolite fingerprinting approach was used to find metabolic changes in *Arabidopsis* upon infection. The most prominent markers that were identified derived from the phenylpropanoid pathway. Quantification of the phenylpropanoids by directed measurements could confirm the data of the non-targeted approach showing an accumulation of sinapoyl glucose, coniferin and diverse lignans already at early stages of infection. To test the contribution of the identified metabolic pathway on susceptibility of *Arabidopsis* against *V. longisporum*, different mutants of the phenylpropanoid pathway were analyzed. One of those was a ferulate-5-hydroxylase mutant (*fah1-2*) which is devoid of sinapate and its esters. This mutant showed a higher susceptibility towards the fungus, underlining the importance of the missing metabolites for the plant during infection. In addition a coniferin accumulation mutant (UGT72E2-OE) showed less stunting and more fungal DNA than wild type plants under infection. This effect might be due to fungal growth inhibiting properties of the deglycosylated coniferin or to an influence on fungal development of coniferin itself.

Additionally implication of suberin and sphingolipids with  $\alpha$ -hydroxy fatty acids in the infection was tested in this thesis. Suberin analyses at early time points of infection as well as infection of suberin mutants did not reveal any importance of this polymer in the infection.

To investigate the functional significance of the  $\alpha$ -hydroxylation in fatty acids of sphingolipids, T-DNA insertion mutants of both *Fatty Acid Hydroxylase* genes (*AtFAH1* and *AtFAH2*) were analyzed in *Arabidopsis*. No phenotype was visible in the single mutant lines but the double mutant showed reduction in leaf size, root length and wrinkled leaves. Ceramide and glucosylceramide profiles of the double mutant showed a strong reduction of sphingolipids with  $\alpha$ -hydroxylated fatty acid moieties and an accumulation of the one without hydroxy group. The total ceramide amount was ten times increased in the double mutant, whereas the glucosylceramide pool was 25 % reduced. Metabolite fingerprinting of the double mutant revealed differences compared to wild type in the metabolome. The most prominent markers were salicylic acid (SA) and its glucoside. Infection of the double mutant with powdery mildew resulted in less fungal colonization whereas infection with *V. longisporum* resulted in stronger stunting and slightly higher fungal DNA amount in infected plants.

In summary it could be shown that the phenylpropanoid pathway is important for the defense response in *Arabidopsis* against *V. longisporum* but fatty acid monomers derived from suberin and sphingolipids seem to play no or only a minor role.

## 6 References

- Abdel-Farid IB, Jahangir M, van den Hondel CAMJJ, Kim HK, Choi YH, Verpoorte R (2009) Fungal infection-induced metabolites in *Brassica rapa*. *Plant Science* **176**(5): 608-615
- Adlercreutz H (2007) Lignans and human health. *Critical Reviews in Clinical Laboratory Sciences* **44**(5-6): 483-525
- Akiyama K, Yamauchi S, Nakato T, Maruyama M, Sugahara T, Kishida T, (2007) Antifungal activity of tetra-substituted tetrahydrofuran lignan, (-)-virgatusin, and its structure-activity relationship. *Bioscience, Biotechnology and Biochemistry* **71**(4): 1028-1035
- Ausubel FM, Brent RE, Kingston DD, Seidmann JR, Smith JA, Struhl K (1993) *Current Protocols in Molecular Biology*, New York: Green Publishing Associates and John Wiley and Sons Inc.
- Ayella AK, Trick HN, Wang W (2007) Enhancing lignan biosynthesis by over-expressing pinoresinol lariciresinol reductase in transgenic wheat. *Molecular Nutrition & Food Research* **51**(12): 1518-1526
- Bannenberg G, Martinez M, Rodriguez MJ, Lopez MA, Ponce de Leon I, Hamberg M, Castresana C (2009) Functional analysis of  $\alpha$ -DOX2, an active  $\alpha$ -dioxygenase critical for normal development in tomato plants. *Plant Physiology* **151**(3): 1421-1432
- Barbara DJ, Clewes E (2003) Plant pathogenic *Verticillium* species: how many of them are there? *Molecular Plant Pathology* **4**(4): 297-305
- Baxter I, Hosmani PS, Rus A, Lahner B, Borevitz JO, Muthukumar B, Mickelbart MV, Schreiber L, Franke RB, Salt DE (2009) Root suberin forms an extracellular barrier that affects water relations and mineral nutrition in *Arabidopsis*. *PLoS Genetics* **5**(5): e1000492
- Bechinger C, Giebel K-F, Schnell M, Leiderer P, Deising HB, Bastmeyer M (1999) Optical measurements of invasive forces exerted by appressoria of a plant pathogenic fungus. *Science* **285**(5435): 1896-1899
- Beckman CH (1987) *The nature of wilt diseases of plants*. St Paul, Minn: APS Press
- Bednarek P, Osbourn A (2009) Plant-microbe interactions: chemical diversity in plant defense. *Science* **324**(5928): 746-748
- Bednarek P, Pislewska-Bednarek M, Svatos A, Schneider B, Doubsky J, Mansurova M, Humphry M, Consonni C, Panstruga R, Sanchez-Vallet A, Molina A, Schulze-Lefert P (2009) A glucosinolate metabolism pathway in living plant cells mediates broad-spectrum antifungal defense. *Science* **323**(5910): 101-106
- Bednarek P, Schneider B, Svatos A, Oldham NJ, Hahlbrock K (2005) Structural complexity, differential response to infection, and tissue specificity of indolic and phenylpropanoid secondary metabolism in *Arabidopsis* roots. *Plant Physiology* **138**(2): 1058-1070

- Beisson F, Li Y, Bonaventure G, Pollard M, Ohlrogge JB (2007) The acyltransferase GPAT5 is required for the synthesis of suberin in seed coat and root of Arabidopsis. *The Plant Cell* **19**(1): 351-368
- Benhamou N (1995) Elicitor-induced resistance in tomato plants against fungal pathogens: ultrastructure and cytochemistry of the induced response. *Scanning Microscopy* **9**(3): 861-880
- Berlanger I, Powelson ML. (2000) Verticillium wilt. *The Plant Health Instructor*. APSnet Plant Disease Lesson
- Bernards MA (2002) Demystifying suberin. *Canadian Journal of Botany* **80**(3): 227-240
- Bessire M, Chassot C, Jacquat AC, Humphry M, Borel S, Petetot JM, Metraux JP, Nawrath C (2007) A permeable cuticle in Arabidopsis leads to a strong resistance to Botrytis cinerea. *The EMBO Journal* **26**: 2158–2168
- Bird D, Beisson F, Brigham A, Shin J, Greer S, Jetter R, Kunst L, Wu X, Yephremov A, Samuels L (2007) Characterization of Arabidopsis ABCG11/WBC11, an ATP binding cassette (ABC) transporter that is required for cuticular lipid secretion. *The Plant Journal* **52**(3): 485-498
- Bishop CD, Cooper RM (1983) An ultrastructural study of vascular colonization in three vascular wilt diseases I. Colonization of susceptible cultivars. *Physiological Plant Pathology* **23**(3): 323-343
- Boerjan W, Ralph J, Baucher M (2003) Lignin Biosynthesis. *Annual Review of Plant Biology* **54**(1): 519-546
- Boggs JM, Koshy KM, Rangaraj G (1988) Influence of structural modifications on the phase behavior of semi-synthetic cerebroside sulfate. *Biochimica et Biophysica Acta (BBA) - Biomembranes* **938**(3): 361-372
- Bollina V, Kumaraswamy GK, Kushalappa AC, Choo TM, Dion Y, Rioux S, Faubert D, Hamzehzarghani H (2010) Mass spectrometry-based metabolomics application to identify quantitative resistance-related metabolites in barley against Fusarium head blight. *Molecular Plant Pathology* **11**(6): 769-782
- Bonaventure G, Beisson F, Ohlrogge J, Pollard M (2004) Analysis of the aliphatic monomer composition of polyesters associated with Arabidopsis epidermis: occurrence of octadeca-cis-6, cis-9-diene-1,18-dioate as the major component. *The Plant Journal* **40**(6): 920-930
- Brader G, Mikkelsen MD, Halkier BA, Tapio Palva E (2006) Altering glucosinolate profiles modulates disease resistance in plants. *The Plant Journal* **46**(5): 758-767
- Brader G, Tas Ñ, Palva ET (2001) Jasmonate-dependent induction of indole glucosinolates in Arabidopsis by culture filtrates of the nonspecific pathogen Erwinia carotovora. *Plant Physiology* **126**(2): 849-860
- Brandfass C, Karlovsky P (2006) Simultaneous detection of Fusarium culmorum and F. graminearum in plant material by duplex PCR with melting curve analysis. *BMC Microbiology* **6**: 4

- Brodersen P, Malinovsky FG, Hématy K, Newman M-A, Mundy J (2005) The role of salicylic acid in the induction of cell death in *Arabidopsis* acd11. *Plant Physiology* **138**(2): 1037-1045
- Brodersen P, Petersen M, Pike HM, Olszak B, Skov S, Oedum N, Joergensen LB, Brown RE, Mundy J (2002) Knockout of *Arabidopsis* ACCELERATED-CELL-DEATH11 encoding a sphingosine transfer protein causes activation of programmed cell death and defense. *Genes & Development* **16**(4): 490-502
- Bromley PE, Li YO, Murphy SM, Sumner CM, Lynch DV (2003) Complex sphingolipid synthesis in plants: characterization of inositolphosphorylceramide synthase activity in bean microsomes. *Archives of Biochemistry and Biophysics* **417**(2): 219-226
- Cahoon EB, Lynch DV (1991) Analysis of glucocerebrosides of rye (*Secale cereale* L. cv Puma) leaf and plasma membrane. *Plant Physiology* **95**(1): 58-68
- Carpinella MC, Ferrayoli CG, Palacios SM (2005) Antifungal synergistic effect of scopoletin, a hydroxycoumarin isolated from *Melia azedarach* L. fruits. *Journal of Agricultural and Food Chemistry* **53**(8): 2922-2927
- Carpinella MC, Giorda LM, Ferrayoli CG, Palacios SM (2003) Antifungal effects of different organic extracts from *Melia azedarach* L. on phytopathogenic fungi and their isolated active components. *Journal of Agricultural and Food Chemistry* **51**(9): 2506-2511
- Chapple CCS, Vogt T, Ellis BE, Somerville CR (1992) An *Arabidopsis* mutant defective in the general phenylpropanoid pathway. *The Plant Cell* **4**(11): 1413-1424
- Chassot C, Nawrath C, Metraux J-P (2007) Cuticular defects lead to full immunity to a major plant pathogen. *The Plant Journal* **49**(6): 972-980
- Chen M, Markham JE, Dietrich CR, Jaworski JG, Cahoon EB (2008) Sphingolipid long-chain base hydroxylation is important for growth and regulation of sphingolipid content and composition in *Arabidopsis*. *The Plant Cell* **20**(7): 1862-1878
- Chomczynski P, Mackey K (1995) Short technical reports. Modification of the TRI reagent procedure for isolation of RNA from polysaccharide- and proteoglycan-rich sources. *BioTechniques* **19**(6): 942-945
- Clay NK, Adio AM, Denoux C, Jander G, Ausubel FM (2009) Glucosinolate metabolites required for an *Arabidopsis* innate immune response. *Science* **323**(5910): 95-101
- Compagnon V, Diehl P, Benveniste I, Meyer D, Schaller H, Schreiber L, Franke R, Pinot F (2009) CYP86B1 is required for very long chain  $\omega$ -hydroxyacid and  $\alpha,\omega$ -dicarboxylic acid synthesis in root and seed suberin polyester. *Plant Physiology* **150**(4): 1831-1843
- Davin LB, Jourdes M, Patten AM, Kim K-W, Vassao DG, Lewis NG (2008) Dissection of lignin macromolecular configuration and assembly: Comparison to related biochemical processes in allyl/propenyl phenol and lignan biosynthesis. *Natural Product Reports* **25**(6): 1015-1090
- Davin LB, Lewis NG (2005) Lignin primary structures and dirigent sites. *Current Opinion in Biotechnology* **16**(4): 407-415
- De Ascensao ARFDC, Dubery IA (2003) Soluble and wall-bound phenolics and phenolic polymers in *Musa acuminata* roots exposed to elicitors from *Fusarium oxysporum* f.sp. cubense. *Phytochemistry* **63**(6): 679-686

- De Leon IP, Sanz A, Hamberg M, Castresana C (2002) Involvement of the Arabidopsis  $\alpha$ -DOX1 fatty acid dioxygenase in protection against oxidative stress and cell death. *The Plant Journal* **29**(1): 61-62
- Dixon GR, Pegg GF (1972) Changes in amino-acid content of tomato xylem sap following infection with strains of *Verticillium albo-atrum*. *Annals of Botany* **36**(1): 147-154
- Dixon RA, Harrison MJ, Lamb CJ (1994) Early events in the activation of plant defense responses. *Annual Review of Phytopathology* **32**: 479-501
- Dixon RA, Paiva NL (1995) Stress-induced phenylpropanoid metabolism. *The Plant Cell* **7**(7): 1085-1097
- Dunker S, Keunecke H, Steinbach P, von Tiedemann A (2008) Impact of *Verticillium longisporum* on yield and morphology of winter oilseed rape (*Brassica napus*) in relation to systemic spread in the plant. *Journal of Phytopathology* **156**(11-12): 689-707
- Dunn TM, Lynch DV, Michaelson LV, Napier JA (2004) A post-genomic approach to understanding sphingolipid metabolism in *Arabidopsis thaliana*. *Annals of Botany* **93**(5): 483-497
- Durrant WE, Dong X (2004) Systemic acquired resistance. *Annual Review of Phytopathology* **42**(1): 185-209
- Eynck C, Koopmann B, Grunewaldt-Stoecker G, Karlovsky P, von Tiedemann A (2007) Differential interactions of *Verticillium longisporum* and *V. dahliae* with *Brassica napus* detected with molecular and histological techniques. *European Journal of Plant Pathology* **118**: 259-274
- Eynck C, Koopmann B, Karlovsky P, von Tiedemann A (2009) Internal resistance in winter oilseed rape inhibits systemic spread of the vascular pathogen *Verticillium longisporum*. *Phytopathology* **99**(7): 802-811
- Fahey JW, Zalcmann AT, Talalay P (2001) The chemical diversity and distribution of glucosinolates and isothiocyanates among plants. *Phytochemistry* **56**(1): 5-51
- Fernie AR, Martinoia E (2009) Malate. Jack of all trades or master of a few? *Phytochemistry* **70**(7): 828-832
- Floerl S (2007) Identifizierung und Charakterisierung extrazellulärer Proteine unter dem Einfluss von *Verticillium longisporum* in *Arabidopsis thaliana* und Raps (*Brassica napus*). Dissertation, Georg-August-University Göttingen
- Floerl S, C. Druebert, H.I. Aroud, P. Karlovsky, Polle A (2010) Disease symptoms and mineral nutrition in *Arabidopsis thaliana* in response to *Verticillium longisporum* infection. *Journal of Plant Pathology* **92**(3): 693-700
- Floerl S, Druebert C, Majcherczyk A, Karlovsky P, Kues U, Polle A (2008) Defence reactions in the apoplastic proteome of oilseed rape (*Brassica napus* var. *napus*) attenuate *Verticillium longisporum* growth but not disease symptoms. *BMC Plant Biology* **8**: 129
- Fradin EF, Thomma BP (2006) Physiology and molecular aspect of *Verticillium* wilt diseases caused by *V. dahliae* and *V. albo-atrum*. *Molecular Plant Pathology* **7**(2): 71-86

- Francis SA, Dewey FM, Gurr SJ (1996) The role of cutinase in germling development and infection by *Erysiphe graminis* f.sp.hordei. *Physiological and Molecular Plant Pathology* **49**(3): 201-211
- Franke R, Briesen I, Wojciechowski T, Faust A, Yephremov A, Nawrath C, Schreiber L (2005) Apoplastic polyesters in Arabidopsis surface tissues - a typical suberin and a particular cutin. *Phytochemistry* **66**(22): 2643-2658
- Franke R, Höfer R, Briesen I, Emsermann M, Efremova N, Yephremov A, Schreiber L, (2009) The *DAISY* gene from Arabidopsis encodes a fatty acid elongase condensing enzyme involved in the biosynthesis of aliphatic suberin in roots and the chalazamicropyle region of seeds. *The Plant Journal* **57**(1): 80-95
- Fraser CM, Thompson MG, Shirley AM, Ralph J, Schoenherr JA, Sinlapadech T, Hall MC, Chapple C (2007) Related Arabidopsis serine carboxypeptidase-like sinapoylglucose acyltransferases display distinct but overlapping substrate specificities. *Plant Physiology* **144**(4): 1986-1999
- Frye CA, Innes RW (1998) An Arabidopsis mutant with enhanced resistance to powdery mildew. *The Plant Cell Online* **10**(6): 947-956
- Gang DR, Kasahara H, Xia Z-Q, Vander Mijnsbrugge K, Bauw G, Boerjan W, Van Montagu M, Davin LB, Lewis NG (1999) Evolution of plant defense mechanisms. *Journal of Biological Chemistry* **274**(11): 7516-7527
- Gayoso C, Pomar F, Novo-Uzal E, Merino F, Martinez de Ilarduya O (2010) The Ve-mediated resistance response of the tomato to *Verticillium dahliae* involves H<sub>2</sub>O<sub>2</sub>, peroxidase and lignins and drives PAL gene expression. *BMC Plant Biology* **10**:232
- Gilbert RD, Johnson AM, Dean RA (1996) Chemical signals responsible for appressorium formation in the rice blast fungus *Magnaporthe grisea*. *Physiological and Molecular Plant Pathology* **48**(5): 335-346
- Glawischnig E (2007) Camalexin. *Phytochemistry* **68**(4): 401-406
- Glazebrook J (2005) Contrasting mechanisms of defense against biotrophic and necrotrophic pathogens. *Annual Review of Phytopathology* **43**(1): 205-227
- Gold J, Robb J (1995) The role of the coating response in *Craigella* tomatoes infected with *Verticillium dahliae*, races 1 and 2. *Physiological and Molecular Plant Pathology* **47**(3): 141-157
- Graça J, Santos S (2007) Suberin: A biopolyester of plants' skin. *Macromolecular Bioscience* **7**(2): 128-135
- Greenberg JT, Silverman FP, Liang H (2000) Uncoupling salicylic acid-dependent cell death and defense-related responses from disease resistance in the Arabidopsis mutant *acd5*. *Genetics* **156**(1): 341-350
- Griffiths DA (1971) The development of lignitubers in roots after infection by *Verticillium dahliae* Kleb. *Canadian Journal of Microbiology* **17**(4): 441-444
- Häffner E, Karlovsky P, Diederichsen E (2010) Genetic and environmental control of the *Verticillium* syndrome in Arabidopsis thaliana. *BMC Plant Biology* **10**(1): 235

- Hagemeyer J, Schneider B, Oldham NJ, Hahlbrock K (2001) Accumulation of soluble and wall-bound indolic metabolites in *Arabidopsis thaliana* leaves infected with virulent or avirulent *Pseudomonas syringae* pathovar tomato strains. *Proceedings of the National Academy of Sciences of the United States of America* **98**(2): 753-758
- Hama H (2010) Fatty acid 2-hydroxylation in mammalian sphingolipid biology. *Biochimica et Biophysica Acta (BBA) - Molecular and Cell Biology of Lipids* **1801**(4): 405-414
- Hamberg M, Sanz A, Castresana C (1999)  $\alpha$ -Oxidation of fatty acids in higher plants - identification of a pathogen-inducible oxygenase (PIOX) as an  $\alpha$ -dioxygenase and biosynthesis of 2-hydroperoxylinolenic acid. *Journal of Biological Chemistry* **274**(35): 24503-24513
- Hammerschmidt R (1999) Phytoalexins: What have we learned after 60 years? *Annual Review of Phytopathology* **37**(1): 285-306
- Hano C, Addi M, Bensaddek L, Cr nier D, Baltora-Rosset S, Dousot J, Maury S, Mesnard F, Chabbert B, Hawkins S, Lain  E, Lamblin F (2006) Differential accumulation of monolignol-derived compounds in elicited flax (*Linum usitatissimum*) cell suspension cultures. *Planta* **223**(5): 975-989
- Harborne JB, Williams CA (2000) Advances in flavonoid research since 1992. *Phytochemistry* **55**(6): 481-504
- Harrison S, Mott E, Parsley K, Aspinall S, Gray J, Cottage A (2006) A rapid and robust method of identifying transformed *Arabidopsis thaliana* seedlings following floral dip transformation. *Plant Methods* **2**(19): 1746-4811
- H fer R, Briesen I, Beck M, Pinot F, Schreiber L, Franke R (2008) The *Arabidopsis* cytochrome P450 CYP86A1 encodes a fatty acid  $\omega$ -hydroxylase involved in suberin monomer biosynthesis. *Journal of Experimental Botany* **59**(9): 2347-2360
- Howard RJ, Ferrari MA, Roach DH, Money NP (1991) Penetration of hard substrates by a fungus employing enormous turgor pressures. *Proceedings of the National Academy of Sciences of the United States of America* **88**(24): 11281-11284
- Huang J, Bhinu VS, Li X, Dallal Bashi Z, Zhou R, Hannoufa A (2009) Pleiotropic changes in *Arabidopsis* f5h and sct mutants revealed by large-scale gene expression and metabolite analysis. *Planta* **230**(5): 1057-1069
- Humphreys JM, Chapple C (2002) Rewriting the lignin roadmap. *Current Opinion in Plant Biology* **5**(3): 224-229
- Imai H, Ohnishi M, Kinoshita M, Kojima M, Ito S (1995) Structure and distribution of cerebroside containing unsaturated hydroxy fatty acids in plant leaves. *Bioscience, Biotechnology and Biochemistry* **59**: 1309-1313
- Inderbitzin P, Davis RM, Bostock RM, Subbarao KV (2011) The ascomycete *Verticillium longisporum* is a hybrid and a plant pathogen with an expanded host range. *PLoS ONE* **6**(3): e18260
- Iven T (2009) Transkriptomanalyse der *Arabidopsis*-Wurzel nach Infektion mit dem pilzlichen Pathogen *Verticillium longisporum* und Identifizierung von transkriptionellen Regulatoren der Pathogenantwort. Dissertation, Georg-August-University G ttingen

- Jez JM, Bowman ME, Noel JP (2002) Role of hydrogen bonds in the reaction mechanism of chalcone isomerase. *Biochemistry* **41**(16): 5168-5176
- Johansson A, Goud J-K, Dixelius C (2006a) Plant host range of *Verticillium longisporum* and microsclerotia density in Swedish soils. *European Journal of Plant Pathology* **114**(2): 139-149
- Johansson A, Staal J, Dixelius C (2006b) Early responses in the *Arabidopsis*-*Verticillium longisporum* pathosystem are dependent on NDR1, JA- and ET-associated signals via cytosolic NPR1 and RFO1. *Molecular Plant-Microbe Interactions* **19**(9): 958-969
- Jones JDG, Dangl JL (2006) The plant immune system. *Nature* **444**(7117): 323-329
- Jones P, Vogt T (2001) Glycosyltransferases in secondary plant metabolism: tranquilizers and stimulant controllers. *Planta* **213**(2): 164-174
- Jung H-JG, Ni W, Chapple CCS, Meyer K (1999) Impact of lignin composition on cell-wall degradability in an *Arabidopsis* mutant. *Journal of the Science of Food and Agriculture* **79**(6): 922-928
- Jung H, Deetz D (1993) Cell wall lignification and degradability. In *Forage Cell Wall Structure and Digestibility*, Jung H, Buxton D, Hatfield R, Ralph J (eds), pp 315-346. Madison, USA: Am Soc Agron
- Kaefer A, Lingner T, Feussner K, Göbel C, Feussner I, Meinicke P (2009) MarVis: a tool for clustering and visualization of metabolic biomarkers. *BMC Bioinformatics* **10**: 92
- Karapapa VK, Bainbridge BW, Heale JB (1997) Morphological and molecular characterization of *Verticillium longisporum* comb. nov., pathogenic to oilseed rape. *Mycological Research* **101**(11): 1281-1294
- Katagiri F, Thilmony R, He SY (2002) The *Arabidopsis thaliana*-*Pseudomonas syringae* interaction. *The Arabidopsis Book*: e0039
- Kaya K, Ramesha CS, Thompson GA (1984) On the formation of alpha-hydroxy fatty acids. Evidence for a direct hydroxylation of nonhydroxy fatty acid-containing sphingolipids. *Journal of Biological Chemistry* **259**(6): 3548-3553
- Keen NT, Littlefield LJ (1979) The possible association of phytoalexins with resistance gene expression in flax to *Melampsora lini*. *Physiological Plant Pathology* **14**(3): 265-280
- Kliebenstein DJ, Rowe HC, Denby KJ (2005) Secondary metabolites influence *Arabidopsis*/*Botrytis* interactions: variation in host production and pathogen sensitivity. *The Plant Journal* **44**(1): 25-36
- Koga J, Yamauchi T, Shimura M, Ogawa N, Oshima K, Umemura K, Kikuchi M, Ogasawara N (1998) Cerebrosides A and C, sphingolipid elicitors of hypersensitive cell death and phytoalexin accumulation in rice plants. *Journal of Biological Chemistry* **273**(48): 31985-31991
- Kolattukudy P (2001) Polyesters in higher plants. In *Biopolyesters* Vol. 71, pp 1-49. Springer Berlin / Heidelberg
- Kunst L, Samuels AL (2003) Biosynthesis and secretion of plant cuticular wax. *Progress in Lipid Research* **42**(1): 51-80

- Kurdyukov S, Faust A, Nawrath C, Bar S, Voisin D, Efremova N, Franke R, Schreiber L, Saedler H, Metraux J-P, Yephremov A (2006a) The epidermis-specific extracellular BODYGUARD controls cuticle development and morphogenesis in Arabidopsis. *The Plant Cell* **18**(2): 321-339
- Kurdyukov S, Faust A, Trenkamp S, Bär S, Franke R, Efremova N, Tietjen K, Schreiber L, Saedler H, Yephremov A (2006b) Genetic and biochemical evidence for involvement of HOTHEAD in the biosynthesis of long-chain  $\alpha$ , $\omega$ -dicarboxylic fatty acids and formation of extracellular matrix. *Planta* **224**(2): 315-329
- Lamb C, Dixon RA (1997) The oxidative burst in plant disease resistance. *Annual Review of Plant Physiology and Plant Molecular Biology* **48**: 251-275
- Landry LG, C. C. Chapple, and R. L. Last (1995) Arabidopsis mutants lacking phenolic sunscreens exhibit enhanced ultraviolet-B injury and oxidative damage. *Plant Physiology* **109**(4): 1159-1166
- Lanot A, Hodge D, Jackson RG, George GL, Elias L, Lim E-K, Vaistij FE, Bowles DJ (2006) The glucosyltransferase UGT72E2 is responsible for monolignol 4-O-glucoside production in Arabidopsis thaliana. *The Plant Journal* **48**(2): 286-295
- Lanot A, Hodge D, Lim E-K, Vaistij F, Bowles D (2008) Redirection of flux through the phenylpropanoid pathway by increased glucosylation of soluble intermediates. *Planta* **228**(4): 609-616
- Lee S-B, Jung S-J, Go Y-S, Kim H-U, Kim J-K, Cho H-J, Park OK, Suh M-C (2009) Two Arabidopsis 3-ketoacyl CoA synthase genes, KCS20 and KCS2/DAISY, are functionally redundant in cuticular wax and root suberin biosynthesis, but differentially controlled by osmotic stress. *The Plant Journal* **60**(3): 462-475
- Lee S-W, Nazar RN, Powell DA, Robb J (1992) Reduced PAL gene suppression in Verticillium-infected resistant tomatoes. *Plant Molecular Biology* **18**(2): 345-352
- Lehfeldt C, Shirley AM, Meyer K, Ruegger MO, Cusumano JC, Viitanen PV, Strack D, Chapple C (2000) Cloning of the SNG1 gene of Arabidopsis reveals a role for a serine carboxypeptidase-like protein as an acyltransferase in secondary metabolism. *The Plant Cell Online* **12**(8): 1295-1306
- Li-Beisson Y (2011) Cutin and Suberin. In eLS. John Wiley & Sons, Ltd
- Li Y, Beisson F, Koo AJK, Molina I, Pollard M, Ohlrogge J (2007) Identification of acyltransferases required for cutin biosynthesis and production of cutin with suberin-like monomers. *Proceedings of the National Academy of Sciences of the United States of America* **104**(46): 18339-18344
- Liang H, Yao N, Song JT, Luo S, Lu H, Greenberg JT (2003) Ceramides modulate programmed cell death in plants. *Genes & Development* **17**(21): 2636-2641
- Lim E-K, Li Y, Parr A, Jackson R, Ashford DA, Bowles DJ (2001) Identification of glucosyltransferase genes involved in sinapate metabolism and lignin synthesis in Arabidopsis. *Journal of Biological Chemistry* **276**(6): 4344-4349
- Lipka V, Dittgen J, Bednarek P, Bhat R, Wiermer M, Stein M, Landtag Jr, Brandt W, Rosahl S, Scheel D, Llorente F, Molina A, Parker J, Somerville S, Schulze-Lefert P (2005) Pre- and postinvasion defenses both contribute to nonhost resistance in Arabidopsis. *Science* **310**(5751): 1180-1183

- Lloyd AJ, William Allwood J, Winder CL, Dunn WB, Heald JK, Cristescu SM, Sivakumaran A, Harren FJM, Mulema J, Denby K, Goodacre R, Smith AR, Mur LAJ (2011) Metabolomic approaches reveal that cell wall modifications play a major role in ethylene-mediated resistance against *Botrytis cinerea*. *The Plant Journal*: epub ahead of print
- Löfgren H, Pascher I (1977) Molecular arrangements of sphingolipids. The monolayer behaviour of ceramides. *Chemistry and Physics of Lipids* **20**(4): 273-284
- Lorenzen M, Racicot V, Strack D, Chapple C (1996) Sinapic acid ester metabolism in wild type and a sinapoylglucose-accumulating mutant of *Arabidopsis*. *Plant Physiology* **112**(4): 1625-1630
- Lulai E (2005) Non-wound-induced suberization of tuber parenchyma cells: A physiological response to the wilt disease pathogen *Verticillium dahliae*. *American Journal of Potato Research* **82**(6): 433-440
- Lynch DV, Dunn TM (2004) An introduction to plant sphingolipids and a review of recent advances in understanding their metabolism and function. *New Phytologist* **161**(3): 677-702
- Lynch DV, Steponkus PL (1987) Plasma membrane lipid alterations associated with cold acclimation of winter rye seedlings (*Secale cereale* L. cv Puma). *Plant Physiology* **83**: 761-767
- Markham JE, Jaworski JG (2007) Rapid measurement of sphingolipids from *Arabidopsis thaliana* by reversed-phase high-performance liquid chromatography coupled to electrospray ionization tandem mass spectrometry. *Rapid Communications in Mass Spectrometry* **21**(7): 1304-1314
- Matyash V, Liebisch G, Kurzchalia TV, Shevchenko A, Schwudke D (2008) Lipid extraction by methyl-tert-butyl ether for high-throughput lipidomics. *Journal of Lipid Research* **49**(5): 1137-1146
- Melotto M, Underwood W, He SY (2008) Role of stomata in plant innate immunity and foliar bacterial diseases. *Annual Review of Phytopathology* **46**(1): 101-122
- Menden B, Kohlhoff M, Moerschbacher BM (2007) Wheat cells accumulate a syringyl-rich lignin during the hypersensitive resistance response. *Phytochemistry* **68**(4): 513-520
- Meyer K, Shirley AM, Cusumano JC, Bell-Lelong DA, Chapple C (1998) Lignin monomer composition is determined by the expression of a cytochrome P450-dependent monooxygenase in *Arabidopsis*. *Proceedings of the National Academy of Sciences of the United States of America* **95**(12): 6619-6623
- Milkowski C, Strack D (2010) Sinapate esters in brassicaceous plants: biochemistry, molecular biology, evolution and metabolic engineering. *Planta* **232**(1): 19-35
- Mitchell AG, Martin CE (1997) Fah1p, a *Saccharomyces cerevisiae* cytochrome *b5* fusion protein, and its *Arabidopsis thaliana* homolog that lacks the cytochrome *b5* domain both function in the  $\alpha$ -hydroxylation of sphingolipid-associated very long chain fatty acids. *Journal of Biological Chemistry* **272**(45): 28281-28288
- Mol L, Scholte K, Vos J (1995) Effects of crop rotation and removal of crop debris on the soil population of two isolates of *Verticillium dahliae*. *Plant Pathology* **44**(6): 1070-1074

- Molina I, Bonaventure G, Ohlrogge J, Pollard M (2006) The lipid polyester composition of *Arabidopsis thaliana* and *Brassica napus* seeds. *Phytochemistry* **67**(23): 2597-2610
- Morrissey JP, Osbourn AE (1999) Fungal resistance to plant antibiotics as a mechanism of pathogenesis. *Microbiology and Molecular Biology Reviews* **63**(3): 708-724
- Nagano M, Ihara-Ohori Y, Imai H, Inada N, Fujimoto M, Tsutsumi N, Uchimiya H, Kawai-Yamada M (2009) Functional association of cell death suppressor, *Arabidopsis* Bax inhibitor-1, with fatty acid 2-hydroxylation through cytochrome b5. *The Plant Journal* **58**(1): 122-134
- Nair RB, Bastress KL, Ruegger MO, Denault JW, Chapple C (2004) The *Arabidopsis thaliana* REDUCED EPIDERMAL FLUORESCENCE1 gene encodes an aldehyde dehydrogenase involved in ferulic acid and sinapic acid biosynthesis. *The Plant Cell* **16**(2): 544-554
- Nakatsubo T, Mizutani M, Suzuki S, Hattori T, Umezawa T (2008) Characterization of *Arabidopsis thaliana* pinorexinol reductase, a new type of enzyme involved in lignan biosynthesis. *Journal of Biological Chemistry* **283**(23): 15550-15557
- Naoumkina MA, Zhao Q, Gallego-Giraldo L, Dai X, Zhao PX, Dixon RA (2010) Genome-wide analysis of phenylpropanoid defence pathways. *Molecular Plant Pathology* **11**(6): 829-846
- Nahlik K., Dumkow M, Bayram Ö, Helmstaedt K, Busch S, Valerius O, Gerke J, Hoppert M, Schwier E, Opitz L, Westermann M, Grond S, Feussner K, Goebel C, Kaefer A, Meinicke P, Feussner I, Braus GH (2010) The COP9 signalosome mediates transcriptional and metabolic response to hormones, oxidative stress protection and cell wall rearrangement during fungal development. *Molecular Microbiology* **78**(4): 964-979.
- Nawrath C (2002) The biopolymers cutin and suberin. In *The Arabidopsis Book*, Somerville C, Meyerowitz E (eds), pp 1-14. Rockville, MD: American Society of Plant Biologists
- Nawrath C (2006) Unraveling the complex network of cuticular structure and function. *Current Opinion in Plant Biology* **9**(3): 281-287
- Njoroge SMC, Vallad GE, Park SY, Kang S, Koike ST, Bolda M, Burman P, Polonik W, Subbarao KV (2011) Phenological and phytochemical changes correlate with differential interactions of *Verticillium dahliae* with broccoli and cauliflower. *Phytopathology* **101**(5): 523-534
- Nürnberg T, Lipka V (2005) Non-host resistance in plants: new insights into an old phenomenon. *Molecular Plant Pathology* **6**(3): 335-345
- Park JH, Suh MC, Kim TH, Kim MC, Cho SH (2008) Expression of glycine-rich protein genes, AtGRP5 and AtGRP23, induced by the cutin monomer 16-hydroxypalmitic acid in *Arabidopsis thaliana*. *Plant Physiology and Biochemistry* **46**(11): 1015-1018
- Parker D, Beckmann M, Zubair H, Enot DP, Caracul-Rios Z, Overy DP, Snowdon S, Talbot NJ, Draper J (2009) Metabolomic analysis reveals a common pattern of metabolic re-programming during invasion of three host plant species by *Magnaporthe oryzae*. *The Plant Journal* **59**(5): 723-737
- Pascher I, Sundell S (1977) Molecular arrangements in sphingolipids. The crystal structure of cerebroside. *Chemistry and Physics of Lipids* **20**(3): 175-191

- Pata MO, Hannun YA, Ng CK-Y (2010) Plant sphingolipids: decoding the enigma of the Sphinx. *New Phytologist* **185**(3): 611-630
- Pedras MSC, Zheng Q-A, Strelkov S (2008) Metabolic changes in roots of the oilseed canola infected with the biotroph *Plasmodiophora brassicae*: phytoalexins and phytoanticipins. *Journal of Agricultural and Food Chemistry* **56**(21): 9949-9961
- Pegg GF, Brady. BL (2002) *Verticillium Wilts*. Wallingford: CABI
- Pickel B, Constantin M-A, Pfannstiel J, Conrad J, Beifuss U, Schaller A (2010) An enantiocomplementary dirigent protein for the enantioselective laccase-catalyzed oxidative coupling of phenols. *Angewandte Chemie International Edition* **49**(1): 202-204
- Picman AK, Schneider EF, Picman J (1995) Effect of flavonoids on mycelial growth of *Verticillium albo-atrum*. *Biochemical Systematics and Ecology* **23**(7-8): 683-693
- Pollard M, Beisson F, Li Y, Ohlgrogge JB (2008) Building lipid barriers: biosynthesis of cutin and suberin. *Trends in Plant Science* **13**(5): 236-246
- Pomar F, Novo M, Bernal MA, Merino F, Barceló AR (2004) Changes in stem lignins (monomer composition and crosslinking) and peroxidase are related with the maintenance of leaf photosynthetic integrity during *Verticillium* wilt in *Capsicum annuum*. *New Phytologist* **163**(1): 111-123
- Quentin MI, Allasia Vr, Pegard A, Allais F, Ducrot P-H, Favery B, Levis C, Martinet S, Masur C, Ponchet M, Roby D, Schlaich NL, Jouanin L, Keller H (2009) Imbalanced lignin biosynthesis promotes the sexual reproduction of homothallic oomycete pathogens. *PLoS Pathogens* **5**(1): e1000264
- Ralph SG, Jancsik S, Bohlmann J (2007) Dirigent proteins in conifer defense II: Extended gene discovery, phylogeny, and constitutive and stress-induced gene expression in spruce (*Picea* spp.). *Phytochemistry* **68**(14): 1975-1991
- Ranathunge K, Thomas RH, Fang X, Peterson CA, Gijzen M, Bernards MA (2008) Soybean root suberin and partial resistance to root rot caused by *Phytophthora sojae*. *Phytopathology* **98**(11): 1179-1189
- Ratzinger A, Riediger N, von Tiedemann A, Karlovsky P (2009) Salicylic acid and salicylic acid glucoside in xylem sap of *Brassica napus* infected with *Verticillium longisporum*. *Journal of Plant Research* **122**(5): 571-579
- Robb J, Lee S-W, Mohan R, Kolattukudy PE (1991) Chemical characterization of stress-induced vascular coating in tomato. *Plant Physiology* **97**(2): 528-536
- Rygulla W, Friedt W, Seyis F, Luhs W, Eynck C, von Tiedemann A, Snowdon RJ (2007) Combination of resistance to *Verticillium longisporum* from zero erucic acid *Brassica oleracea* and oilseed *Brassica rapa* genotypes in resynthesized rapeseed (*Brassica napus*) lines. *Plant Breeding* **126**(6): 596-602
- Sambrook J, Fritsch EF, Maniatis T (1989) *Molecular cloning: a laboratory manual*, 2nd edn. Cold Spring Harbor NY: Cold Spring Harbor Laboratory.
- Sanger, F., Nicklen, S., and Coulson, A.R. (1977) DNA sequencing with chain-terminating inhibitors. *Proceedings of the National Academy of Sciences of the United States of America* **74**: 5463-5467.

- Sasaki-Sekimoto Y, Taki N, Obayashi T, Aono M, Matsumoto F, Sakurai N, Suzuki H, Hirai MY, Noji M, Saito K, Masuda T, Takamiya K-i, Shibata D, Ohta H (2005) Coordinated activation of metabolic pathways for antioxidants and defence compounds by jasmonates and their roles in stress tolerance in *Arabidopsis*. *The Plant Journal* **44**(4): 653-668
- Schnurr J, Shockey J, Browse J (2004) The acyl-CoA synthetase encoded by LACS2 is essential for normal cuticle development in *Arabidopsis*. *The Plant Cell* **16**(3): 629-642
- Schweizer P, Felix G, Buchala A, Muller C, Metraux JP (1996) Perception of free cutin monomers by plant cells. *The Plant Journal* **10**(2): 331-341
- Shi L, Bielawski J, Mu J, Dong H, Teng C, Zhang J, Yang X, Tomishige N, Hanada K, Hannun YA, Zuo J (2007) Involvement of sphingoid bases in mediating reactive oxygen intermediate production and programmed cell death in *Arabidopsis*. *Cell Research* **17**(12): 1030-1040
- Sinlapadech T, Stout J, Ruegger MO, Deak M, Chapple C (2007) The hyper-fluorescent trichome phenotype of the *brt1* mutant of *Arabidopsis* is the result of a defect in a sinapic acid:UDPG glucosyltransferase. *The Plant Journal* **49**(4): 655-668
- Sperling P, Heinz E (2003) Plant sphingolipids: structural diversity, biosynthesis, first genes and functions. *Biochimica et Biophysica Acta* **1632**(1-3): 1-15
- Suh MC, Samuels AL, Jetter R, Kunst L, Pollard M, Ohlrogge J, Beisson F (2005) Cuticular lipid composition, surface structure, and gene expression in *Arabidopsis* stem epidermis. *Plant Physiology* **139**(4): 1649-1665
- Talboys PW (1972) Resistance to vascular wilt fungi. *Proceedings of the Royal Society of London Series B Biological Sciences* **181**(1064): 319-332
- Tang D, Simonich MT, Innes RW (2007) Mutations in LACS2, a long-chain acyl-coenzyme A synthetase, enhance susceptibility to avirulent *Pseudomonas syringae* but confer resistance to *Botrytis cinerea* in *Arabidopsis*. *Plant Physiology* **144**(2): 1093-1103
- Tappe H (2008) *Verticillium longisporum* induced gene expression in *Arabidopsis thaliana*. Dissertation, Georg-August-University Göttingen
- Ternes P, Wobbe T, Schwarz M, Albrecht S, Feussner K, Riezman I, Cregg JM, Heinz E, Riezman H, Feussner I, Warnecke D (2011) Two pathways of sphingolipid biosynthesis are separated in the yeast *Pichia pastoris*. *Journal of Biological Chemistry* **286**(13):11401-11414
- Thatcher LF, Manners JM, Kazan K (2009) *Fusarium oxysporum* hijacks COI1-mediated jasmonate signaling to promote disease development in *Arabidopsis*. *The Plant Journal* **58**(6): 927-939
- Tjamos SE, Flemetakis E, Paplomatas EJ, Katinakis P (2005) Induction of resistance to *Verticillium dahliae* in *Arabidopsis thaliana* by the biocontrol agent K-165 and pathogenesis-related proteins gene expression. *Molecular Plant-Microbe Interactions* **18**(6): 555-561
- Townley HE, McDonald K, Jenkins GI, Knight MR, Leaver CJ (2005) Ceramides induce programmed cell death in *Arabidopsis* cells in a calcium-dependent manner. *Biological Chemistry* **386**(2): 161-166

- Tronchet M, Balagué C, Kroj T, Jouanin L, Roby D (2010) Cinnamyl alcohol dehydrogenases-C and D, key enzymes in lignin biosynthesis, play an essential role in disease resistance in Arabidopsis. *Molecular Plant Pathology* **11**(1): 83-92
- Uemura M, Yoshida S (1984) Involvement of plasma membrane alterations in cold acclimation of winter rye seedlings (*Secale cereale* L. cv Puma). *Plant Physiology* **75**: 818-826
- Umemura K, Ogawa N, Yamauchi T, Iwata M, Shimura M, Koga J (2000) Cerebroside elicitors found in diverse phytopathogens activate defense responses in rice plants. *Plant and Cell Physiology* **41**(6): 676-683
- Umezawa T, Davin LB, Lewis NG (1990) Formation of the lignan, (-) secoisolariciresinol, by cell free extracts of *Forsythia intermedia*. *Biochemical and Biophysical Research Communications* **171**(3): 1008-1014
- Vailhé MAB, Migné C, Cornu A, Maillot MP, Grenet E, Besle JM, Atanassova R, Martz F, Legrand M (1996) Effect of modification of the O-methyltransferase activity on cell wall composition, ultrastructure and degradability of transgenic Tobacco. *Journal of the Science of Food and Agriculture* **72**(3): 385-391
- van Kan JAL (2006) Licensed to kill: the lifestyle of a necrotrophic plant pathogen. *Trends in Plant Science* **11**(5): 247-253
- van Loon LC, Rep M, Pieterse CMJ (2006) Significance of inducible defense-related proteins in infected plants. *Annual Review of Phytopathology* **44**(1): 135-162
- VanEtten HD, Mansfield JW, Bailey JA, Farmer EE (1994) Two classes of plant antibiotics: phytoalexins versus "phytoanticipins". *The Plant Cell Online* **6**(9): 1191-1192
- Vanholme R, Demedts B, Morreel K, Ralph J, Boerjan W (2010) Lignin biosynthesis and structure. *Plant Physiology* **153**(3): 895-905
- Viaud MC, Rollin P, Latxague L & Gardrat C (1992) Synthetic studies on indole glucosinolates. 1. Synthesis of glucobrassicin and its 4-methoxy and 5-methoxy derivatives. *Journal of Chemical Research*: 207
- Vogel J, Somerville S (2000) Isolation and characterization of powdery mildew-resistant Arabidopsis mutants. *Proceedings of the National Academy of Sciences of the United States of America* **97**(4): 1897-1902
- Vogt T (2010) Phenylpropanoid Biosynthesis. *Molecular Plant* **3**(1): 2-20
- von Malek B, van der Graaff E, Schneitz K, Keller B (2002) The Arabidopsis male-sterile mutant *dde2-2* is defective in the *ALLENE OXIDE SYNTHASE* gene encoding one of the key enzymes of the jasmonic acid biosynthesis pathway. *Planta* **216**(1): 187-192
- Wang H, Li J, Bostock RM, Gilchrist DG (1996) Apoptosis: A functional paradigm for programmed plant cell death induced by a host-selective phytotoxin and invoked during development. *The Plant Cell Online* **8**(3): 375-391
- Wang W, Yang X, Tangchaiburana S, Ndeh R, Markham JE, Tsegaye Y, Dunn TM, Wang G-L, Bellizzi M, Parsons JF, Morrissey D, Bravo JE, Lynch DV, Xiao S (2008) An inositolphosphorylceramide synthase is involved in regulation of plant programmed cell death associated with defense in Arabidopsis. *The Plant Cell* **20**(11): 3163-3179

- Ward JL, Forcat S, Beckmann M, Bennett M, Miller SJ, Baker JM, Hawkins ND, Vermeer CP, Lu C, Lin W, Truman WM, Beale MH, Draper J, Mansfield JW, Grant M (2010) The metabolic transition during disease following infection of *Arabidopsis thaliana* by *Pseudomonas syringae* pv. tomato. *The Plant Journal* **63**(3): 443-457
- Warnecke D, Heinz E (2003) Recently discovered functions of glucosylceramides in plants and fungi. *Cellular and Molecular Life Sciences* **60**(5): 919-941
- Wilhelm S (1955) Longevity of the Verticillium wilt fungus in the laboratory and field. *Phytopathology* **45**(3): 180-181
- Williams JS, Hall SA, Hawkesford MJ, Beale MH, Cooper RM (2002) Elemental sulfur and thiol accumulation in tomato and defense against a fungal vascular pathogen. *Plant Physiology* **128**(1): 150-159
- Woloshuk CP, Kolattukudy PE (1986) Mechanism by which contact with plant cuticle triggers cutinase gene expression in the spores of *Fusarium solani* f. sp. pisi. *Proceedings of the National Academy of Sciences of the United States of America* **83**(6): 1704-1708
- Wuyts N, Lognay G, Swennen R, De Waele D (2006) Nematode infection and reproduction in transgenic and mutant *Arabidopsis* and tobacco with an altered phenylpropanoid metabolism. *Journal of Experimental Botany* **57**(11): 2825-2835
- Xiao F, Mark Goodwin S, Xiao Y, Sun Z, Baker D, Tang X, Jenks MA, Zhou J-M (2004) *Arabidopsis* CYP86A2 represses *Pseudomonas syringae* type III genes and is required for cuticle development. *The EMBO Journal* **23**(14): 2903-2913
- Xie DX, Feys BF, James S, Nietoroostro M, Turner JG (1998) COI1: An *Arabidopsis* gene required for jasmonate-regulated defense and fertility. *Science* **280**(5366): 1091-1094
- Zeise K, von Tiedemann A (2001) Morphological and physiological differentiation among vegetative compatibility groups of *Verticillium dahliae* in relation to *Verticillium longisporum*. *Journal of Phytopathology* **149**(7-8): 469-475
- Zeise K, von Tiedemann A (2002) Host specialization among vegetative compatibility groups of *Verticillium dahliae* in relation to *Verticillium longisporum*. *Journal of Phytopathology* **150**(3): 112-119
- Zhang G, Slaski JJ, Archambault DJ, Taylor GJ (1997) Alternation of plasma membrane lipids in aluminum-resistant and aluminum-sensitive wheat genotypes in response to aluminum stress. *Physiologia Plantarum* **99**(2): 302-308
- Zhang S-H, Yang Q, Ma R-C (2007) *Erwinia carotovora* ssp. *carotovora* infection induced "defense lignin" accumulation and lignin biosynthetic gene expression in chinese cabbage (*Brassica rapa* L. ssp. *pekinensis*). *Journal of Integrative Plant Biology* **49**(7): 993-1002
- Zhou L, Hu Q, Johansson A, Dixelius C (2006) *Verticillium longisporum* and *V. dahliae*: infection and disease in *Brassica napus*. *Plant Pathology* **55**(1): 137-144

## 7 Abbreviations

1D-SOM	one dimensional self organizing map
1MI3G	1-methyl-indol-3-ylmethyl glucosinolate
4HI3G	4-hydroxy-indol-3-ylmethyl glucosinolate
4MI3G	4-methyl-indol-3-ylmethyl glucosinolate
ABA	abscisic acid
At	<i>Arabidopsis thaliana</i>
<i>atpr</i>	<i>Arabidopsis thaliana pinoresinol reductase</i>
<i>A. tumefaciens</i>	<i>Agrobacterium tumefaciens</i>
amu	atomic mass unit
<i>B. cinerea</i>	<i>Botrytis cinerea</i>
<i>B. napus</i>	<i>Brassica napus</i>
BSTFA	Bis(trimethylsilyl)-trifluoroacetamide
C4H	cinnamate-4-hydroxylase
CaCl <sub>2</sub>	calcium chloride
CAD	cinnamyl alcohol dehydrogenase
CCoAOMT	caffeoyl CoA O-methyltransferase
CD	Czapec Dox
cl.	cluster
CoA	coenzyme A
<i>coi1-t</i>	<i>coronatine insensitive 1</i> T-DNA insertion line
Col 0	<i>Arabidopsis thaliana</i> ecotype Columbia 0
CTAB	cetyltrimethylammoniumbromide
Da	Dalton
DAD	diode array detector
<i>dde2-2</i>	<i>delayed dehiscence 2-2</i>
ddH <sub>2</sub> O	double distilled water
DIR	dirigent protein
DNA	deoxyribonucleic acid
dNTP	deoxyribonucleosid triphosphate
dpi	days post infection
dw	dry weight
<i>E. coli</i>	<i>Escherichia coli</i>
EDTA	ethylene diamine tetra acetate
ESI	electrospray ionization

---

eV	electron volt
<i>F. oxysporum</i>	<i>Fusarium oxysporum</i>
F5H	ferulate-5-hydroxylase
FAE	formaldehyde-acetic acid-ethanol
<i>fah1</i>	<i>fatty acid hydroxylase 1</i>
<i>fah1-2</i>	<i>ferulate-5-hydroxylase 1-2</i>
<i>fah2</i>	<i>fatty acid hydroxylase 2</i>
Fe(III)SO <sub>4</sub>	iron sulfate
FID	flame ionization detector
Fig.	figure
FW	fresh weight
xfx	<i>fah1xfah2</i>
g	gram
<i>G. cichoracearum</i>	<i>Golovinomyces cichoracearum</i>
GC	gas chromatography
gluc	glucoside
<i>gpat5-1</i>	<i>glycerol phosphate acyltransferase 5-1</i>
GUS	β-glucuronidase
h	hour
HCl	hydrochloric acid
HPLC	high performance liquid chromatography
HR	hypersensitive reaction
I3G	indol-3-ylmethyl glucosinolate
IPC	inositol phosphoryl ceramide
JA	jasmonic acid
KCl	potassium chloride
KOH	potassium hydroxide
l	liter
LCB	long chain base
m	milli
M	molar (mol l <sup>-1</sup> )
m/z	mass to charge
MgSO <sub>4</sub>	magnesium sulfate
min	minute
mRNA	messenger RNA
MS	mass spectrometer
MS-medium	Murashige & Skoog medium

---

MTBE	methyl- <i>tert</i> -butyl ether
NaNO <sub>3</sub>	sodium nitrate
NaOH	sodium hydroxide
NaCl	sodium chloride
OD	optical density
<i>P. syringae</i>	<i>Pseudomonas syringae</i>
PAL	phenylalanine ammonia lyase
PCD	programmed cell death
PCR	polymerase chain reaction
PDA	potato dextrose agar
PDB	potato dextrose broth
pH	negative decadic logarithm of the proton concentration
PR	pathogenesis related
<i>ref1-s</i>	<i>reduced epidermal fluorescence 1</i> SALK line
Rg	research group
rha	rhamnoside
RNA	ribonucleic acid
RP-HPLC	reverse phase HPLC
RT-PCR	reverse transcriptase PCR
s	second
SA	salicylic acid
SAG	salicylic acid glucoside
SAR	systemic acquired resistance
SD	standard deviation
SE	standard error
<i>sng1-1</i>	<i>sinapoyl glucose accumulator 1-1</i>
Tab.	table
TOF	time of flight
UGT	UDP-glucose transferase
UPLC	ultra performance liquid chromatography
UV	ultraviolet
<i>V. albo-atrum</i>	<i>Verticillium albo-atrum</i>
<i>V. dahliae</i>	<i>Verticillium dahliae</i>
<i>V. longisporum</i>	<i>Verticillium longisporum</i>
v/v	volume per volume
VL	<i>Verticillium longisporum</i>
w/v	weight per volume

## 8 Appendix

### 8.1 Infection markers detected by metabolite fingerprinting analyses

**Tab. S1: Phenylpropanoid markers of *V. longisporum* infected *Arabidopsis* leaves detected by the metabolite fingerprinting approach.**

cluster	rt	m/z	detected ion	db hit	theor. mass	+/-	ident.
19	2.5	387.1283	[M+H] <sup>+</sup>	1-sinapoyl glucose	386.1213	+	√
21	4.0	591.1700	[M-H] <sup>-</sup>	1,2-bissinapoyl glucose	592.1792	+	√
16	1.3	360.1644	[M+NH <sub>4</sub> ] <sup>+</sup>	coniferin	342.1315	+	
17	1.7	390.1811	[M+NH <sub>4</sub> ] <sup>+</sup>	syringin	372.1420	+	
27	1.6	372.1285	[M+NH <sub>4</sub> ] <sup>+</sup>	caffeoylquinic acid	354.0951	+	
28	2.7	151.075	[M+H] <sup>+</sup>	p-coumaroyl alcohol	150.0681	+	
26	3.0	543.1835	[M+Na] <sup>+</sup>	pinosresinol glucoside	520.1945	+	√
24	2.6	683.2521	[M+H] <sup>+</sup>	pinosresinol diglucoside	682.2473	+	√
26	3.0	523.2155	[M+H] <sup>+</sup>	lariciresinol glucoside	522.2101	+	√
27	2.6	685.2668	[M+H] <sup>+</sup>	lariciresinol diglucoside	684.2629	+	
25	2.9	363.1812	[M+H] <sup>+</sup>	secoisolariciresinol	362.1729	+	
27	2.8	581.1285	[M+H] <sup>+</sup>	syringaresinol glucoside	580.2156	+	
17	4.1	489.1381	[M+H] <sup>+</sup>	phrymarolin I	488.1319	+	
25	3.4	373.1277	[M+H] <sup>+</sup>	sesamolinal	372.1209	+	
25	2.7	355.1179	[M+H] <sup>+</sup>	sesamin	354.1103	+	
24	2.7	535.1788	[M+H] <sup>+</sup>	sesamolinal glucoside	534.1715	+	
6	3.1	593.1498	[M-H] <sup>-</sup>	kaempferol-3-galactoside-7-rhamnoside	594.1585	- (35 dpi)	√
6	3.4	577.1555	[M-H] <sup>-</sup>	kaempferol-3-rhamnoside-7-rhamnoside	578.1636	- (35 dpi)	√
25	2.7	741.2227	[M-H] <sup>-</sup>	naringin-4-glucoside	742.2320	+	
23	3.4	579.1702	[M-H] <sup>-</sup>	naringin	580.1792	+	

rt: retention time; m/z: mass to charge ratio; db hit: database hit (databases used: KEGG, Knapsack, LipidMaps, AraCyc); +: compound with higher intensity in the infected samples compared to controls, -: compound with lower intensity in the infected sample compared to controls, ident.: markers identified by comparison with authentic standards or fragmentation patterns

**Tab. S2: Comparison of markers detected in samples of root cut infection and of root dip infection.**

Material of root cut infection was analyzed at 10, 21 and 35 dpi, material of root dip infections at 21 dpi.

db hit	theor. mass	+/-	root cut	root dip
1-sinapoyl-glucose	386.1213	+	✓	✓
1,2-bissinapoyl-glucose	592.1792	+	✓	✓
coniferin	340.0794	+	✓	✓
coniferylaldehyde glucoside	340.1158	+	x	✓
syringin	372.1420	+	✓	✓
caffeoylquinic acid	354.0951	+	✓	✓
p-coumaroyl alcohol	150.0681	+	✓	✓
pinoselinol glucoside	520.1945	+	✓	✓
pinoselinol diglucoside	682.2473	+	✓	✓
lariciresinol glucoside	522.2101	+	✓	✓
lariciresinol diglucoside	684.2629	+	✓	✓
secoisolariciresinol	362.1729	+	✓	✓
syringaresinol glucoside	580.2156	+	✓	x
phrymarolin I	488.1319	+	✓	✓
sesamolol	372.1209	+	✓	✓
sesamin	354.1103	+	✓	✓
sesamolol glucoside	554.1737	+	✓	✓
kaempferol-3-galactoside-7-rhamnoside	594.1585	-	35 dpi	✓
kaempferol-3-rhamnoside-7-rhamnoside	578.1636	-	35 dpi	✓
naringin-4-glucoside	742.2320	+	✓	✓
naringin	580.1792	+	✓	✓
indol-3-ylmethyl-glucosinolate	448.0610	+	10/21 dpi	✓
1-methoxy-indol-3-ylmethyl glucosinolate	478.0716	+	✓	✓
4-methoxy-indol-3-ylmethyl glucosinolate	478.0716	+	21 dpi	✓
4-hydroxy-indol-3-ylmethyl glucosinolate	464.0471	+	x	✓

db hit: database hit (databases used: KEGG, knapsack, lipid maps, metacyc); +: compound with higher intensity in the infected samples compared to controls, -: compound with lower intensity in the infected sample compared to controls; root cut: markers in samples of the root cut infection (10, 21 and 35 dpi), root dip: markers in samples of the root dip infection (21 dpi); ✓: markers detected, x: markers not detected

## 8.2 Quantification of infection markers of root dip infected plants

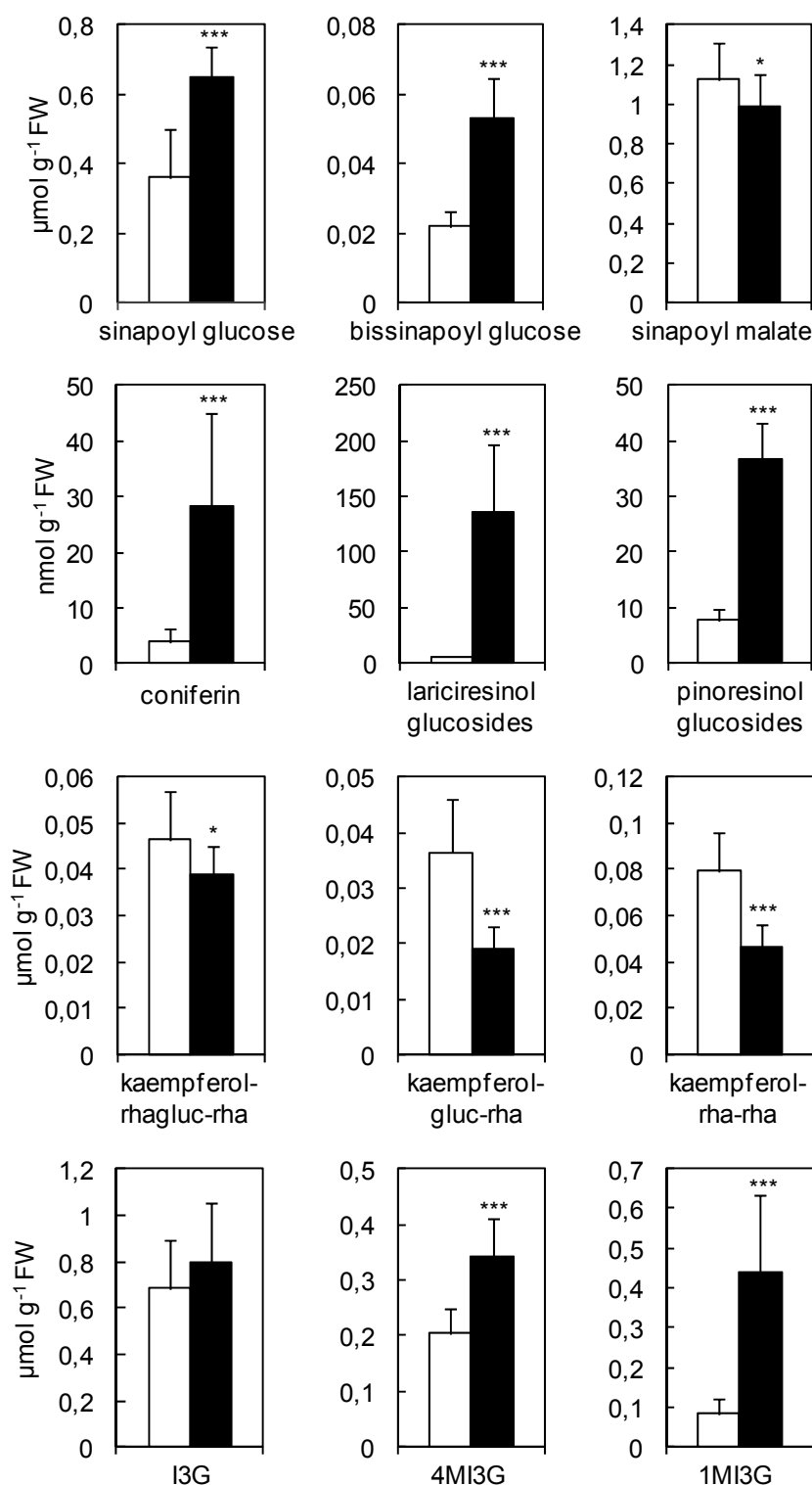


**Fig. S1: Quantification of phenylpropanoids and indoles in root dip infected plants.**

Plants were infected by root dip infection and harvested at 21 dpi. Methanolic extracts of leaf material of controls (white bars) and infected plants (black bars) were measured by RP-HPLC-DAD. Mono- and dilignols were analyzed after deglycosylation of the sample with  $\beta$ -glucosidase from almonds. Each data point represents the mean value of 16 samples from four independent experiments  $\pm$ SD. Asterisks indicate significant differences between control and infected plants according to student's t-test (\*  $p \leq 0.05$ , \*\*\*  $p \leq 0.001$ ).

### 8.3 Mutants examined in infections with *V. longisporum*

Tab. S3: Mutants lines tested for their susceptibility against *V. longisporum*.

Linie	literature	effected gene	susceptibility
<i>fah1-2</i>	(Chapple et al, 1992)	ferulate-5-hydroxylase defect	++
<i>ref 1_s</i>		aldehyde-dehydrogenase defect	+/-
<i>sng1-1</i>	(Lorenzen et al, 1996)	sinapoyl glucose:malate sinapoyltransferase defect	+/-
UGT72E1 -OE	(Lanot et al 2008)	glycosyltransferase overexpressed	+/-
UGT72E2 -OE	(Lanot et al, 2006)	glycosyltransferase overexpressed	--
UGT72E3-OE	(Lanot et al, 2008)	glycosyltransferase overexpressed	+/-
C4H:F5H	(Meyer et al, 1998)	ferulate-5-hydroxylase overexpressed	(-)
<i>atpr1-1xatpr2</i>	(Nakatsobu et al, 2008)	pinorensinol reductase defect	+/-
<i>nac42</i>		transcription factor defect	+/-
NAC42_20		transcription factor overexpressed	+/-
NAC42_6		transcription factor overexpressed	+/-
<i>cad4</i>		cinnamyl alcohol dehydrogenase defect	+/-
<i>cad5</i>		cinnamyl alcohol dehydrogenase defect	+/-

+: higher susceptibility, -: lower susceptibility, +/-: similar susceptibility compared to wild type

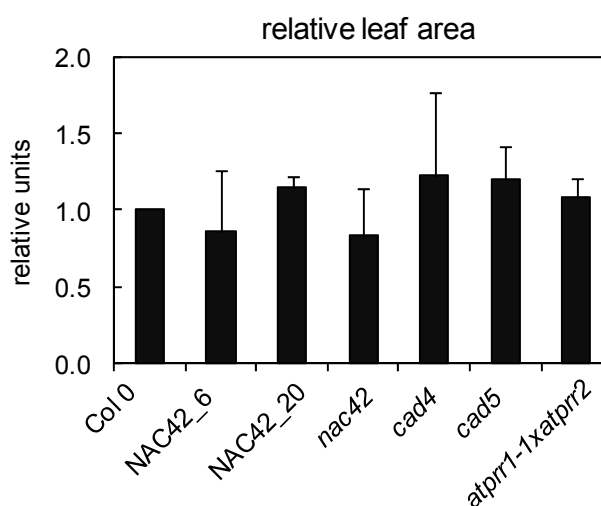
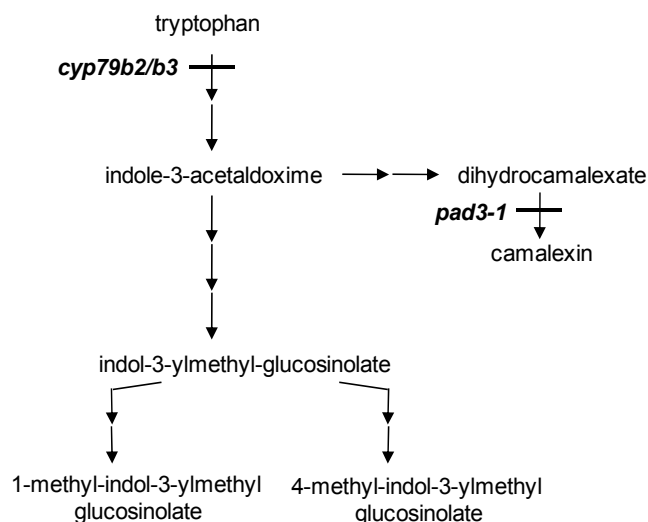


Fig. S2: Relative leaf area of mutant plants from the phenylpropanoid pathway infected with *V. longisporum*.

Infection of different phenylpropanoid mutants by root dip infection; NAC42: transcription factor which influences CCoAOMT, *cad*: cinnamyl alcohol dehydrogenase mutants, *atpr1-1xatpr2*: pinorensinol reductase double mutant. The relative leaf area was determined at 21 dpi: The leaf area of infected plants was divided by the leaf area of control plants and the results of the mutant plants were set in relation to the value of the wild type. The mean value of at least three independent experiments is show  $\pm$ SD.

## 8.4 Infection of the *cyp79b2/b3* mutant with *V. longisporum*



**Fig. S3: Mutants in the indole glucosinolate and camalexin pathway.**

Positions of the general indole mutant *cyp79b2/b3* and of the camalexin mutant *pad3-1* in the pathway are shown.

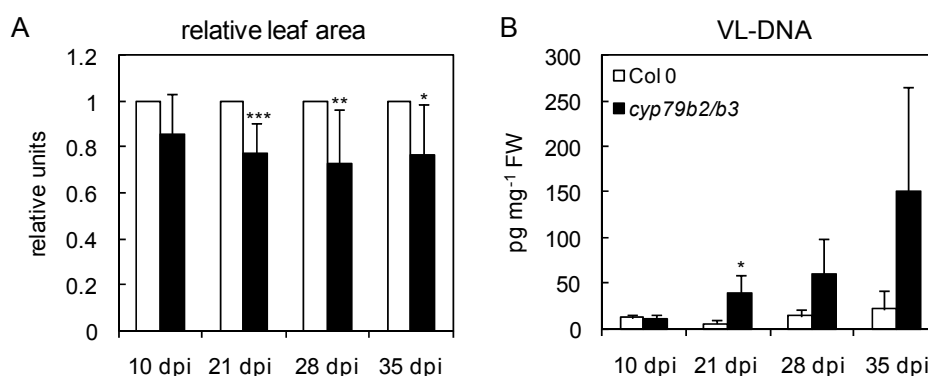


**Fig. S4: Infection of the *cyp79/b3b2* mutant with *V. longisporum* by root cut infection.**

Col 0 (white bars) and *cyp79b2/b3* (black bars) plants were infected by root cut infection and harvested at the indicated time points. A) Determination of the relative leaf area: The leaf area of infected plants was divided by the leaf area of control plants and the results of the mutant plants were set in relation to the value of the wild type. The mean values of seven independent experiments are shown  $\pm$ SD. B) Determination of VL-DNA in infected leaves. Mean values of three independent experiments were shown  $\pm$ SE. Asterisks indicate significant differences between control and infected plants according to student's t-test (\*= $p \leq 0.05$ , \*\*= $p \leq 0.01$ , \*\*\*= $p \leq 0.001$ ). The VL-DNA analysis was performed in the group of Prof. Karlovsky (Göttingen).

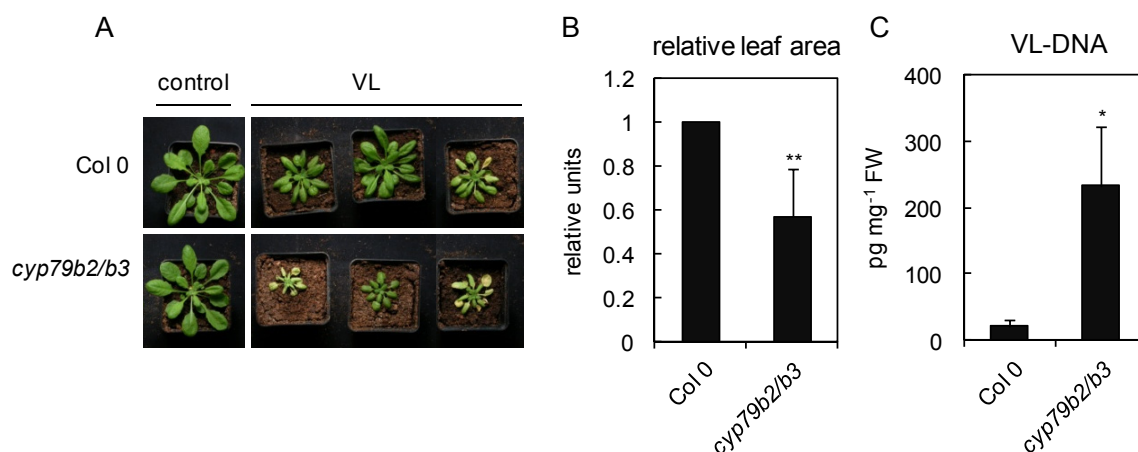


**Fig. S5: Infection of the *cyp79b2/b3* mutant with *V. longisporum* by root dip infection.**

Col 0 and *cyp79b2/b3* plants were infected by root dip infection and harvested at 21 dpi. A) Pictures of infected and control plants at 21 dpi. B) The leaf area was determined from pictures taken of the rosettes of the plants: The leaf area of infected plants was divided by the leaf area of control plants and the results of the mutant plants were set in relation to the value of the wild type. The mean values of five independent experiments are shown  $\pm$ SD. C) Determination of VL-DNA in infected leaves. Mean values of ten samples of three independent experiments were shown  $\pm$ SE. Asterisk indicate significant differences between control and infected plants according to student's t-test (\*  $p \leq 0.05$ , \*\*  $p \leq 0.01$ ). The VL-DNA analysis was performed in the group of Prof. Karlovsky (Göttingen).

## 8.5 Infection and metabolite analysis of sinapate ester mutants

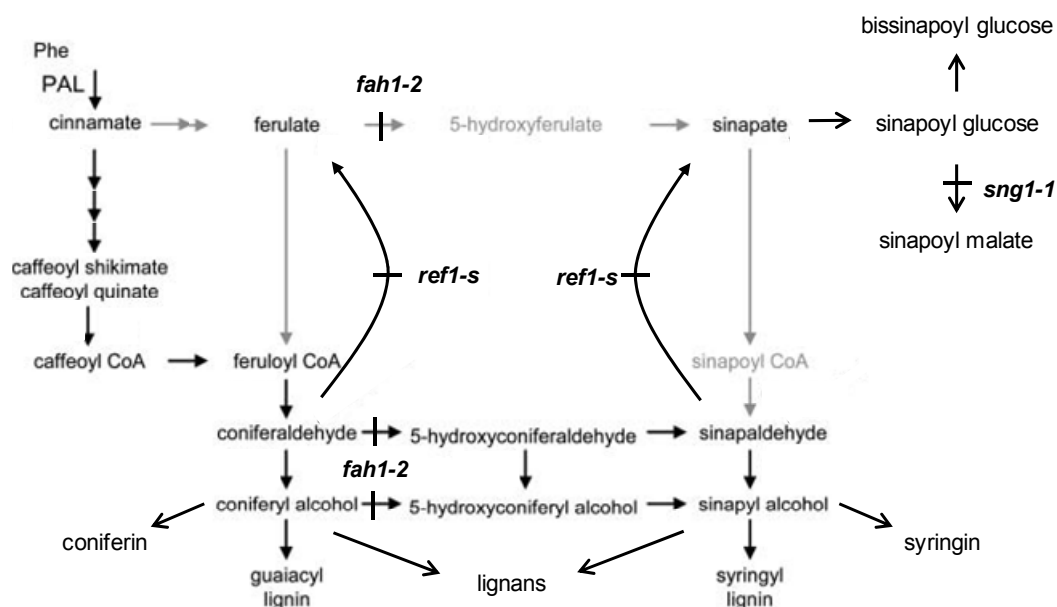


**Fig. S6: Position of the sinapate ester mutants *fah1-2*, *ref1-s* and *sng1-1* in the phenylpropanoid pathway.**

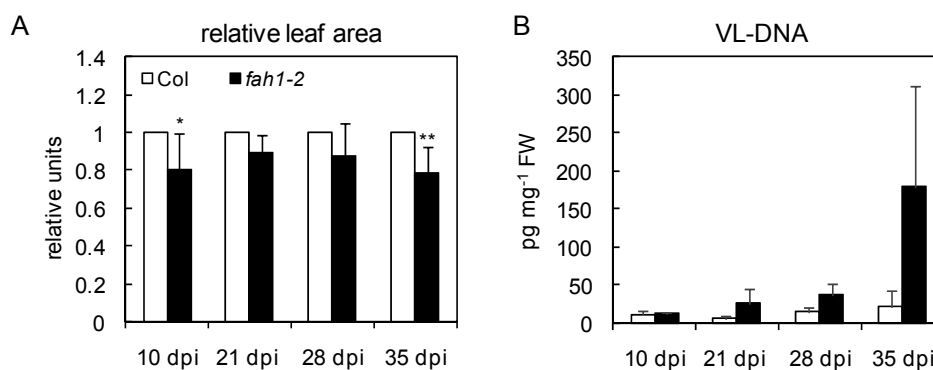


**Fig. S7: Infection of the *fah1-2* mutant with *V. longisporum* by root cut infection.**

Col 0 (white bars) and *fah1-2* (black bars) plants were infected by root cut infection and harvested at the indicated time points. A) Determination of the relative leaf area: The leaf area of infected plants was divided by the leaf area of control plants and the results of the mutant plants were set in relation to the value of the wild type. The data represent the mean values of seven independent experiments. B) Determination of VL-DNA in infected leaves. The mean values of three independent experiments are shown  $\pm$ SD. Asterisks indicate significant differences between control and infected plants according to student's t-test (\*  $p \leq 0.05$ , \*\*  $p \leq 0.01$ ). The VL-DNA analysis was performed in the group of Prof. Karlovsky (Göttingen).

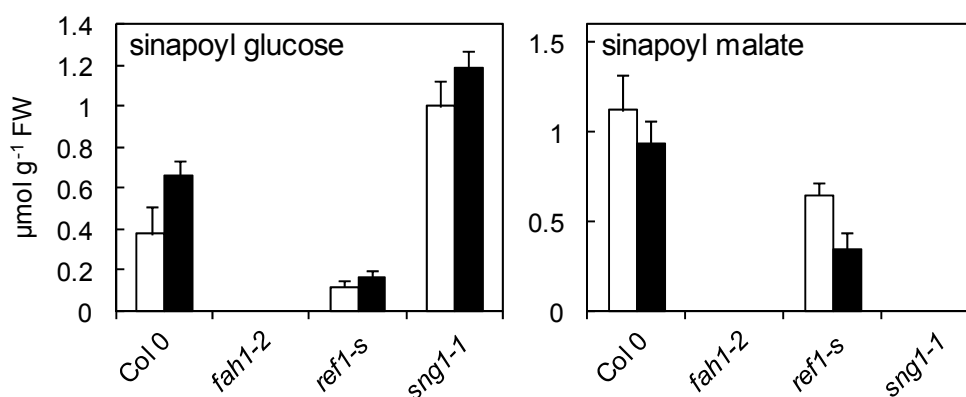


**Fig. S8: Determination of sinapate esters in mutants of sinapate ester biosynthesis.**

Plants were infected by root dip infection and harvested at 21 dpi. Methanolic extracts of leaf material of controls (white bars) and infected plants (black bars) were measured by RP-HPLC-DAD. Each data point represents the mean value of eight samples from two independent experiments  $\pm$ SD.

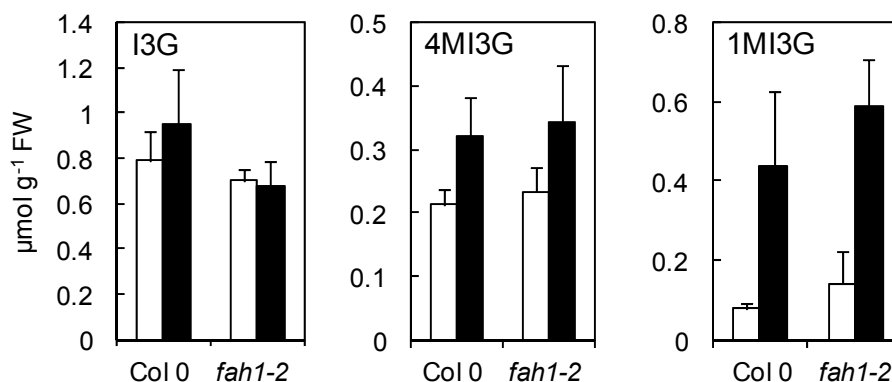


**Fig. S9: Determination of indole glucosinolates in *fah1-2* mutants.**

Col 0 and *fah1-2* plants were infected by root dip inoculation and harvested at 21 dpi. Quantification of indole glucosinolates was performed by RP-HPLC-DAD of *V. longisporum* infected (black bars) and control (white bars) plants. Each data point represents the mean value of eight biological replicates from two independent experiments  $\pm$ SD.

## 8.6 Infection of C4H:F5H plants with *V. longisporum*

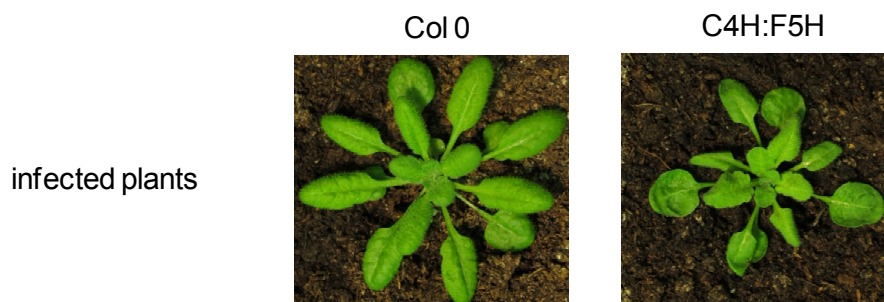


**Fig. S10: Infection symptoms of the C4H:F5H mutant.**

Col 0 and C4H:F5H plants were infected by root dip infection. Pictures were taken at 17 dpi. C4H:F5H showed leaves with less tension especially at the leaf tips.

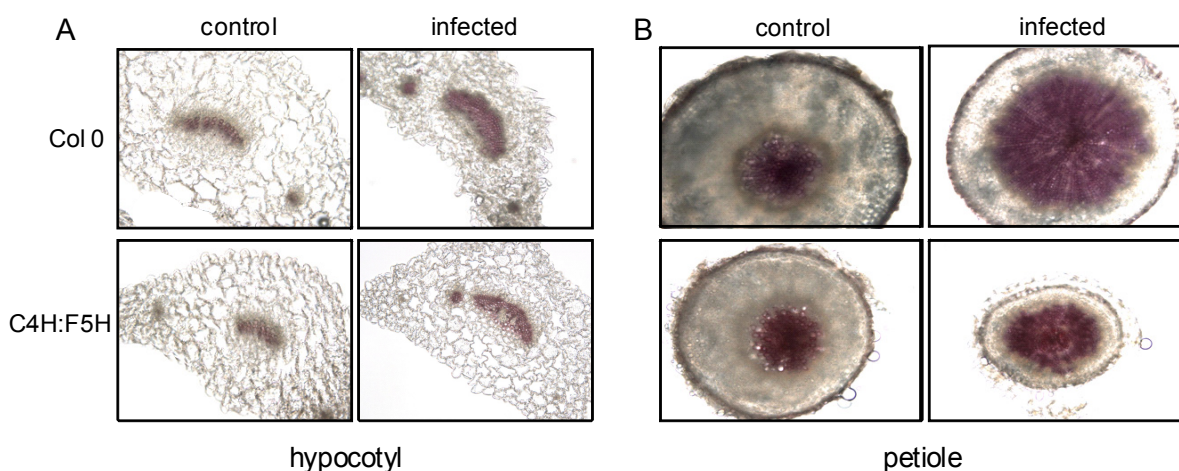


**Fig. S11: Lignin staining of hypocotyls and petioles of infected C4H:F5H mutants.**

Col 0 and C4H:F5H plants were infected by root dip infection. At 21 dpi petioles (A) and hypocotyls (B) were harvested. For easier cutting material was paraffin embedded before handsections were performed. The cuts were stained with phloroglucin/HCl for lignified tissue and examined under the microscope with 400 times magnification. The pictures represent results of three independent experiments.

## 8.7 Lignans in the infection with *V. longisporum*

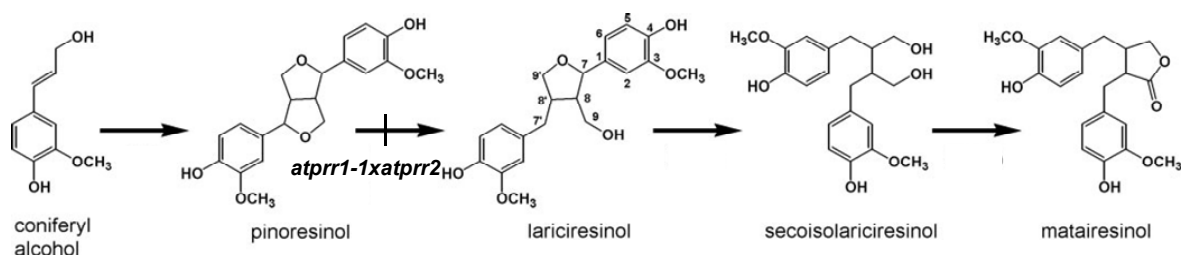


**Fig. S12: Position of the pinoresinol reductase double mutant (*atpr1-1xatpr2*) in the lignan biosynthetic pathway (modified from Nakatsobu et al, 2008).**

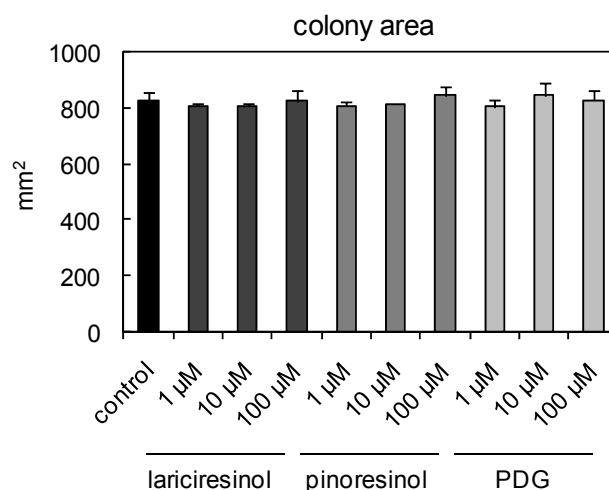


**Fig. S13: Influence of different lignans on *V. longisporum* growth.**

PDB plates were supplemented with pinoresinol, lariciresinol or pinoresinol diglucoside (PDG) in indicated concentrations. After inoculation, the fungus was grown for 17 days on these plates. Pictures of colonies were taken under a binocular and the area was measured. Mean values were calculated from two independent plates  $\pm$ SD.

## 8.8 Infection of JA mutants with *V. longisporum*

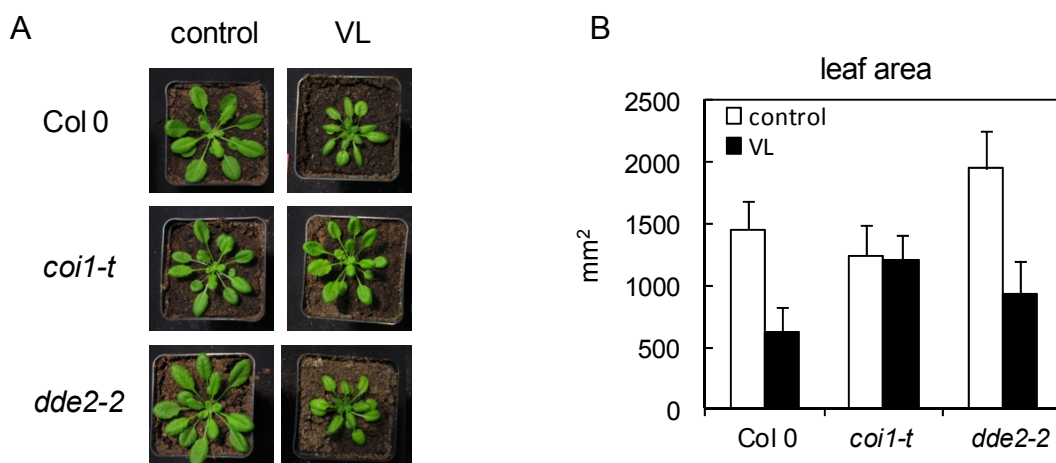


**Fig. S14: Infection of JA mutants with *V. longisporum*.**

Col 0, *coi1-t* and *dde2-2* were infected by root dip infection. A) Pictures of control and infected plants at 14 dpi. B) Leaf area data of control (white bars) and infected (black bars) plants. Homozygous *coi1-t* plants were detected by PCR genotyping after harvest of the control and infected plants. Each bar represents the mean value of nine biological replicates  $\pm$ SD.

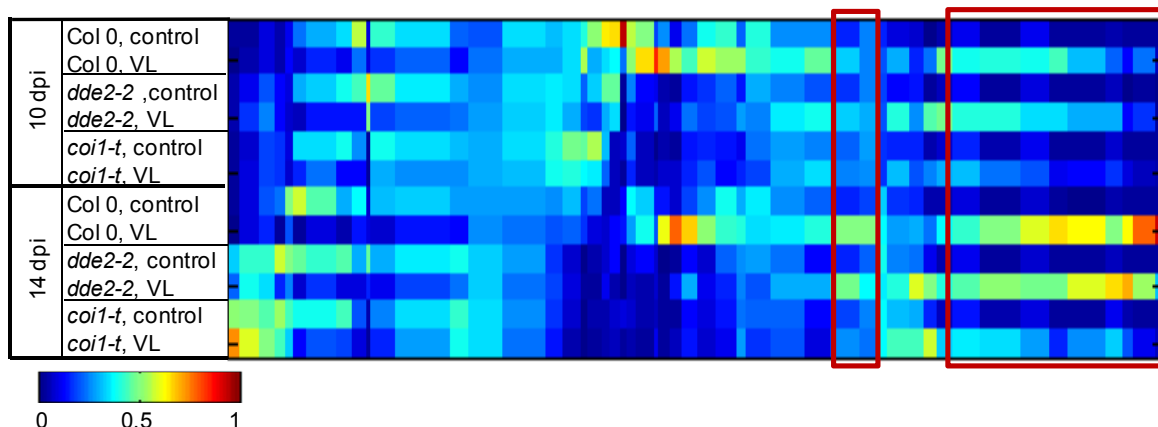


**Fig. S15: 1D-SOM of markers of the undirected fingerprinting of Col 0, *dde2-2* and *coi1-t* plants infected with *V. longisporum*.**

Col 0, *dde2-2* and *coi1-t* plants were infected by root dip infection and harvested at the indicated time points of infection. Homozygous *coi1-t* plants were detected after harvest by PCR analysis. Leaf material of three independent samples was extracted by two phase partitioning, leading to a methanol phase with polar substances and a chloroform phase with non-polar substances. Shown markers derived from measurements of the methanol phase. Each sample was measured twice. Clusters used for reclustering are marked in the red boxes.

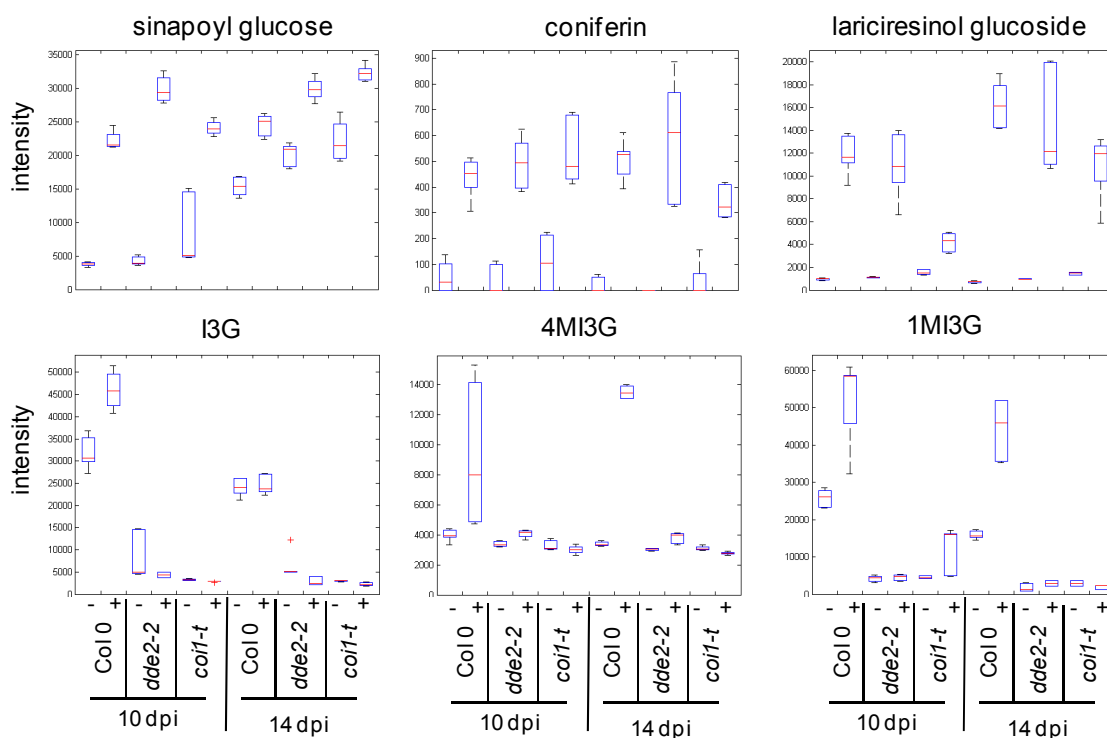


**Fig. S16: Phenylpropanoid and indole markers of the metabolite fingerprinting of *V. longisporum* infected Col 0, *coi1-t* and *dde2-2* leaf material.**

Col 0, *dde2-2* and *coi1-t* plants were infected by root dip infection and harvested at the indicated time points of infection. Homozygous *coi1-t* plants were detected after harvest by PCR analysis. Leaf material of three independent samples was extracted by two phase partitioning leading to a methanol phase with polar substances and a chloroform phase with non-polar substances. Shown markers derived from measurements of the methanol phase. Each sample was measured twice. -: control samples, +: samples of infected material

## 8.9 Determination of ceramides and glucosylceramides in the *fah*-mutants

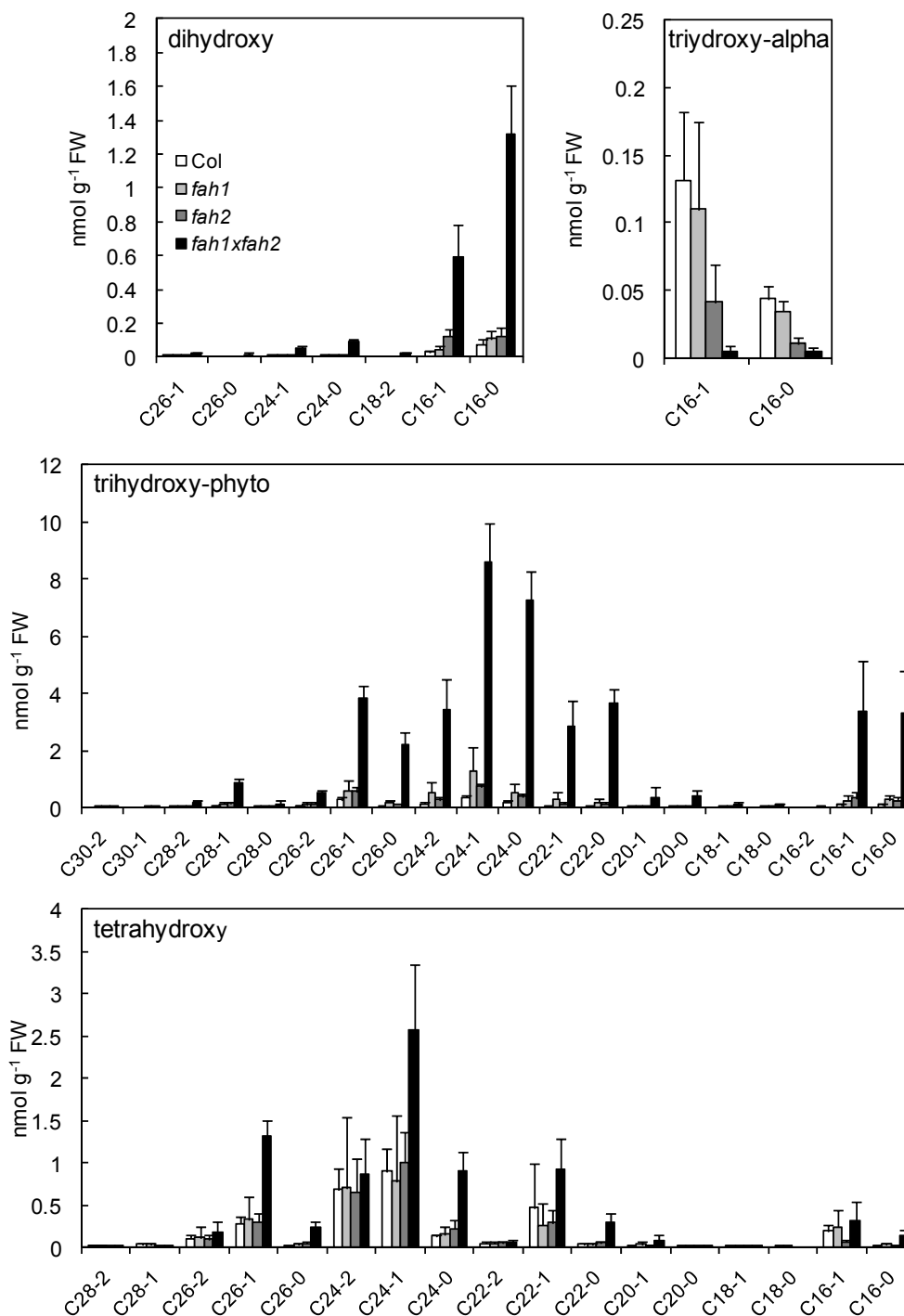


**Fig. S17: Determination of ceramide species in  $\alpha$ -hydroxylase mutant plants.**

Col 0 (white bars), *fah1* (bright grey bars), *fah2* (dark grey bars) and *fah1xfah2* (black bars) plants were grown for 35 days under long day conditions. Ceramides were extracted from the leaf material by chloroform:methanol extraction, SPE-separation and alkaline hydrolysis. Extracted ceramides were analyzed by UPLC-MS by Kirstin Feussner. Nomenclature: first number represents the chain length of the fatty acid moiety, the second number represents the number of double bonds in the molecule. The data represent the mean value of six biological replicates from two independent experiments.

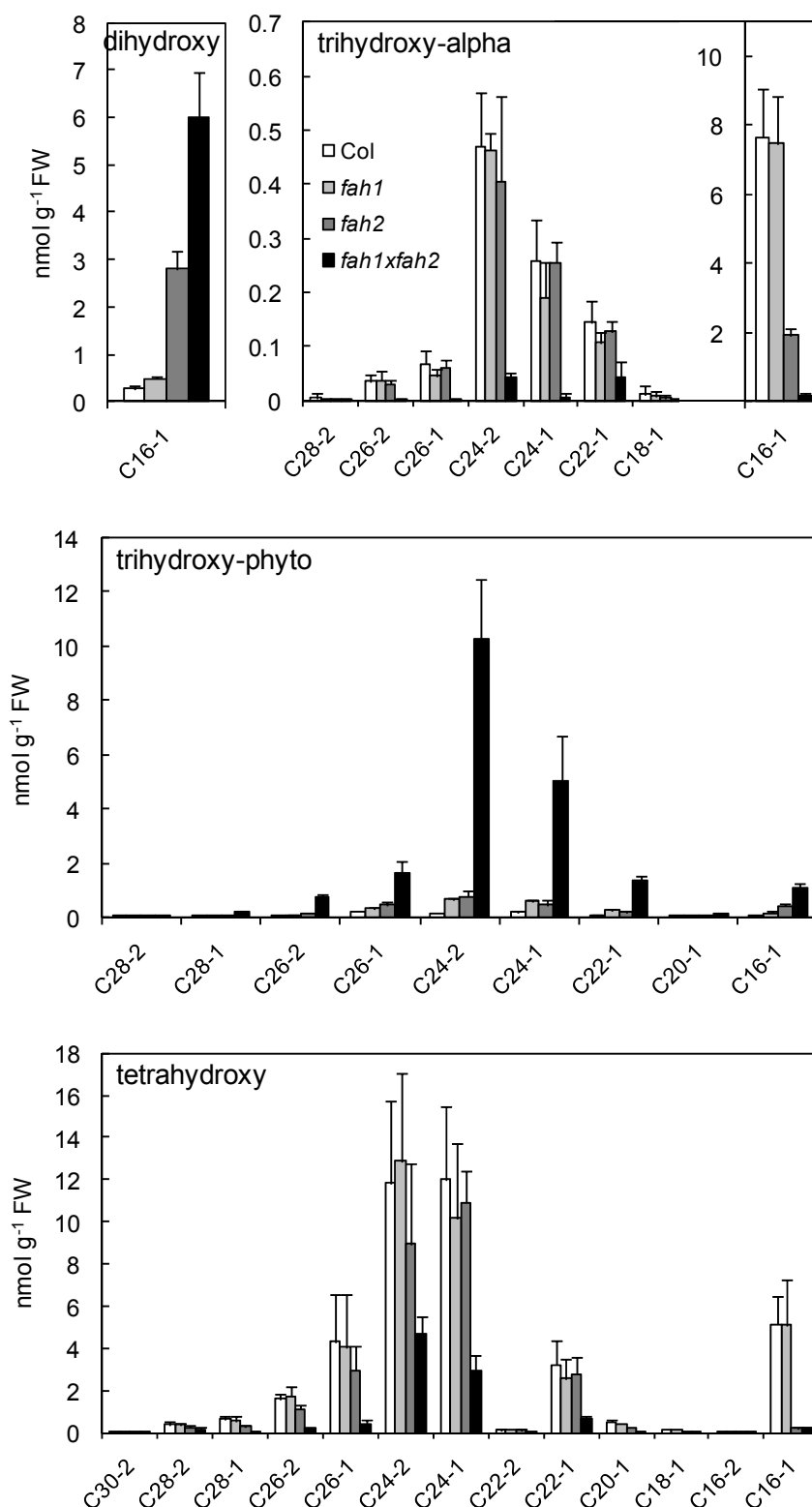


**Fig. S18: Determination of glucosylceramide species in  $\alpha$ -hydroxylase mutant plants.**

Col 0 (white bars), *fah1* (bright grey bars), *fah2* (dark grey bars) and *fah1xfah2* (black bars) plants were grown for 35 days under long day conditions. Glucosylceramides were extracted from the leaf material by chloroform:methanol extraction, SPE-separation and alkaline hydrolysis. Extracted ceramides were analyzed by UPLC-MS by Kirstin Feussner. Nomenclature: the first number represents the chain length of the fatty acid moiety, the second number represents the number of double bonds in the molecule. The data represent the mean value of six biological replicates from two independent experiments.

## Danksagung

Hiermit möchte ich bei allen bedanken, die zur Entstehung dieser Arbeit beigetragen und mich bei der Fertigstellung unterstützt haben.

Ein besonderer Dank gilt Prof. Dr. Ivo Feußner für die Überlassung des Themas, die gute Betreuung, die Unterstützung bei allen Fragen und die hilfreichen Diskussionen. Auch möchte ich mich für die Möglichkeit bedanken, viele verschiedene Tagungen besuchen zu können.

Prof. Dr. Wolfgang Dröge-Laser danke ich für die Bereitschaft, das Koreferat zu übernehmen.

Bei Dr. Kirstin Feußner möchte ich mich für die zahlreichen UPLC-Messungen, die Auswertungen und die immer wieder neuen Berechnungen bedanken. In diesem Zusammenhang danke ich auch Dr. Peter Meinecke, Alexander Kaefer und Manuel Landesfeind aus der Abteilung Bioinformatik für die Entwicklung und Bereitstellung des MarVis-Tools zur Auswertung der ungerichteten Messungen.

Dr. Cornelia Herrfurth danke ich für die Einführung in die Analytik und die Hilfe bei den Arbeiten mit HPLC, GC und GC-MS sowie für MS/MS- und Phytohormon-Messungen.

Bei Dr. Ellen Hornung bedanke ich mich für ihre Hilfe bei allen molekularbiologischen Arbeiten dieser Arbeit, für das Korrekturlesen und für die leckeren Kuchen ohne Obst.

Dr. Tim Iven möchte ich für die Phytohormon-Messungen und die Zusammenarbeit bei den Indol-Mutanten danken.

Bei den Mitgliedern der Verticillium-Forschergruppe bedanke ich mich für die gute Zusammenarbeit, insbesondere bei Christine Drübert aus der Arbeitsgruppe von Prof. Dr. Polle für die gemeinsamen Versuche zu Beginn meiner Arbeit und bei Anjali Ralhan aus der Arbeitsgruppe von Prof. Dr. Gatz für die Hilfe bei der Root-Dip-Infektion und für das Material der coi-Infektion. Danken möchte ich auch Prof. Dr. Petr Karlovsky und Heike Rollwage für die VL-DNA Messungen.

Außerhalb der Forschergruppe bedanke ich mich bei Marnie Schwarz aus der Arbeitsgruppe von Prof. Dr. Lipka, die die Mehltau-Infektionen durchgeführt hat.

Bei Dr. Alfred Baumann aus Halle bedanke ich mich für die Sinapatester-Standards und bei Dr. Matthias Bischoff aus der Arbeitsgruppe von Prof. Dr. Lutz F. Tietze (Göttingen) für die Synthese des 4MI3G Standards.

Desweiteren sei verschiedenen Personen für die Bereitstellung von Arabidopsis-Saatgut gedankt: Prof. Dianna Bowles für die UGT72E-OE Samen, Prof. Mike Pollard für die Suberin-Mutanten (*cyp86a1-2*, *cyp86b1-2*, *gpat5-1*) und Prof. Clint Chapple für die C4H:F5H-Samen. Außerdem danke ich Alina Mosblech für das *coi1-t* –Saatgut.

Ich danke Susanne Mester für die Versorgung meiner Pflanzen, für die vielen gesiebten Samen und die Unmengen an gedämpfter Erde.

Sabine Freitag danke ich für zahlreiche Hilfen im Labor, für verschiedene Extraktionen und Erste-Hilfe-Leistungen an der HPLC. Auch Pia Meyer danke ich für die Hilfe mit Pflanzen und PCRs, für zahlreiche Extraktionen für die UPLC und für die Begrünung der Etage. Den beiden möchte ich auch ganz besonders für den Spaß im Labor, die Unterstützung bei Problemen aller Art und das immer offene Ohr danken.

Den Studenten Urs Benning, Alexandra Matei und Lilli Haid danke ich für die fleißige Mitarbeit und das Interesse an dem Projekt.

Allen Mitarbeitern der Abteilung Biochemie der Pflanze danke ich für das gute Arbeitsklima und die Hilfe bei Fragestellungen aller Art, besonders sei hier noch Dr. Florian Brodhun erwähnt, der diese Arbeit sehr hilfreich Korrektur gelesen hat.

Ich bedanke mich auch bei meinen Eltern für die immerwährende Unterstützung, sowie meiner Schwester für das tapfere Ertragen all meiner Fragen und das pingelige Korrekturlesen.

Ganz besonders möchte ich mich bei Martin für das unendliche Verständnis bedanken, das er für mich und meine Arbeit aufgebracht hat.

## Lebenslauf

### Persönliche Daten

Name: Stefanie König (geb. Götze)  
 Geburtstag: 17.07.1981  
 Geburtsort: Hannover  
 Staatsangehörigkeit: deutsch

### Wissenschaftlicher Bildungsweg

seit 04/2008 Wissenschaftliche Mitarbeiterin in der Abteilung Biochemie der Pflanze der Universität Göttingen bei Prof. Dr. Ivo Feußner zur Anfertigung der Dissertation mit dem Thema: *Phenylpropanoids and long chain fatty acid derivatives in the interaction of Arabidopsis thaliana and Verticillium longisporum* im Rahmen der DFG geförderten Forschergruppe FOR546

01/2007 - 03/2008 Stipendiatin im Graduiertenkolleg 1342 der DFG am Institut für Pharmazeutische Biologie der Universität Würzburg in dem Projekt: *Posttranslational activation of mitogen activated protein kinases by oxylipins*, betreut von Prof. Dr. Roitsch

10/2006 - 12/2006 Wissenschaftliche Hilfskraft am Institut für Pflanzenernährung der Leibniz Universität Hannover

01/2006 - 09/2006 Anfertigung der Diplomarbeit am Institut für Pflanzenernährung der Universität Hannover bei Prof. Dr. Horst mit dem Titel: *Peroxidasen im Blattapoplasten – Einfluß der Wirkung von Silizium auf die Mangan-Toleranz von Vigna unguiculata*

10/2001 - 10/2006 Biologie-Studium an der Leibniz Universität Hannover  
 Abschluss: Diplom  
 Hauptfach: Botanik  
 Nebenfächer: Biochemie, Pflanzenernährung

### Freiwilliges Ökologisches Jahr

09/2000 - 08/2001 Freiwilliges Ökologisches Jahr bei der AG für Naturschutz Herringhausen-Stirpe-Oelingen, Osnabrück

### Schulbildung

07/2000 Abitur  
 1993 - 2000 Gymnasium: Wilhelm-Raabe-Schule, Hannover  
 1991 - 1993 Orientierungsstufe Anderten, Hannover  
 1987 - 1992 Grundschule: Kurt-Schumacher-Schule, Hannover

## Erklärung

Hiermit versichere ich, dass ich die vorliegende Arbeit selbständig verfasst und keine anderen als die angegebenen Hilfsmittel und Quellen verwendet habe.

Göttingen, September 2011

Stefanie König